JPRS-UEE-90-011
24 OCTOBER 1990

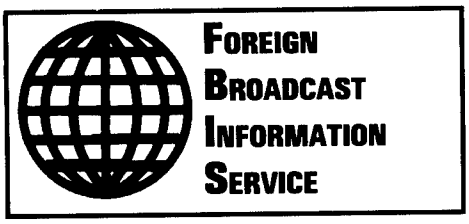

JPRS Report

Science & Technology

USSR: Electronics & Electrical Engineering

Science & Technology
USSR: Electronics & Electrical Engineering

JPRS-UEE-90-011 *24 OCTOBER 1990*

CONTENTS

Broadcasting, Consumer Electronics

Antennas, Propagation

Circuits, Systems

Transportation

Industrial Electronics, Control Instrumentation

Computers

Power Engineering

Industrial Applications

Quantum Electronics, Electro-Optics

Solid State Circuits

UDC 621.397.132.129:006

Achievements and Problems of High-Definition Television

907K0280A Moscow TEKHNIKA KINO I TELEVIDENIYA in Russian No 5, May 90 pp 16-27

[Article by V. A. Khleborodov]

[Abstract] A global model has been developed for the system which will provide high-definition television, including the channels of signal distribution and the supply of video cassettes and disks. Television centers, the core of the system, must be able to use a number of different standards (i.e., 525-line and 625-line formats) in analog or digital mode. They should be able to issue standard signals by ground communications, satellite, cable, disks, or cassettes. The viewer could choose high-quality or high-definition television with a full frequency band or a reduced frequency band. Home television sets would support both.

The International Consulting Committee on Radio plans to choose a global studio standard. The parameters of a variety of proposed standards are presented in tables. The committee feels that the future of high-definition television is irrevocably linked with digital equipment, and thus, a digital standard.

The advantages and disadvantages of each standard are discussed, and the information presented in the tables is expanded. Figures 3; tables 2; references 15: 8 Russian 7 Western.

UDC 621.397.13:629.783+621.397.444

Satellite Television: What's Between the Lines of International Agreements?

907K0280B Moscow TEKHNIKA KINO I TELEVIDENIYA in Russian No 5, May 90 pp 46-52

[Article by A. P. Altayskiy]

[Abstract] A new multilateral convention to prevent unauthorized secondary transmission of signals from satellites has being drafted. The convention is couched in the terms of international publishing law, and this makes it possible to individual governments to implement their own means of suppressing piracy.

Article 1 defines the terms of the agreement according to legal standards. Article 2 defines the jurisdiction of the convention and makes governments responsible for preventing transmission to or from their territory of any signal by any transmission device for which the signal is not intended. The convention is to remain in effect for 20 years, and does not encompass ground communications. Article 3 outlines what may and may not be directly broadcast. Article 4 expands upon the exclusions to Article 3.

In Article 5, the juridical status of the signal transmitted to the satellite remains in effect, barring other resolutions. The convention is not retroactive. Article 6 protects the interests of those who invest in programs. Article 7 fully supports national laws on misuse by monopolies.

Satellite TV Reception: Antennas for 11-to-12 GHz Band

907K0281A Moscow RADIO in Russian No 4, Apr 90 pp 48-53, 88

[Article under the rubric "Video Techniques" by G. Tsurikov, A. Kvitko, and V. Fadeyev, Moscow]

[Abstract] A direct-broadcasting-from-satellite system using the 11-to-12 GHz band (the STV-12 system) is nearing completion in the USSR. Detailed directions, geared to the radio amateur, are given for constructing a 1.5.-m-diameter single-mirror parabolic receiving antenna. The horn feed is described, dimensioned for a 1.5-m, 160°-aperture reflector for use with Moskva receiving equipment. The antenna's gain equals 42.5 dB, pattern width at -3 dB level about 1.5°, first-few-minor-lobe level of -25 dB, noise temperature with an elevation tilt of 10° and more not higher than 60 K, and voltage standing-wave ratio about 1.4. A rotating support using a so-called polar suspension for the reflector is recommended and the screw-and-nut mechanism for rotating the antenna on its polar axis is described in detail. The steel pipe used for the support is 90 to 100 mm in diameter and has a wall thickness of 4 to 5 mm to withstand 25-to-30-m/s winds. Fiberglass-reinforced plastic is recommended for the most complicated step of making the reflector. The form for molding the plastic reflector can be made from cement mortar or a sand-and-water-glass mixture on a wire frame. The procedure for aiming the antenna at satellites is described. The use of a theodolite is recommended for greater accuracy. Final adjustments for receiving the strongest signal are enumerated. Figures 14.

4USTsT Televisions. Control Units: 1. Push Button System

907K0281B Moscow RADIO in Russian No 4, Apr 90 pp 54-56

[Article under the rubric "Video Techniques" by V. Zakharov, Moscow]

[Abstract] There are several modifications of type 4USTsT televisions with various control unit designs. The soft-touch pushbutton control system for the Rubin 51/61 TTs405D television set is described. The A9 control unit consists of an MVP-2 program selector module and a display and switching board. It also contains variable resistors for picture brightness, color saturation and contrast control and sound volume control. The television also features treble and bass controls, a sound shut-off button and jacks for connecting a tape recorder or external loudspeaker and headphones. The

control button system makes it possible to select one of eight TV programs by pushing the proper button and to tune each of the eight control buttons to any VHF or UHF TV channel in three subbands. The preset channel selector subband is switched in by the transmission of voltages through three circuits. When the set is turned on it is ready to receive the program to which the first button has been tuned. The eighth button makes it possible for the TV set to work with a video tape recorder. The control unit incorporates a type KR1106KhP2 microcircuit functioning as an electronic switch. Designed for use in TV electronic tuners, this microcircuit makes it possible to select a program and store it, switch the tuning voltage, control the subband selection switches, and to generate signals for controlling a seven-element digital display and for blocking automatic frequency tuning (AFT). The microcircuit incorporates 16 output switches: eight tuning switches, seven display switches and an AFT blocking pulse generator. The control system's operation is described in detail. Trimmer resistors are used to store the required tuning voltage for the television channel of the program selected, which is shown by means of a type ILTs1-1/9 vacuum-tube display. Figures 3.

Calculation of Equalizer by Means of Elektronika B3-34 Microcalculator

907K0281C Moscow RADIO in Russian No 4, Apr 90 p 59

[Article under the rubric "Audio Engineering" by D. Kuznetsov, Chelyabinsk]

[Abstract] Calculation of an equalizer by means of the Elektronika B3-34 Microcalculator was discussed earlier in RADIO, No 6, 1987. Here a simpler procedure is discussed for the calculation of band filters and for the selection of parts. A calculation program for the Elektronika B3-34 is presented. Four identical capacitors each are needed for each band for a stereophonic equalizer. The first step of the procedure is to select capacitors having monotonically decreasing capacitances and with intervals close to the intervals between the equalizer's frequency bands. It is possible to use capacitors having the same capacitance value for the filters of two adjacent frequency bands, or to increase the interval between capacitances. Then the necessary Q factor is selected (Q = 1.4 to 1.7 for a 10-band equalizer), and then the gain, the interval between frequency bands in octaves, and the equalizer's bottom frequency (usually 31.5 Hz for a 10-band equalizer). Then the rated values of the resistors are calculated according to the program. Resistances are calculated for the first frequency band, and then the resonance frequency of the next filter is calculated. The filters' parameters are calculated successively in the order of increasing frequency. Resistance values are rounded to the nearest standard values. The filter circuit chosen constitutes an inverting operational amplifier with frequency-dependent negative feedback. A voltage follower is added to the equalizer's input. The tolerances for deviation of the parts' rated values from the calculated become tougher as the number of equalizer bands increases. The calculation procedure discussed is much simpler than the one published before. However, the simplified formulas used for calculating the parameters of band filters and their elements result in poorer accuracy of the end results. Figures 1.

UDC 621.397.743(47+57)

Cable Television: What are the Prospects? Part 2

907K0306A Moscow TEKHNIKA KINO I TELEVIDENIYA in Russian No 6, Jun 90 pp 43-48

[Article by A. Barsukov]

[Abstract] The First All-Union Seminar on Cable Television MZhK [not further expanded] was held in Sverdlovsk in mid-February 1990. More than twenty cities were represented. There is great interest in the creation of local television studios for cable and satellite television services. A report was given at the conference proposing the creation of a departmental system of business communications for the exchange of digital information.

At present the Gorizont satellite has no room to implement this service. It has been proposed that two improved Gorizont-M satellites be launched to organize a network of departmental communications.

The equipment and costs of implementing receiving and transmission points are discussed. There is a lengthy discussion of existing international conventions and foreign legislation regulating cable and satellite television and video cassettes. Terms of the convention are defined and examples given. Steps that the USSR should take to regulate cable and satellite television and video cassettes to protect copyright laws are discussed.

UDC 778.5TV:621.397.132.129

Creative, Production, and Economic Features of Creating Films Using the Technology of High-Definition Television

907K0306B Moscow TEKHNIKA KINO I TELEVIDENIYA in Russian No 6, Jun 90 pp 55-57

[Article by M. L. Nemirovskaya, Ye. Ye. Ogurtsova]

[Abstract] There are plans for the introduction in 1995 of daily six-hour experimental high-definition television broadcasting in the Soviet Union.

The economic advantages of high definition television are discussed and a description is given of the production of the Soviet high-definition film presented at the Second World Festival of Electronic Cinematography. The film was awarded the Golden Astrolabe. The film was made in the Soviet Union, and edited in the United States.

Once the use of the cameras was mastered, filming proceeded at a faster pace than typical 35-mm filming. This leads to savings of time, material, and labor, which should stimulate the development of this technology.

The only negative comment was made by cameramen, who thought the equipment could be lighter and more compact. Directors were greatly impressed with the opportunities provided by the new technology, and actors found that their work was made easier.

UDC 621.397.7:621.397.132

The HSV-400 Color Video System to Analyze Rapidly Occurring Events

907K0306C Moscow TEKHNIKA KINO I TELEVIDENIYA in Russian No 6, Jun 90 pp 65-66

[Article by A. Ya. Khesin]

[Abstract] NAS (Japan) has introduced the new HSV-400 video system. It is comprised of the following units:

V-11 television camera, 6 and 12 dB amplification, mechanical gate which opens at 1/2500, 1/5000, 1/10000 seconds, which can handle 200-400 fields/second.

V-24 strobing unit, strobing at 1/50,000 seconds (20 μs) with a 200 W light source.

Variable objective camera O = 1:1.2, focal lengths of 12.5-75 mm.

V-302-E video recorder (PAL system) using VHS cassettes, 200 fields/second, 262.5 lines/field (six images/frame) or 400 fields/second, 131.25 lines/field (11 images/frame).

Color video monitor (any standard monitor for the PAL or NTSC system can be used)

V-84 control unit: stop, start, change recording mode, fast forward, fast reverse, freeze frame, captioning, eject tape, frame-by-frame examination. Time can be indicated on the screen. Monochrome or color recording. Indexing of limited number of frames for later reference.

Connecting cables and stand. Additional supplies can also be purchased: second television camera, illumination source, power pack, computer equipment to process and print data (for PS/2 or IBM AT systems).

Operates on 120, 220, 240 V, consumes 580-640 VA. Can be used at 0-40 degrees centigrade and relative humidities of 30-80 percent. Figures 3.

UDC 628.977.1

On Microprocessor Lighting Control Systems

907k0316a Moscow SVETOTEKHNIKA in Russian No 5, May 90 pp 1-3

[Article by Ya. A. Kungs, B. A. Oshchepkov, Sibtsvetmetenergo, Krasnoyarsk]

[Abstract] A microprocessor lightning control system consisting of a control microprocessor, an interface, control units (which receive digital signals from the processor and send control signals into the outgoing lines), local and remote control relays for turning ON or OFF the lighting fixtures, and a photo relay controlling the illuminance in work areas is described. The device was used to analyze the fixed and variable cost components necessary for operating the microprocessor, the control units, and other elements of the circuit. The total savings and net profit were used as the economic factor evaluation criteria. The limit of economic feasibility of using this device is examined for the MS-2702 "Elektronika" controller. The analysis shows that given a lighting power demand controlled by the device of over 500 kW, the use of microprocessor control is expedient. References 7: 6 Russian, 1 Western; figures 2; tables 1.

UDC 621.326.032.1.001:669.295:62-426

On The Efficiency of Titanium Filament Supports in Incandescent Lamps

907K0316B Moscow SVETOTEKHNIKA in Russian No 5, May 90 pp 5-7

[Article by N. P. Kiseleva, M. N. Koshina, O. M. Muratov, All-Union Light Source Institute imeni A. N. Lodygin]

[Abstract] Titanium and its alloys have many considerable advantages over other materials used as incandescent lamp getters. The use of compact titanium wires as both a getter and a structural member in incandescent lamps is examined. A wire with a 1 mm diameter was made in a laboratory; to degas it, the aquadag-free wire was annealed with RF currents in a 10^{-2} Pa vacuum at 800°C for 20 min. The luminous and electric parameters of the lamps were examined. Test results of vacuum and gas-filled incandescent lamps with titanium supports show: compared to aluminized molybdenum supports, titanium maintains its gettering properties during the entire service life and retains its shape; the use of titanium supports is gas-filled lams as both a getter and a structural member is complicated; commercial production and subsequent testing of wires with a 0.12 mm diameter is expedient. The authors are grateful to L. A. Lupacheva for help with microstructural analyses. Reference 2; figures 4; table 2.

UDC 621.32:615.831.76:001.5

Medical Studies of Ultraviolet Lamps

907K0316C Moscow SVETOTEKHNIKA in Russian No 5, May 90 p 7

[Article by T. V. Balyasnikova, A. V. Leonov, N. V. Mamontova, Gorkiy Medical Institute imeni S. M. Kirov]

[Abstract] The lack of luminous flux in erythematous ultraviolet light sources limits their applications in preschool care institutions and school. The hygienic efficiency of LB UF-36 lamps was examined over a two-year period on over 200 six-year old children. The results on both children exposed for five months and unexposed children were analyzed. The daily prophylactic dose of ultraviolet radiation was within 1/8-1/6 of the minimum erythema dose. The mean classroom illuminance was 50 lx with a peak of 400 lx. Analytical data show that the composite (luminous and ultraviolet) flux has a favorable effect on children, especially their eyes. The authors conclude that research should continue and that the range of irradiating and illuminating plants should be expanded not only in schools but in rooms where adults spend considerable time and that commercial production of the LB UF-36 lamps is needed. References 2.

UDC 628.94.002

Conveyor-Type Ion Treatment of Tungsten Wires

907K0316D Moscow SVETOTEKHNIKA in Russian No 5, May 90 p 24

[Article by A. N. Abiyaka, L. N. Orlikov, Ye. V. Chikin, Sibelektrosvet Tomsk Production Association and Tomsk Automatic Control System and Radio Electronics Institute]

[Abstract] In electric lamp production, the tungsten wire used as the filament material must be treated beforehand to remove the graphite coat which serves as a lubricant during the drawing and protects tungsten from oxidation. A device developed for the ion treatment of wires is described; it consists of a cylindrical body which houses a plasma generator formed by a cylindrical anode and a grid. The wire is pulled through the device at a 1-5 m/s rate; the treated hot wire passes a nitrogen- or helium-filled tube. The dependence of the discharge voltage and current, gas type, and pulling rate on the wire treatment characteristics is analyzed. The treatment rate can be controlled by the accelerating voltage while the annealing, by the current. The process can be easily automated using a pressure regulator with a discharge current feedback. The device can be used to treat a number of other materials, such as molybdenum and steel. After minor design modifications, wires made from different materials can be treated simultaneously. References 2; figures 2.

UDC 628.955.032.4

New Injection Molding Material

907K0316E Moscow SVETOTEKHNIKA in Russian No 5, May 90 p 27

[Article by Z. P. Openkina, V. V. Surzhenko, S. S. Fedeyev, All-Union Scientific Research Institute of Lighting Engineering]

[Abstract] A new casting material based on self-stopping polypropylene compositions used for making insulating parts for electrical devices developed by the Pilot Scientific Production Association Plastpolimer together with the All-Union Scientific Research Institute of Lighting Engineering is described. It was tested at the Ardatov Lighting Plant pursuant to GOST 361-85; the test reveals that the material meets all the specifications and is capable of withstanding electric and mechanical loads developing in the course of normal operation. The composition is made by injection molding in domestic and imported machines; the process does not require pretreatment and the mold does not need preheating. Compared to the phenol plastic used today, the new material has a number of advantages, such as a small shrinkage spread, good mold filling, high accuracy and stability of geometric dimensions, and minimal raw material losses. The principal specifications of the material pursuant to TU 6-05-05-417-89 are cited. Commercial production of the new material is expected in 1991 resulting in a saving of 2,796 rubles per ton of material. Tables 1.

UDC 550.388.2

Double Stimulated Scattering of Electromagnetic Waves in Ionospheric Plasma

907K0210A Moscow GEOMAGNETIZM I AERONOMIYA in Russian Vol 30 No 1, Jan 90 pp 82-89

[Article by A.N. Karashtin and M.Sh. Tsimring, Gorkiy Scientific Research Institute of Radiophysics]

[Abstract] Double stimulated scattering of a high-frequency electromagnetic wave upon its oblique incidence on a plane layer of magnetically active isothermal plasma is considered, this electromagnetic wave riding on a low-frequency fast magnetic sound wave which propagates perpendicularly to the plasma concentration gradient and almost perpendicularly across the external magnetic field. Analysis of this process is based on the system of Maxwell equations and the wave equation for magnetic sound in a nonuniform high-frequency electric field. The plasma concentration is regarded as the sum of a quiescent component and a perturbation in the sound wave. The solution to those equations yields the amplitude of the threshold field intensity of an incident electromagnetic wave field for its double stimulated scattering, corresponding to a zero power reflection coefficient. In the case of an ionospheric layer there is no analytical expression obtainable for the threshold field and, therefore, the equations must be solved by numerical methods. Calculations for the F- layer above moderate latitudes have yielded data on the dependence of that threshold field on the angle (85.5-88.5°) which the sound wave vector makes with the magnetic field vector (frequency of electromagnetic wave 9.31 MHz, angle of incidence 6°) and on the frequency of the electromagnetic wave (6-10 MHz, angle of incidence 6°). The results indicate that experimental observation of double stimulated scattering in the ionosphere is feasible, with the aid of test equipment such as the "Sura" apparatus, and they indicate the conditions under which this should be possible. Figures 3; references 10.

UDC 550.388.2:523.98

Nocturnal Peaking of Ionization within F-Layer above Cuba: Relation to Solar Activity

907K0210B Moscow GEOMAGNETIZM I AERONOMIYA in Russian Vol 30 No 1, Jan 90 pp 98-106

[Article by L. Lois, J. Perez, B. Laso, N. Jakowski, and R. Landrock, Institute of Geophysics and Astronomy, Cuban Academy of Sciences, and Institute of Space Research, GDR Academy of Sciences]

[Abstract] Nocturnal peaking of ionization within the ionospheric F- layer above Cuba is analyzed statistically on the basis of measurements made over the 1974-80 period. The principal indicators here are the electron concentration N_F and the critical frequency f_0F2, auxiliary measurements with a Faraday polarimeter having yielded data on the Faraday angle needed for determination of the N_F and data on the layer thickness according to the Bradley-Dudeney model having been used for determination of the altitudinal N(h) profile widening. The method of analysis is based on approximation of the two ionization indicators as linear functions of time during both rise and fall periods. The statistical analysis is based on 746 events of N_F peaking and 1308 events of f_0F2 peaking. As a supplementary indicator of ionization changes was calculated the integral ionization intensity corresponding to various rates of nocturnal changes. The data cover periods of weak and strong solar activity, in winter, in summer, and during equinoxes. The anomalous peaking of ionization is, on the basis of this study, correlated with plasma transport along global magnetic lines of force dependent not only on the geography and on the season but also appreciably on the solar activity. During periods of weak solar activity these nocturnal peaks occur almost every night in winter, most intensely about solstice time, and only sporadically in summer. During periods of strong solar activity these nocturnal peaks, of shorter duration but higher intensity, reach their maximum levels in summer. Figures 6; references 24.

UDC 550.388.2

Oblique Sounding of Ionosphere With Continuous Linearly Frequency- Modulated Signals

907K0210C Moscow GEOMAGNETIZM I AERONOMIYA in Russian Vol 30 No 1, Jan 90 pp 107-112

[Article by V.A. Ivanov, V.P. Uryadov, V.A. Frolov, and V.V. Shumayev, Mari Polytechnic Institute]

[Abstract] The ionosphere above moderate latitudes was sounded with continuous linearly frequency-modulated short-wave radio signals in an experiment using rhombic transmitter and receiver antennas. Measurements were made along the 2700 km long Alma Ata - Gorkiy route over the June-July 1987 period, noteworthy being the appearance of a wideband $2E_s$ mode on the distance-frequency characteristics, then along the 5800 km long Khabarovsk - Gorkiy route over the 13 March - 3 April 1988 period coinciding with magnetic storms and a much more probable appearance of the 3F2 Pedersen mode during morning or evening hours. The authors thank L.M. Yerukhimov, N.A. Mityakov, V.S. Maksimov, E.G. Mirmovich, N.A. Kurmuzakov, N.D. Krupenyy, A.M. Leonov, N.G. Serebryanitskiy, and I.V. Popkov for assisting in the experiments. Figures 4; references 10.

UDC 551.466.1

Measurement of 'Sea Surface - Radar Signal' Modulation Transfer Function at 3-cm Wavelength

907K0224A Gorkiy IZVESTIYA VYSSHIKH UCHEBNYKH ZAVEDENIY: RADIOFIZIKA in Russian Vol 33 No 1, Jan 90 pp 3-11

[Article by A.D. Rozenberg, Institute of Oceanology, USSR Academy of Sciences]

[Abstract] Measurements with a pulsed coherent navigational radar at the 3-cm wavelength were made during the June-September 1972 period along the Black Sea coast, for a validation of this method of determining the parameters of sea ripple from the frequency characteristics of signals scattered by the sea surface and then on this basis calculating the modulation transfer function. The radar station was installed on a cape, its equipment including an echo resonator cavity for storage of the signal phase and then a high-frequency phase shifter before one of the two heterodyne mixer mixer. This mixer was followed by an intermediate-frequency amplifier, this amplifier and the one behind the other mixer feeding signals to a phase detector followed by a peak detector which also received signals from a range selector through a strobing circuit. Output signals from the peak detector were recorded on magnetic tape along with output signals from a d.c. string ondograph, the latter having been mounted on a buoy 400 m away from the coast and 60 m under the water surface. The antenna was mounted on a mast 12 m above sea level, on the beach 50 m behind the water front, the grazing angle being variable over the 1-4.5° range for distances covering the 150-750 m range. Measurements were made under calm conditions, each measurement was made with vertically polarized andhorizontally polarized signals. The readings have been analyzed for "instantaneous" frequency spectra of wave energy and spectral density at the upper cutoff frequency (100 Hz), also for determination of upper and lower 3 db corner frequencies. From these spectra has been obtained the modulation transfer function, which depends on the wind velocity as well as on the range, on the angle of signal incidence, and strongly on the signal polarization. An evaluation of the results has yielded values of the coherence function comparable with those based on earlier measurements from platforms, but 1.5-2 time lower absolute values of the modulation transfer function. The author thanks I.A. Leykin for helpful discussions. Figures 4; tables 1; references 8.

UDC 621.396

Effect of Near Fields on Local Perturbation of Earth-to-Ionosphere Distance

907K0224B Gorkiy IZVESTIYA VYSSHIKH UCHEBNYKH ZAVEDENIY: RADIOFIZIKA in Russian Vol 33 No 1, Jan 90 pp 12-16

[Article by A.P. Nikolayenko, Institute of Radio Astronomy, UkSSR Academy of Sciences]

[Abstract] The problem of diffraction of a infralow-frequency electromagnetic field by a local inhomogeneity within the cavity between Earth and ionosphere is solved on the basis of the Stratton-Chu integral equation with Green's function in the Born approximation of the perturbation theory and so as to reveal how the near fields influence the solution. The cavity between Earth and ionosphere is assumed to be excited by a vertical electric dipole on the surface of Earth and the resulting local inhomogeneity in the lower ionosphere above that field source is assumed to be a circular with a diameter much smaller than the wavelength of the electromagnetic radiation, the configuration of the problem being an axisymmetric one. Considering vertical propagation of radio waves describable by null-mode normal field component and using the conventional dispersion law, calculations yield the perturbation of an otherwise uniform Earth-to-ionosphere distance (altitude of the ionospheric layer above Earth). The physical significance of the results is, disregarding the curvature of the Earth surface, that such a local change in that distance (altitude) is equivalent to the change in the current moment of the field source. The electrostatic component of the field at the lower boundary of the ionosphere is much more perturbed than its induced component and even more so than its radiation component, the thickness of the ionospheric layer into which the field penetrates being approximately equal to the altitude of its lower boundary. The author thanks G.I. Makarov, V.V. Kirillov, and Yu.P. Galyuk for helpful discussion and constructive critique. Figures 1; tables 1; references 5.

UDC 538.566

Influence of Terrain Relief on Low-Frequency Electromagnetic Field

907K0224C Gorkiy IZVESTIYA VYSSHIKH UCHEBNYKH ZAVEDENIY: RADIOFIZIKA in Russian Vol 33 No 1, Jan 90 pp 17-21

[Article by O.G. Kozina and G.I. Makarov, Leningrad State University]

[Abstract] The effect of geometrical nonuniformity such as a surface relief on the performance of low-frequency antennas is analyzed, convex and concave cylindrical surface deformities being considered whose dimensions are much smaller than the radiation wavelength in vacuum and which cut the level surface or, in the more general case of a curving surface, the plane tangent to it at any angle from $\pi/2$ to π (hill) and from π to 3π (valley). The analysis is based on the Leontovich relation between tangential electric and magnetic field components, assuming that both principal radii of surface curvature are larger than the radiation in the lower medium. Analysis of the problem in the complex plane with the Meixner condition at the edge, after several conformal transformations, leads to the Laplace equation which here needs to be solved for a half-plane with Neumann boundary conditions only. The effect of terrain nonuniformity, characterized by the ratio of the tangential magnetic field components at a surface deformity and at a level surface respectively, is found to increase with decreasing distance from the antenna and with increasing width of that deformity: the field radiated by an antenna on level ground becomes weaker at a hill and stronger at a valley. Figures 4; references 9.

UDC 538.574.6

Asymptotic Differential Radiation Conditions for Three-Dimensional Diffraction Problems

907K0224D Gorkiy IZVESTIYA VYSSHIKH UCHEBNYKH ZAVEDENIY: RADIOFIZIKA in Russian Vol 33 No 1, Jan 90 pp 85-92

[Article by A.B. Samokhin and S.V. Tsvetkov, Moscow Institute of Radio Engineering, Electronics, and Automation]

[Abstract] Asymptotic differential boundary conditions of order- 0([<s]up-3) accuracy are proposed for the three-dimensional diffraction problem, these boundary including transverse space derivatives so that such a high accuracy becomes attainable. As a consequence, however, there would be several several solutions to this boundary-value problem rather than a unique one. The problem is regularized by insertion of a corrective term containing fourth-order transverse space derivatives into the differential operator so as to ensure, without lowering the accuracy of the approximations, uniqueness of the solution to a strongly elliptical equation more appropriate than the conventional Maxwell equations for the electric field. The problem is formulated in a bounded region first, for solution by the method of finite elements on the basis of which it can then be solved approximately for a boundless region. The boundary conditions are then particularized for diffraction be a sphere with a given radius in a homogeneous and isotropic medium, considering an electric field which outside that sphere satisfies the Helmholtz vector equation in a spherical system of coordinates. Uniqueness of the solution to such a boundary-value problem, if one exists, is established by theorem on the basis of the Cauchy-Bunyakovskiy inequality, whereupon its existence is established by demonstrating that the problem is one of the Fredholm kind. References 11.

UDC 621.371.36.029.63

Saturated Intensity Fluctuations of Radio Waves Propagating Through Solar Plasma

907K0235A Gorkiy IZVESTIYA VYSSHIKH UCHEBNYKH ZAVEDENIY: RADIOFIZIKA in Russian Vol 33 No 2, Feb 90 pp 135-142

[Article by S.N. Rubtsov, O.I. Yakovlev, and A.I. Yefimov, Institute of Radio Engineering and Electronics, USSR Academy of Sciences]

[Abstract] Saturated intensity fluctuations of radio waves propagating through the solar plasma are analyzed on the basis of experimental data provided by "Venera-15,16" spacecrafts during 1984 explorations, a theory of such fluctuations and mathematical models having been developed earlier on the basis of explorations of the terrestrial ionosphere. The solar plasma was sounded with decametric (32 cm) and centimetric (5 cm) radio waves skirting the sun as close as 100-2.5 solar radii. The results are evaluated in terms of asymmetry and kurtosis factors, both depending on the flicker index and on the nearest distance of the radio beam to the sun. On this basis are then calculated the frequency spectra and the autocorrelation functions of these fluctuations. They indicate that random focusing occurs when 32 cm radio waves approach the sun within 13-16 solar radii and intensity spikes appear when 5 cm radio waves approach the sun within 3-7 solar radii. The spectra of these fluctuations indicate a maximum spectral density within the 0.1-0.3 Hz frequency range, in close agreement with the theory. Figures 6; tables 1; references 15.

UDC 550.388.2

Phase Perturbation in Strong Radio Waves Reflected by Ionospheric F-Layer

907K0235B Gorkiy IZVESTIYA VYSSHIKH UCHEBNYKH ZAVEDENIY: RADIOFIZIKA in Russian Vol 33 No 2, Feb 90 pp 143-149

[Article by V.V. Belikovich, Ye.A. Benediktov, V.A. Zyuzin, G.P. Komrakov, M.Yu. Krasilnikov, A.V. Prokofyev and A.V. Tolmacheva, Scientific Research Institute of Radio Physics]

[Abstract] An experimental study of strong radio waves reflected by the ionspheric F-layer was made with the aid of sounding radio waves in December 1986, November 1987, and December 1988, at two radio frequencies: 4.785 GHz and 5.828 GHz. The apparatus of the "Sura" facility included a cophasal antenna array for reception of signals with two mutually orthogonal linear polarizations (12 dipoles for each polarization), a phase shifter gang for resolution of two circular polarizations corresponding to ordinary and extraordinary magnetoionic wave components respectively, a selective receiver having a bandwidth of approximately 40 kHz, followed by a phase detector and an amplitude detector. The data reveal fast phase variations in the strong ordinary wave component upon impingement of a strong radio wave on the F-layer and intense signal scattering near the mirror reflection level, evidently owing to formation of prominent artificial periodic inhomogeneities in the field of a strong standing radio wave as the strictional force is compounded by strictional parametric instability. Figures 2; references 13.

UDC 550.388.1

Methodological Accuracy of Signal Delay Readings During Radio Sounding of Ionosphere

907K0235C Gorkiy IZVESTIYA VYSSHIKH UCHEBNYKH ZAVEDENIY: RADIOFIZIKA in Russian Vol 33 No 2, Feb 90 pp 150-154

[Article by Yu.K. Kalinin, V.Ye. Kunitsyn and L.L. Rozhdestvenskaya, Moscow State University]

[Abstract] Use of solitary digital ion probes for radio sounding of the ionosphere along oblique paths is analyzed

for accuracy of signal group delay readings, subsequent calculation of the three-dimensional electron concentration distribution in the ionosphere not being possible on the basis of these readings but being done along smooth profiles of a laminar ionosphere. The effect of three-dimensional inhomogeneities associated with nonuniformity of the electron concentration on readings of the group delay of signals from an ion probe is evaluated in the approximation of an isotropic ionosphere and scalar radio waves, namely radio waves whose electric field satisfies the Helmholtz equation. The dispersion relation is established at the high-frequency limit (wave number $k \rightarrow \infty$) by the stationary phase method, first assuming local uniformity of three- dimensional electron concentration fluctuations within an ionospheric layer and then considering a thin statistically homogeneous layer with large-scale inhomogeneities. The results of analysis and calculations indicate that measuring the signal group paths in the ionosphere accurately within the 1-5 km Fresnel radius is adequate for reconstruction of the regular ionosphere profile but not for determining the statistical characteristics of three-dimensional ionospheric inhomogeneities, which requires measuring the variations of those paths. References 4.

UDC 551.501.85

Characteristics of Wind Field in Clouds Based on Readings of Noncoherent Radar

907K0235D Gorkiy IZVESTIYA VYSSHIKH UCHEBNYKH ZAVEDENIY: RADIOFIZIKA in Russian Vol 33 No 2, Feb 90 pp 164-169

[Article by V.M. Melnikov, Main Geophysical Observatory]

[Abstract] Inasmuch as the two characteristics of the wind field in clouds and clusters measurable by a Doppler radar are the mean velocity of hydrometeors in the direction of the sounding radio beam and the width of the velocity spectrum of scatterers within the radar pulse range, the mean velocity of hydrometeors being simply equal to half the product of Doppler frequency shift and wavelength of the radio beam but the width of the scatterer velocity spectrum being equal to half the product of that wavelength and the spectrum broadening. Measurement of that spectrum broadening with a noncoherent radar is considered, the four independent and thus additive causes of this effect being turbulence, vertical wind gradient, gravity precipitation of particles, and radio beam width. Measurement of these four spectrum broadening components involves estimation of their standard deviations, calculation of the signal correlation coefficient, and determination of the frequency of signal mean-value crossovers as well as of the mean modulus of the difference between successive pulses. Such measurements were made in the Leningrad region with automated instruments including Fourier analyzers. An evaluation of data pertaining to selected clouds, assuming a Gaussian ergodic echo signal, reveal how the radar output signal indicating the mean difference between wind velocities depends on the width of the scatterer velocity spectrum and on the echo signal power correlation coefficient. It thus is feasible, by use of "outer" coherence, to measure the difference between wind velocities without measuring the width of the scatter velocity spectrum. Figures 4; references 9.

UDC 533.933

Magnetic Instability of Nonhomogeneous Plasma in Field of Strong Electromagnetic Wave

907K0235E Gorkiy IZVESTIYA VYSSHIKH UCHEBNYKH ZAVEDENIY: RADIOFIZIKA in Russian Vol 33 No 2, Feb 90 pp 170-176

[Article by A.I. Alber, A.A. Zharov, T.M. Zaboronkova, I.G. Kondratyev, and Z.N. Krotova, Scientific Research Institute of Radiophysics]

[Abstract] Magnetic instability of a weakly nonhomogeneous plasma in the field of a strong incident high-frequency electromagnetic wave is considered, particularly the hydrodynamic diffusion stage of this instability characterized by a mean free path of electrons much shorter than the length of the electromagnetic wave in the plasma region coinciding with the region where the amplitude of the electric field component becomes nonuniform as plasma resonance is approached. The plasma is assumed to be a plane-laminar one with a linear electron concentration profile. The wave is assumed to be a normally incident monochromatic one. The vector equation describing the quasi-static magnetic field generated by such a wave in such a plasma involves the frequency of electron-ion collisions and a nonlinear current, the latter calculated by the Hertz method including only ten moments. The problem of instability evolution is solved for a quasi-static magnetic field orthogonal to both the electron concentration gradient and to the electric field component of the incident wave, in the approximation of a slowly varying amplitude of the longitudinal wave field component and a high electron-ion collision frequency. Small-scale perturbations of the quasi-static magnetic field during instability evolution are calculated on the basis of an analytical solution to the corresponding system of equations. Analysis of large-scale perturbations requires a numerical solution, upon regularization of the problem by phenomenological accounting for the fact that interaction of the current and the quasi-electrostatic field is slightly delocalized. These perturbation are found to be still relatively small-scale ones within the region of negative diffusion. Figures 4; references 7.

UDC 621.396.677

Diffraction of Electromagnetic Waves by Thin Shields of Variable Configuration

907K0235F Gorkiy IZVESTIYA VYSSHIKH UCHEBNYKH ZAVEDENIY: RADIOFIZIKA in Russian Vol 33 No 2, Feb 90 pp 226-230

[Article by V.V. Martsafey, I.G. Shvayko, and G.F. Tsalimov, Odessa Institute of Electrical Communications Engineering]

[Abstract] The problem of diffraction of electromagnetic waves is solved by a time-efficient new method for the design of antenna arrays with variable configuration. The problem is assumed to be a two-dimensional one, corresponding to diffraction by a thin shield, and reducible to the Fredholm integral equation of first or second kind. The method of solution, following reduction of the integral equation to a well-conditioned system of linear algebraic equations, involves collocation with piecewise-uniform interpolation. Deletion of an n-th row and an n-th column from the original MxN matrix yields a new matrix for a shield with a hole the location of which corresponds to the n-th element of that original matrix. Subsequent deletions of rows and columns will correspond to insertion of additional holes or expansion of existing ones, shortening and narrowing the shield being effected by deletion of peripheral columns and rows. The time required for computing a new matrix is much shorter than that required for computing the original one, inasmuch as the algorithms are the same and can be executed simultaneously. The method is very expedient for estimating the dependence of the antenna performance characteristics on the size and the location of gaps between mirror segments of a reflector antenna, for design of multislot antennas mounted on any kind of surface, design of multislot shields for optimization of electromagnetic apparatus, and for shaping the radiation pattern of an aperture by varying the flange. The procedure is demonstrated on diffraction of E-polarized or H-polarized waves emerging from the open end of a plane waveguide of finite length with a variable-length plane solid flange, a "perforated" solid flange, or a a laminated flange, assuming that the waveguide has been excited by a current filament. The solution by this method of a model diffraction problem, namely diffraction of a normally incident electromagnetic wave by and ideally conducting ribbon, is compared with the solution of this problem on the basis of the same integral equation without extraction of the root singularity and with its solution by separation of variables in an elliptical system of coordinates. Calculations of the directive gain in both principal and reverse directions for each kind of flange are found to be made most economically and with satisfactory accuracy even the corner points by the proposed method. Figures 5; references 8.

UDC 538.574.6

Peculiarities Characterizing Reflection of Spherical Electromagnetic Wave by Anisotropic Dielectric Medium

907K0235G Gorkiy IZVESTIYA VYSSHIKH UCHEBNYKH ZAVEDENIY: RADIOFIZIKA in Russian Vol 33 No 2, Feb 90 pp 249-252

[Article by F.G. Bass, A.A. Bulgakov, and S.I. Khankina, Institute of Radiophysics and Electronics, USSR Academy of Sciences]

[Abstract] Reflection of a spherical electromagnetic wave by a solid anisotropic dielectric medium is analyzed and specifically the side waves which emerge when the angle of incidence is larger than the critical one, these side waves propagating not only through the medium in which both the point source of such a wave and the receiver receiver are located but also partly through that dielectric medium. The medium containing the source and the receiver is assumed to be a homogeneous dielectric one in the half-space $y > 0$. The dielectric reflector medium is assumed to be a uniaxial crystal with its optical axis in the plane of the interface perpendicular to the z- axis. In accordance with the theory of reflection and refraction, the field of the incident spherical wave is represented as the sum of two plane waves polarized so that $E_y = 0$ and $H_y = 0$ respectively. Both an ordinary wave with div $E = 0$ and an extraordinary wave with div $D = 0$ can be found to propagate through the crystal, with $E_z = 0$ and $H_z = 0$ respectively. There remains then only an E_x component. In the ambient medium this component represents superposition of the incident wave and the reflected one. In the crystal this component represents superposition of the ordinary wave and the extraordinary one. On the basis of this model, with each wave described by a surface integral and with the appropriate expression for the reflection coefficient, the amplitudes of both side waves have been calculated numerically as functions of the azimuth angle in positively uniaxial crystals ($m^2 > n^2$) as in GaAs-TiO_2 and AgCl-SiO_2 systems or in negatively uniaxial crystals ($m^2 < n^2 < 1$ as in CsBr-$NaNO_3$ and KRS6-($NaNO_3$,TlCl,TlBr) systems. The results yield information about the crystallographic axes of such crystals, which accordingly can be determined from measurement of both ordinary and extraordinary side waves. Figures 2; references 6.

UDC 621.396.677

Numerical Analysis of Compact Polygon for Antenna Radiation Pattern Measurement With Collimator

907K0235H Gorkiy IZVESTIYA VYSSHIKH UCHEBNYKH ZAVEDENIY: RADIOFIZIKA in Russian Vol 33 No 2, Feb 90 pp 253-255

[Article by E.M. Inspektorov and G.I. Rusetskaya, Gomel State University]

[Abstract] Measurement of antenna radiation patterns by the collimator method is considered, which involves a numerical analysis of a compact polygon. The collimator is formed by the antenna, typically a reflector antenna having the shape of a segment of a parabolic cylinder rotating about a pivot at the center point on its surface, and mirror which is also a segment of a parabolic cylinder. The exciter, the third element of the polygon facing the mirror, represents a cophasal array of electric current filaments with the phase center at the focus of that mirror. Both antenna and mirror have rounded edges and both are assumed to be ideally conducting, the mirror being much wider than the antenna. As the radiation pattern of such an antenna is regarded the angular distribution of the field produced at the focus of the parabolic antenna by currents induced on the mirror. The currents induced on both antenna and mirror surfaces by an external source such as the exciter are determined theoretically from the solution to the corresponding Fredholm integral equation of the second kind and the E_z component of the field at the observation point is then determined accordingly. Numerical calculations based on measurements in the polygon will be sufficiently accurate when the function describing the radiation pattern of the antenna is constant over the antenna aperture angle and zero on both sides beyond that angle, when the exciter is exactly matched to the feeder and to the ambient space, and when diffraction and shadowing by the exciter are negligible. Calculations have been made for two different antenna-mirror-exciter configurations and, for comparison, with the antenna in free space. Figures 4; references 4.

[UDC 517.587:621.396.677.494

Formation of Nulls in Antenna Radiation Pattern by Method of Orthogonal Aperture Polynomials

907K0298A Kiev IZVESTIYA VYSSHIKH UCHEBNYKH ZAVEDENIY: RADIOELEKTRONIKA in Russian Vol 33 No 5, May 90 pp 3-7

[Article by V.I. Gusevskiy]

[Abstract] The method of orthogonal aperture polynomials, an extension of the least squares method, is applied to optimum synthesis of the phase distribution in the aperture of an antenna array with the necessary number of nulls in certain direction, this method being more computation-efficient than minimization of nonlinear functionals under nonlinear constraints by the method of nonlinear programming and not being subject to any constraints on the number of array elements or on the geometry of the array contour. The method is demonstrated on a linear phased antenna array with a known amplitude distribution over its aperture and with a finite set of M directions in which its radiation pattern must have dips. The sequence of orthonormalized polynomials $_n(x)$ on the normalized aperture [-1,1] which satisfies the relations Integral from -1 to 1 of $p_n(x)p_m(x)\rho(x)dx = 1$ for n = m and 0 for n not = m is defined by the function $\rho(x)$, while the sought phase distribution $\Phi(x)$ which satisfies the system of integral equations $f(_q$ (value of normalized radiation pattern in far field in direction at angle Φ_q from normal to antenna aperture) = (1/2)Integral from -1 to 1 of $e^{-iklxsin\varphi+ i\Phi(x)}\rho(x)dx = 0$ for q = 1,2,...,M is expanded into a series $\Phi(x) = kl\Sigma\, c_n p_n(x)$ from n = 2 to n = N (k = $2\pi/\lambda$, λ- wavelength, c_n- sought Fourier coefficients of synthesized phase distribution, N- number of Fourier harmonics). The number of directions M is equal to N- 2, inasmuch as the Fourier coefficient of the fundamental (first) harmonic determines the a'priori prescribed angular coordinates of the equivalent linear phase front and thus the orientation of the major lobe. The term $e^{i\Phi(x)}$ is replaced with the $1+ ikl\Sigma\, c_n{}^1 p_n(x)$ segment of its Taylor series expansion, whereupon the nulls are formed so as to minimize the reduction of antenna gain along the axis of the major lobe. A numerical analysis of this method of phase distribution synthesis has revealed that minimum reduction of gain is attained by using only odd harmonics for formation of dips, a paradox from the standpoint of conventional antenna theory and design but not when orthogonal odd harmonics are used. The method is demonstrated on a 10λ long linear phased antenna array with a 0.5λ distance between elements and a uniform amplitude distribution. The method can be extended to two-dimensional phased antenna arrays with any contour, including multiply-connected ones. Figures 4; tables 1; references 3.

UDC 621.396.677.494:62.391.24

Determination of Space Spectrum from Samples of Signals Transformed in Adaptive Antenna Array

907K0298B Kiev IZVESTIYA VYSSHIKH UCHEBNYKH ZAVEDENIY: RADIOELEKTRONIKA in Russian Vol 33 No 5, May 90 pp 7-12

[Article by V.N. Manzhos, V.N. Kokin, and V.G. Parfenyuk]

[Abstract] Superresolution algorithms are synthesized for adaptive estimation of the space spectrum of noise signals from samples of antenna output signals, the estimated angular parameter α_i of the i-th signal being the coordinate of the i-th stationary point in the space spectrum and the estimation being done algebraically by an equidistant antenna array. The procedure is based on the assumption each of M elements in an equidistant array puts out a separate sample of signals and takes into account transformation of signals by special devices in the antenna such as phase shifters, adders, subtractors, etc. It essentially involves search of the weight vector-column $R(\alpha)$ which will minimize the antenna output power $P(\alpha) = R^*(\alpha)\Phi_A R(\alpha)$, where $\Phi_A = A\Phi A^*$ is the correlation matrix of transformed signals and A is the square MxM nondegenerate and generally complex transformation matrix. The space spectrum is estimated accordingly, first by the method of maximum likelihood involving use of Lagrange multipliers in search of the weight vector $R(\alpha)$ which will minimize the antenna output power $P(\alpha)$ under the linear constraint

$R^*(\alpha)X_A(\alpha) = 1$, where $X_A = AX(\alpha)$ is the transformed amplitude-phase-distribution vector. It is then estimated by the method of maximum entropy involving an analogous procedure, but with the amplitude-phase-distribution vector X_A vector replaced by the i-th column of matrix A. It is also estimated by the method of eigenvectors involving minimization of the antenna output power $P(\alpha)$ under the quadratic constraint $R^*(\alpha)AA^*R(\alpha)$, with the Lagrange multiplier μ equal to the smallest eigenvalue of the Hermitian $B = [A^{-1}*A^{-1}\Phi_A$ and the weight vector $R(\alpha)$ being the eigenvector of matrix B corresponding to $\mu = \mu_{min}$. Estimates of parameter α are by any of these three methods found as coordinates of the maxima of the power output function or as roots of the complex polynomial $F(\alpha) = [A^*R(\alpha)]^*X(\alpha)$, spurious roots needing to be eliminated from the set of M roots in the latter case. The maximum likelihood method of estimating parameter α and the space spectrum is demonstrated on an antenna array with a phase shifter. Both this method and the method of eigenvectors are demonstrated on an antenna array with a main receiver channel and compensating ones whose radiation patterns have minima in the direction of the useful signal. The method of eigenvectors is also demonstrated on such an antenna array with compensating channels not immune to the useful signal. Figures 2; references 5.

UDC 621.396.67:621.316.36

Effect of Spherical Dielectric Shielding Cap on Radiation Pattern of Aperture Antenna

907K0298C Kiev IZVESTIYA VYSSHIKH UCHEBNYKH ZAVEDENIY: RADIOELEKTRONIKA in Russian Vol 33 No 5, May 90 pp 16-19

[Article by Ye.M. Kats and B.A. Panchenko]

[Abstract] The radiation pattern of an aperture antennas covered by a spherical dielectric shielding cap is calculated with the aid of Green's tensor functions and expansion into series of spherical harmonics, the effect of such a cap on that radiation pattern being analyzed by treating the antenna aperture as the open end of a circular or rectangular waveguide operating in a fundamental mode so as to eliminate the need for solution of both inner and outer problems. Inasmuch as accounting for the effect of any shielding cover requires only stipulation of a specific two-dimensional distribution the magnetic current over the aperture, a circular waveguide operating in the H_{11} mode and having a single or multilayer spherical dielectric cap mounted on its flange has been selected for demonstration. The radiation pattern of a such a covered aperture antenna in the H-plane and in the E-plane is calculated analytically, this being possible owing to the fast convergence of each series in spherical harmonics. The results of numerical calculations based on varying the inside radius of the cap as well as the thickness of its equally thick dielectric layers and the permittivity of their material indicate how the width of the antenna radiation pattern in both planes depends on these three parameters. Figures 3; references 1.

UDC 621.391.25:621.391.268

Discrimination of Discretely Encoded Signals From Interference in Acoustooptic Correlator With Time Integration

907K0298D Kiev IZVESTIYA VYSSHIKH UCHEBNYKH ZAVEDENIY: RADIOELEKTRONIKA in Russian Vol 33 No 5, May 90 pp 24-28

[Article by A.S. Gurevich and G.S. Nakhmanson]

[Abstract] An acoustooptic correlator with time integration is described and its performance as discriminator of discretely encoded signals is analyzed, its capability of processing in real time extending to signals with a base of 10^6-10^8 in a wide frequency range. It includes an ultrasonic light modulator in which coherent light coming from a semiconductor laser through a collimator is modulated by discrete acoustic signals coming from an encoder mixed with interference. This modulator output signals pass through a pair of integrating lenses with different focal lengths and with a spatial filter between them in the Fourier transformation plane to an optoelectronic system which consists of an integrating photodetector array in the recording plane and a resolver. For the purpose of analysis, the modulator is assumed to receive an array of signals with a different code sequence of phase or frequency shift each and to receive light of a certain wavelength from a point source. This light is modulated by a reference signal identical to the phase-shift or discretely frequency-shift keyed input signal so that its intensity will vary correspondingly about some constant positive level without ever dropping to zero. The modulator operates typically in the Bragg diffraction mode with the light incident at the angle $_B = \sin^{-1}\lambda/2\Lambda$ (λ- wavelength of light, Λ- wavelength of sound corresponding to the center frequency of the modulator passband) and its intensity then I(t) varying in time. After transformation by the lenses and 90° phase shift in the spatial filter, its intensity distribution in the photodetector plane will be I(x,t) = I(t)[1+] WX(t- x/V-τ[<s]up2 (V- velocity of acoustic wave in modulator aperture, $W = 2\pi J\Delta n_{max}/\lambda$ denoting the phase modulation index, J- length of acoustooptic interaction space, n- mean refractive index of modulator medium, Δn_{max}- amplitude of index fluctuation during passage of acoustic signal of unit power, x- space coordinate, t- time, τ- time delay from incidence of light to reception of acoustic signal). Assuming that the modulator receives an additive mixture of encoded signals plus a stationary interference with zero mean and $<(t_1)n(t_2)> = B(t_1 - t_2)$ correlation function, two correlator performance characteristics are calculated for the typical case of a small phase modulation index $W << 1$. One of these characteristics is the output signal-to-noise ratio, normalized to the input signal-to-interference ratio, as a function of distance (number of photodetector element) from the photodetector element which puts out the strongest

signal, under conditions of matched reception with either complete or partial coincidence of code elements in the received signal pulse sequences and code elements in the reference pulse sequences. The other characteristic is the probability of correct signal discrimination and its dependence on the input signal-to-interference ratio. Figures 3; references 5.

UDC 621.376.3

Effect of Quantization of Reference Signal on Efficiency of Digital Correlator Processing Discretely Frequency-Shift Keyed Compound Signals

907K0298E Kiev IZVESTIYA VYSSHIKH UCHEBNYKH ZAVEDENIY: RADIOELEKTRONIKA in Russian Vol 33 No 5, May 90 pp 32-36

[Article by Yu.V. Vetrov, K.V. Fedorov, and I.A. Tsikin]

[Abstract] The feasibility of increasing the speed of a digital correlator processing compound signals by decreasing the number of multiplications is considered, one possible way being quantization of the reference signal into few levels. This is demonstrated specifically on a correlator of discretely frequency-shift keyed signals, assuming that the signal appears with together with an additive stationary noise and taking into account the systematic quantization error. The process discretization step must be selected so as to exclude any multiple of any frequency in the frequency-time grid. The instantaneous phase φ_i of any incoming signal S in the [begin set]$S^{(q)}$,$S^{(q-1)}$[end set] set replaced by a constant value C_q (q = 1,2,...,Q) of the reference signal at level q is then uniformly distributed over the range corresponding to each quantization step q, the probability of it falling within that range being $P_q = 2\Delta\varphi^{(q)}/2\pi$ ($\Delta\varphi^{(q)} = \varphi^{(q)} - \varphi^{(q-1)}$). The efficiency of such a correlator in terms of the output signal-to-noise ratio, depends on the Q values C_q of the quantized reference signal and is lower than that of such a correlator without quantization of the reference signal, but can be maximized by optimum quantization of the reference signal. Its optimum values C_q found by differentiation of the output signal-to-noise ratio with respect to each and found to differ minimally from the true values of the reference signal. The limits of the phase ranges $\varphi^{(q-1)}$,$\varphi^{(q)}$ must then also be optimized. Two suboptimum but simple modes of quantization of the reference signal are considered, uniform amplitude quantization into Q levels and uniform phase quantization into 2Q levels, a numerical analysis indicating an only very small penalty in correlator efficiency in both cases. Figures 1; references 4.

UDC 621.396:681.7.069.32

Multichannel Timing Search of Pulse Signals by One-Electron Photodetectors

907K0298F Kiev IZVESTIYA VYSSHIKH UCHEBNYKH ZAVEDENIY: RADIOELEKTRONIKA in Russian Vol 33 No 5, May 90 pp 36-41

[Article by K.Ye. Rumyantsev]

[Abstract] Timing the arrival of a light pulse during its search in both space and time by means of a one-electron photodetector is considered, such a photodetector recording separately each photoelectron which has departed from its cathode and emitting a sequence of one-electron pulses during the scan of a space element. The flux of such pulses is passed through an amplitude discriminator with an optimum discrimination threshold for dark current pulses. The timing of the pulse arrival is based on the receiver knowing the repetition period of incident light signals and recording during the first period up to first N discrimination events, which are then analyzed during the second pulse repetition period. When no discrimination event takes place during the first period, then no signal is assumed to have arrived and the search proceeds with scanning the next space element. Improvement of this signal timing method by addition of a second signal processing channel is evaluated, assuming that every one-electron pulse triggers the threshold device and ignoring dark current pulses. A probability analysis based on a Poisson flux of one-electron pulses representing background radiation reveals that tolerance of two spurious discrimination events raises the false-alarm probability. Lowering the latter requires light pulses of shorter duration from the transmitter, the difference and the thus incurred penalty not being very large, while addition of a second channel eases appreciably the transmitter requirements by allowing its pulse repetition rate (which must not be lower than the repetition rate of background radiation pulses) and thus also the average power to be lowered to one fifth. The advantage continues to increase upon addition of a third and more signal processing channels, a larger number of channels ensuring the same probability of correct light pulse detection in the presence of a larger number of background radiation pulses. A numerical analysis of searching a source of 0.53 μ light submerged in background radiation of 10^{-5} μW intensity corresponding to a photoelectron count of 2.65×10^6/s indicates that a 0.9 probability of correct detection is possible with an at least 0.9405 probability of a light pulse arriving and an at least 0.9516 probability of a background pulse arriving, 3.5 being the average required number of photoelectrons per light pulse. Figures 2; references 3.

UDC 621.3.049.77

Speed of Superhigh-Speed Very-Large-Scale Integrated Silicon Devices at Low Temperatures

907K0298G Kiev IZVESTIYA VYSSHIKH UCHEBNYKH ZAVEDENIY: RADIOELEKTRONIKA in Russian Vol 33 No 5, May 90 pp 49-54

[Article by A.N. Bubennikov]

[Abstract] The problem of increasing the speed of superhigh-speed very-large-scale integrated silicon devices such as bipolar transistors in nonsaturating logic elements as the ambient temperature drops from 300 K to 77.3 K is considered, their reliability increasing as

thermal mechanisms of processes which cause their degradation become weaker. One fundamental way is to minimize the logic swing without loss of interference immunity margin. The requirements are demonstrated on emitter-coupled logic consisting of current switches and emitter followers. Paraphase control, which suppresses cophasal interference, combined with use of diodes as the load on switches can lower the logic swing to 10 mV at 77.3 K while ensuring high absolute and relative interference immunity. This is technologically achieved by minimization of the product $\varepsilon\rho$ (ε- dielectric permittivity of SiO_2 substrate, ρ- electrical resistivity of metal or metallized interconnections), as the degree of integration characterized by the ratio A_{chip}/h^2 (A_{chip} - chip area, h - lithographic dimension) is being raised. The most appropriate both physical and technological criterion of performance optimization with respect to maximum speed is minimum total time delay, which is best achieved by use of two-step output voltage switches on bipolar transistors of one type or better yet on complementary bipolar transistors drawing minimal power and ensuring minimal output resistance. It is accordingly necessary to minimize the emitter-collector time delay, which depends on the impurity distribution in the active region of a bipolar transistor as well as on the critical time constant equal to the surface resistance of the active base region times the capacitance of the collector junction. Segmentation of interconnections will, moreover, minimize sluggishness of signal transmission from one logic element to another. The second criterion of performance optimization is maximum current transfer ratio β, its smallness at low temperatures being principally due to a narrower forbidden band in the emitter region of heavily doped bipolar transistors but also due to "freezing in" of charge carriers and to recombination in the p-n junction, so that its temperature dependence needs to be weakened. Various high-quality bipolar transistors have been successfully developed, among them heavily doped polysilicon transistors and silicon heterojunction transistors with amorphous or microcrystalline emitter and an almost temperature-independent beta, so that production of superhigh-speed very-large-scale integrated logic for cryogenic apparatus is becoming feasible. Figures 3; references 7.

UDC 621.396.677.499:621.391.825

Raising Efficiency of Pulse Interference Suppression in Adaptive Antenna Arrays

907K0298H Kiev IZVESTIYA VYSSHIKH UCHEBNYKH ZAVEDENIY: RADIOELEKTRONIKA in Russian Vol 33 No 5, May 90 pp 55-56

[Article by Ye.I. Glushankov and N.A. Gusev]

[Abstract] Improving the immunity of adaptive antenna arrays to pulse interference is examined, considering also simultaneous suppression of parasitic amplitude modulation of the useful signal. The basic methods of achieving this involve imposition of constraints on the major lobe of the radiation pattern in the time domain and in the frequency domain as well as in the space domain. The principle is demonstrated on compensation of pulse interference by means of spatial filters preceding the adaptive signal processor. Such a filter is formed by a transformation matrix which converts pulse interference into a continuous one and thus prevents undersuppression or even nonsuppression of interference, namely nonsuppression of a pulse which follows a suppressed one after a time interval longer than the antenna adaptation time, while the adaptive processor is preferably based on a single-duty algorithm. The effectiveness of this arrangement is indicated by the difference between the rising signal-to-interference+noise ratio and the constant one at the output of an antenna with and without a transformation matrix respectively. Figures 4; references 1.

UDC 621.315.51.61:537.868.4

Statistical Synthesis of Multilayer Material Transparent to Radio Waves

907K0298I Kiev IZVESTIYA VYSSHIKH UCHEBNYKH ZAVEDENIY: RADIOELEKTRONIKA in Russian Vol 33 No 5, May 90 pp 68-70

[Article by P.P. Skurskiy]

[Abstract] A statistical method is proposed for synthesis of a multilayer material transparent to radio waves. It is based on the premise that M blanks of each layer are available and M different materials can be made of them. The three characteristic parameters of each layer (dielectric permittivity, loss tangent, thickness) vary, owing to imprecision of the technological process, and are treated as random variables with given probability distributions and with a known subset of their permissible values. The performance characteristics of each material, also random variables, depend not only on those characteristics of its layers but also on the wavelength of the electromagnetic radiation in vacuum and on its angle of incidence. A common radio engineering problem, namely synthesis of a material for a given power transmission coefficient within a given tolerance range, is solved on the basis of this statistical model. The subset of known permissible parameter values is replaced with its discrete analog in the x_i,x_j plane parameter values pertaining to i-th layer and its j-th blank. The problem is then solved by the Monte Carlo method, as demonstrated on synthesis of a 7-layer compensator material for a power transmission coefficient not smaller than 0.96 to electromagnetic waves within a $\lambda_{max}:\lambda_{min}$ = 1.2 band linearly polarized in a perpendicular plane and incident at angles within the 0-45° sector. Calculations have been programmed for a BESM-6 high-speed computer. Figures 2; tables 1; references 2.

UDC 621.371.3.01

Distribution of Fluctuations of Spherical Waves in Far Field Behind Chaotically Behaving Planar Shield

907K0161A Moscow RADIOTEKHNIKA I ELEKTRONIKA in Russian Vol 35 No 1, Jan 90 pp 12-20

[Article by S.M. Golynskiy]

[Abstract] Scattering of spherical waves by a chaotically behaving planar shield is analyzed in a plane behind the latter and parallel to it, this problem serving as a model for radiometric sounding of the ionosphere either from a spacecraft above the latter or from the surface of Earth. First is considered a spherical monochromatic wave diverging from a point source and passing through such a shield which modulates it randomly in space so as to cause fluctuations of the wave behind it. The modulation pattern is determined by the transmittance of the shield, a function whose modulus and argument (coordinates in any plane of observation to the shield) characterize amplitude and phase modulation respectively. This function is assumed to have a statistically uniform distribution, namely a constant mean value equal to its modulus immediately behind the shield and zero mean fluctuations. Its fluctuation component is assumed to have cumulants and the latter, of any order, to be absolutely integrable. The asymptotic distribution of fluctuations of a diverging wave sufficiently far behind such a phase shield is found to be an approximately elliptical-normal one when the phase fluctuations of the shield are very small and the effective wave parameter is larger than 1 or a spherical-normal one when the phase fluctuations of the shield are very large and the effective wave parameter is much larger than 2. The asymptotic distribution of fluctuations of a converging spherical wave which passes through such a phase shield is found to approach a normal one from the shield to the focal point and then, as the wave again diverges, to become denormalized with increasing distance beyond that point. The author thanks V.D. Gusev for attentiveness and helpful comments. Figures 2; references 15.

UDC 523.42-852:621.396.96

Refraction of Radio Waves Sounding Polar Atmosphere of Venus

907K0161B Moscow RADIOTEKHNIKA I ELEKTRONIKA in Russian Vol 35 No 1, Jan 90 pp 21-29

[Article by O.I. Yakovlev, V.N. Gubenko, and S.S. Matyugov]

[Abstract] Refraction of radio waves in the atmosphere above both northern and southern polar regions of Venus is analyzed on the basis of data obtained from "Jupiter-Venus" and "Venus-15,16" space probes, the refraction pattern being characterized by the altitudinal profiles of the angle of refraction angle, of the referred refractive index, and of the refractive attenuation. The index profile appears to follow a power law with a corresponding monotonic signal attenuation below 59 km, a zone with a uniform mean vertical temperature gradient, and to become an exponential one above 59 km up to 87 km. The angle profiles above the two polar regions are found not to differ, except within the narrow 58-60 km tropopause zone most likely owing to a different variability of the atmosphere The data are compared with those on the equatorial region and little difference is found except within that tropopause zone. The evaluation of relevant data includes altitudinal profiles of the electric field of decimetric (32 cm) radio waves, these profiles being consistent with the other results.

UDC 621.396.96:781.3

Estimating Power of Optical Probing Signal in Turbid Medium

907K0161C Moscow RADIOTEKHNIKA I ELEKTRONIKA in Russian Vol 35 No 1, Jan 90 pp 34-38

[Article by E.V. Pikkel, V.D. Samoylov, and M.S. Chukin]

[Abstract] The power of an optical probing echo signal returning to the receiver after passage through a turbid and, therefore, scattering medium is calculated by an analytical method based on the integrodifferential equation of radiation transfer in the low-angle approximation. This power is expressed in terms of effective beam and field-of-vision radii, effective beam divergence angle, effective radii of transmitter and receiver apertures, and radius of the reflecting inhomogeneity. The expression simplifies when the inhomogeneity is smaller than the transmitter aperture and the latter is smaller than or equal to the receiver aperture. The reflection coefficient, which depends on the displacement of the inhomogeneity relative to the probing beam, is approximated as an exponential function of that displacement in a two-dimensional Cartesian system of coordinates. References 7.

UDC 621.391.01

Superresolution Limit for Reconstruction of Signals

907K0161D Moscow RADIOTEKHNIKA I ELEKTRONIKA in Russian Vol 35 No 1, Jan 90 pp 68-87

[Article by Ye.L. Kosarev]

[Abstract] The existence of an absolute superresolution limit for reconstruction of signals which exceeds both the Rayleigh limit and the diffraction limit is established on the basis of Shannon's theorem, without restricting the

signal spectrum to a finite one or the problem to a parametric one. The problem of signal reconstruction is then solved by the maximum likelihood method and an improved version of the M.Z. Tarasko procedure for iterations in the direction close to the gradient of the logarithmic likelihood function, assuming a binomial or Poisson distribution of the readings at each individual point and a polynomial distribution of all values. The dependence of the superresolution limit on the signal-to-noise ratio has been determined on the basis of numerical experiments for either two or three narrow lines with Gaussian profiles and four different kinds of kernel K(x,y) appearing in the linear integral equation of the first kind and representing the instrument characteristic:

$$K(\tau) = e^{-\tau^2}$$

$$K(\tau) = 1/(1 + \tau^2)$$

$$K(\tau) = \sin\tau/\tau$$

$$K(\tau) = (\sin\tau/\tau)^2$$

$$\tau = (x - y)/D$$

This method of signal reconstruction is further considered for processing readings of nuclear magnetic resonance in heavy-fermion superconductors such as UBe_{13}. In conclusion, superresolution is evaluated from the standpoint of the uncertainty principle. The author thanks L.A. Vaynshteyn (deceased) and K.Sh. Zigangirov for interest and critical comments, Ye.R. Podolyak and V.I. Gelfgat for assistance in running the signal reconstruction programs on a computer. Figures 9; references 40.

UDC 537.533.3

Spatial and Time-of-Flight Focusing in Electrostatic Lens With Two Planes of Symmetry

907K0161E Moscow RADIOTEKHNIKA I ELEKTRONIKA in Russian Vol 35 No 1, Jan 90 pp 125-133

[Article by S.B. Bimurzayev and Ye.M. Yakushev]

[Abstract] Characteristics of electrostatic lenses with two planes of symmetry used for focusing transient fluxes of charged particles in instruments like time-of-flight mass spectrometers is analyzed, considering that the performance of these instruments will be influenced by time-of- flight aberrations and spatial aberrations in such a lens. Flight calculations are made for an electron moving from an initial plane z = a to an arbitrary other plane z = b in a system of rectangular coordinates x_1,x_2,z where the z-axis is collinear with the axis of symmetry of the electrostatic field and planes x_1z, x_2z are its planes of symmetry. Its time of flight in such a system is calculated as the sum of its time of flight along the z-axis plus two terms of a power series representing up to N-th order integral chromatic aberration, two terms of a power series representing second-order geometrical aberration, and a two terms of a power series representing third-order mixed aberration. These calculations are based on the equations of projections of paraxial trajectories in an electrostatic field with a quadrupole component and yield the coefficients characterizing those various modes of time-of-flight aberration. References 5.

UDC 535.853.22:534.29

Collinear Acoustooptical Diffraction in Two Crystals

907K0161F Moscow RADIOTEKHNIKA I ELEKTRONIKA in Russian Vol 35 No 1, Jan 90 pp 175-178

[Article by V.G. Zakharov and V.N. Parygin]

[Abstract] Replacement of a single "long" crystal with two "short" ones for acoustooptic interaction in devices such as an acoustooptic filter is considered, operation of these devices being based on the phenomenon of collinear acoustooptical diffraction in an anisotropic medium. Here light passes from one crystal to the next while the acoustic wave in the second crystal originates from an independent second piezoelectric transducer, both transducers being excited by a common oscillator but a phase shifter being placed between the oscillator and the second transducer so that an additional phase shift can be imparted to the signal entering the second crystal and thus control the efficiency of conversion. The resultant divergence of sound is smaller, moreover, inasmuch as the second crystal appears as a "new" source. The performance of such a device is analyzed theoretically on the basis of a system of two short equations describing collinear diffraction of light waves by a Gaussian sound beam. The solution for one crystal, which is then replaced replaced with one of double length and with two short ones, yields for each case the dependence of the intensity of diffracted light on the product of distance traveled and light-sound synchronization index, and in the case of two crystals on the additional phase shift, also the dependence of the acoustooptic interaction pattern on the sound divergence index. A comparison of their performance on this basis under otherwise identical conditions with optimum phase matching in each indicates less blurring but a higher lateral peak with two crystals than with one crystal of double length, both schemes being almost equivalent in terms of filter bandwidth. Figures 4; references 5.

UDC 621.383.82

One-Electron Pulse and Pulse Response Characteristic of Real Photomultipliers

907K0161G Moscow RADIOTEKHNIKA I ELEKTRONIKA in Russian Vol 30 No 1, Jan 90 pp 179-181

[Article by N.B. Glukhovskaya and G.D. Petrukhin]

[Abstract] The two principal performance characteristics of real photomultipliers with some degree of nonhomo-

geneity, namely the shape of a one-electron pulse and of the transient response, are calculated for the basic scheme with at least two additional interelectrode gaps having different time constants than those of the regular dynode-dynode and dynode-anode gaps. The calculations are based on refinement of Shubnikov's and involve two convolutions, a three-dimensional one and a four-dimensional one, of exponential time-of-flight distribution functions characterizing passage of electrons through individual photomultiplier stages. The pulse current and the response current as functions of time have been calculated numerically according to this theoretical model for FEU-115 photomultiplier consisting of three nonhomogeneous stages in cascade under 112 V with an anode sensitivity of 10 A/lm. For an experimental validation of this model, both rise time of the response current and duration of the transient were measured in accordance with the applicable Standard procedure. The agreement is found to be typically within 7 percent. Figures 2; references 2.

UDC 621.317.794

Noise in High-Speed Superconducting Bolometers

907K0161H Moscow RADIOTEKHNIKA I ELEKTRONIKA in Russian Vol 35 No 1, Jan 90 pp 182-191

[Article by A.D. Tkachenko and I.A. Khrebtov]

[Abstract] A series of high-speed superconducting bolometers has been built on a cylindrical aluminum substrates, 8 mm in diameter and 5 mm long, for an evaluation of their noise characteristics. Anodization of their surfaces produced 5-70 μm thick Al_2O_3 insulation layers on which were vacuum-deposited 30-100 nm thick Sn or Sn + Pb superconducting sensor films (critical temperature approximately 3.7 K and 4.2 K respectively) with an electrical surface resistance in the normal state varying over the 0.2-200 Ω/square range. The high-resistance sensors were produced by first vacuum-depositing an approximately 1 nm thick Au interlayer. For comparison, some bolometers were built without the insulation layer. The bolometers were placed inside a helium cryostat, with a copper block mounted to the bottom of the helium reservoir through a teflon gasket filtering out temperature fluctuations in boiling helium. Measurements covering the spectral range from 1 Hz to 100 kHz have yielded the dependence of the noise voltage and the volts-per-watt sensitivity on the bias current, on the temperature, and on the base resistance. For analysis and evaluation of the results, the low-resistance bolometers are considered and here 1/f- noise is identified as the principal component most likely attributable to a thermal mechanism. The high-resistance bolometers are considered next and here, too, 1/f-noise is identified as the principal component but attributable to a magnetic mechanism, the accompanying residual component being more likely associated with the resistive state during superconducting transition rather than with thermal flicker which should have been suppressed by the Au interlayer. Measurements have also yielded the threshold power flux ($W/Hz^{-1/2}$. According to these experimental data, which confirm the results of theoretical calculations, the lowest noise level is found in Sn + Au bolometers with an electrical surface resistance corresponding to an approximately 0.5 and thus nearly maximum absorption coefficient. Figures 5; tables 1; references 21.

UDC 537.874.6.01

Diffraction of Surface Waves on Dielectric Plate by Metal Cylinder

907K0227A Moscow RADIOTEKHNIKA I ELEKTRONIKA in Russian Vol 35 No 2, Feb 90 pp 241-251

[Article by V.I. Kalinichev and N.M. Solovyev]

[Abstract] Diffraction of surface waves traveling along a dielectric plate by a closed circular cylinder above the plate and parallel to it is analyzed for dependence of the phase shift and the dissipated power on the geometrical parameters of the structure. The problem is reduced to successive reflections of waves by the cylinder and the plate, assuming that the steady-state amplitude and phase distribution of these waves satisfies the condition of a self-consistent field. The resultant field, sum of the incident one and the scattered one, satisfies not only the Helmholtz equation everywhere outside the cylinder but also the condition of zero tangential components of the E-vector at the cylinder contour surface, and the condition of continuity of the tangential components of both E and H vectors at the dielectric-vacuum (free space) boundary. The integral equation of the second kind for the spectral density, which characterizes the amplitude and phase distribution of plane electromagnetic waves over the spectrum of a cylindrical source is formulated and then solved analytically for an E_1-wave and for an H_1-wave. The spectral density depends in the first case on both longitudinal and normal components of the volume current density and in the second case on its sole transverse component. With asymptotic convergence of the free term established, each integral equation is reduced to an infinite system of linear algebraic equations for the respective reflection and transmission coefficients as elements of the scattering matrix. The solution to each, existing and unique in the Hilbert l_2-space, is obtained by the method of reduction with an a' priori given accuracy. The power radiation pattern is calculated by the method of steepest descent. Numerical solutions have been obtained for a plate material with a relative dielectric permittivity of 10, an ideally conducting cylinder, and $d_0/a = 0.5$ (d_0- minimum gap width, 2a- plate thickness), letting $ka = 0.455$ for an E_1 wave with a 1.4 phase lag coefficient and $ka = 0.313$ for an H_1 wave with a 2.2 phase lag coefficient ($k = \omega c$, ω-radian frequency of wave, c- speed of light). Figures 5; references 8.

UDC 537.874.6.01

Comparative Accuracy Evaluation of Numerical and Asymptotic Solutions to Problem of Diffraction of Plane Electromagnetic Wave by Periodic Surface of Ideal Conductor

907K0227B Moscow RADIOTEKHNIKA I ELEKTRONIKA in Russian Vol 35 No 2, Feb 90 pp 258-266

[Article by V.A. Korneyev, A.G. Mikheyev, Ye.Yu. Rabotnova, and A.S. Shamayev]

[Abstract] The two-dimensional Helmholtz equation for the problem of diffraction of an obliquely incident plane E-polarized or H-polarized electromagnetic wave by a periodically irregular surface (period b = 2π) of an infinitely long ideally conducting cylinder, with the plane of incidence normal to the axis of the cylinder, has been solved asymptotically in the Kirchhoff approximation and with the third expansion term added as well as numerically by the Krylov-Bogolyubov method after reduction to an integral equation of the second kind for the longitudinal field components and then to a system of algebraic equations for the constant coefficients of the characteristic functions. Both solutions have yielded the amplitudes and the phases of the complex surface currents J_E,J_H and the amplitudes of reflected waves as functions of the normal coordinate, of the angle of incidence, and of the wave number, also the backscattering coefficient at low resonance frequencies as a function of the surface rise and of the angle of incidence. The more nearly exact numerical solution was obtained for both Dirichlet and Neumann boundary conditions with wave numbers ranging from 1.5 to 7.5 and with an "energy defect" not larger than 10^{-3}. An analysis of the results indicates that refinement of Kirchhoff's asymptotic by addition of the third expansion term has not improved its accuracy. Figures 5. references 6.

UDC 621.372.85

Characteristics of Radiator Consisting of Flanged Waveguide and Metal Strip

907K0227C Moscow RADIOTEKHNIKA I ELEKTRONIKA in Russian Vol 35 No 2, Feb 90 pp 275-280

[Article by I.K. Kuzmichev and D.G. Seleznev]

[Abstract] An adjustable millimetric-wave radiator consisting of a flanged plane waveguide and a metal strip is designed by scaling down its centimetric-wave prototype and subsequent refinement to ensure adequate wideband matching to the feeder. As a specific configuration is considered one with the metal strip narrower than and symmetrically parallel to the flange at the exit end of the waveguide, the distance between them being much smaller than the radiation wavelength λ. Two coefficients representing the fractions of excitation energy transmitted beyond the strip and reflected back into the waveguide are calculated for a narrow waveguide from the solution to a system of linear algebraic equations of the second kind for the coefficients of a series expansion, in basis functions, of the field at the mirror surface of a resonator cavity. They are calculated as functions of the distance between flange and strip over the 0-0.06 range of the distance-to-wavelength ratio, for strips whose width equals one half- wavelength and successive odd multiples thereof. The results indicate that the coupling between radiator and ambient space can be regulated by means of a strip of a certain width, namely by varying the distance of this strip from the waveguide flange, resonance on the plunger wave occurring with the strip at some distance from the flange. As the width of the strip is increased, this critical distance becomes smaller and so becomes the amplitude of the resonance. The optimum distance corresponding to maximum transmission of energy, almost all, into the ambient space has been established experimentally and found to be equal to the width of the waveguide (behind the flange) plus 0.04λ ([g–] radiation wavelength). The radiation pattern is also calculated accordingly. The experiment was performed with a waveguide including a smooth reducing transition from its 3.6x1.8 mm^2 segment to its 3.6x0.12 mm^2 segment. The radiator was excited with waves within the 4 mm band modulated at a frequency of 1 kHz. In addition to the radiation pattern was also measured the VSWR, the latter depending on the ratio of the oscillator frequency to the frequency which corresponds to the minimum absolute value of the equivalent reflection coefficient. Adequate matching over the 0.85-1.1 range of this ratio, based on the VSWR = 1.4 criterion, was found to be attainable with such a radiator. Figures 5; references 4.

UDC 621.39.677.49

Optimum Adaptive Antenna Arrays for Communication and Navigation Systems

907K0227D Moscow RADIOTEKHNIKA I ELEKTRONIKA in Russian Vol 35 No 2, Feb 90 pp 335-340

[Article by Yu.I. Choni]

[Abstract] Two new alternative criteria are proposed for optimization of Applebaum adaptive antenna arrays, the conventional one being maximum generalized signal-to-(interference+noise) ratio or in equivalent terms a final steady-state weight vector w_∞ which will minimize the functional $\Phi_1(w) = P_i + \gamma[w-] w_O[<]sup2 (P_i$- effective power of interference signals including internal noise at the antenna output, w_0- initial weight vector, γ-scale factor). The first of these criteria is minimizing the functional $\Phi_2(w) = P_i + \gamma F_O[<]sup2$ (F- instantaneous radiation pattern, F_0- initial radiation pattern). The second of these criteria is minimizing the functional $\Phi_3(w)= P_i+ \gamma[(]]F[-][F<]inf0[)]]^2$. The results of numerical calculations based on each of these criteria indicate that, with orthogonal radiation patterns of individual array elements, design according to the first new

criterion yields the same optimum vector as well as the same functional and the same array structure as design according to the conventional criterion, while design according to the second new criterion yields a different optimum weight vector even when the radiation patterns of individual array elements are orthogonal. Figures 3; references 13.

UDC 621.391.01

Efficiency of Radio Signal Quantization

907K0227E Moscow RADIOTEKHNIKA I ELEKTRONIKA in Russian Vol 35 No 2, Feb 90 pp 349-357

[Article by I.A. Golyanitskiy]

[Abstract] Multidigital binary quantization of radio signal mixtures is analyzed and evaluated, taking into account nonlinearity of quantizers and unavoidable ambiguity of signal or interference extraction from their mixture. The classical quantization criterion is applied to three additive mixtures of a radio signal and a radio interference with amplitude and phase modulation each. In the first mixture the interference-to-signal amplitude ratio is much smaller than 1 and the signal-to-interference power ratio correspondingly much larger than 1. In the second mixture both ratios are equal to 1. In the third mixture the interference-to-signal amplitude ratio is much larger than 1 and the signal-to-interference power ratio correspondingly much smaller than 1. Binary quantization of a strong signal (first mixture) is shown to result in a large decrease of the signal-to-interference ratio, inasmuch the power of the quantized signal is almost equal to the dispersion of the quantization error, while binary quantization of a weak signal (third mixture) is shown to result in a large increase of the signal-to-interference ratio. Binary quantization is analyzed again upon introduction of quantization noise, namely the difference between quantized signal+interference mixture and quantized signal, as a new criterion of quantization efficiency pertaining to radio signals much stronger than, much weaker than, and equal to radio interference. Next is considered M-level quantization, specifically 3-level quantization, taking into account that nonstationarity of a signal+interference mixture makes the result of quantization dependent on the instant of time and on the utilized segment of the quantizer amplitude characteristic. As an example of a 3-level quantizer is considered a limiter with a 2c wide insensitivity zone $z(y) = 0$ between $z(y) = d$ when input $y > +c$ and $z(y) = -d$ when input $y < -c$, an asymptotically linear multidigital (r digits) one with $z(y) = -z(-y)$ and $z(t) = A\cos\Phi$ output as a function of time t for $M = 2^{r-1}$ quantization levels. Its efficiency is evaluated according to another new criterion, namely the relative error $\delta = 1 - \sigma_y^2/\sigma_z^2$ of estimating the dispersion σ_z^2 of its output process by letting σ_z^2 be proportional to $(1 + M/4)^2$ (when r is finite up to 10) and the dispersion of the input process σ_y^2 be equal to $< A^2(t) >$. References 8.

UDC 621.391.01

Adaptive Robust Detection of Signals

907K0227F Moscow RADIOTEKHNIKA I ELEKTRONIKA in Russian Vol 35 No 2, Feb 90 pp 363-371

[Article by Yu.G. Sosulin and S.L. Salikov]

[Abstract] Synthesis of adaptive robust detectors by modification of plain robust ones is outlined, plain robust detectors based on Huber M- estimates being synthesized for operation under conditions where the probability density distribution of noise is known within a given accuracy class P(b,q) (q = integral from -b to +b over p(x)dx, p(x) is symmetric and continuous on the interval [-a,a] of the probability density distribution). An adaptive robust detector is synthesized specifically for deterministic signals, the procedure being analogous for such a detector of a quasi- deterministic signals with random initial phase as well as for such a detector of a coherent or noncoherent pulse sequences. In accordance with the algorithm of estimating parameter b for any fixed q, the problem is to select q so to minimize the error of that estimate. Optimum values of q have been obtained for four kinds of noise: with Weibull, Laplace, normal, and log normal probability density distributions respectively. The performance characteristics of this adaptive robust detector of deterministic signals, namely both correct-detection and false-alarm probabilities as well as the detection threshold appropriately modified so as to ensure stabilization of the false-alarm probability, are described analytically and then evaluated numerically on the basis of statistical simulation for given values of parameters b (1.28) and q (0.8), given size n of the adapting sample, and given size N of the reading sequence (n = N = 30, 50, 100). A comparison of these performance characteristics with those of a nonadaptive robust M-detector indicates that an adaptive one will adequately stabilize the false-alarm probability with a small n-sample already. Figures 2; references 5.

UDC 621.382.323.01

Computer Modeling of High-Speed Pulse Shapers on GaAs Field-Effect Power Transistors

907K0227G Moscow RADIOTEKHNIKA I ELEKTRONIKA in Russian Vol 35 No 2, Feb 90 pp 406-410

[Abstract] A complete large-signal equivalent circuit diagram of a subnanosecond (1-5 GHz) pulse shaping switch on a GaAs field-effect power transistor is constructed, to facilitate modeling of such a device on a Standard 1022 computer for design and performance analysis according to the universal NAP-2 program. The circuit includes not only external reactances but also internal transistor reactances, namely the nonlinearly voltage- dependent Schottky-barrier and transfer capacitances. Calculations on the basis of this model have yielded the pulseform of both the load voltage and the

gate voltage as well as the dependence of the drain switching time and of the shaper output switching time on both the load resistance and the gate resistance, also the dependence of the load current amplitude on the load resistance. The model was applied to five series AP602, two series AP603, one series AP610, one series AP910, and two series AP915 transistors produced in the USSR. On the basis of these data, which agree closely with experimental ones, can be estimated the limiting values of pulse parameters to serve as reference for the design such pulse shapers. Figures 5; tables 2; references 6.

UDC 621.372.852

Tunable Quasi-Optical Cell for 2-mm Wave Band

907K0227H Moscow RADIOTEKHNIKA I ELEKTRONIKA in Russian Vol 35 No 2, Feb 90 pp 415-420

[Article by A.A. Vertiy, S.P. Gavrilov, and V.N. Derkach]

[Abstract] A quasi-optical absorption cell for the 2-mm wave band has been designed and tested, a planar cell which consists of a layer of an absorbing medium between a metal mirror and a tunable reflector. The latter is formed by a multilayer stack of four identical metal wire gratings and correspondingly three equally wide adjustable-width gaps in free space. Each grating consists of six identical wires (straight cylinders) and is split into two wings of three symmetrically about the common axis. The period of all four gratings is the same and adjustable without limit. This cell can, in effect, be regarded as a plane-parallel Fabry-Perot interferometer operating in the reflection mode. Its optical characteristics of this cell, namely its reflection and transmission coefficients for a normally incident wave, are evaluated by treating it as a half-space containing a paramagnetic medium with a complex refractive index $\tilde{N}_s = n_s - jk_s'$ where $n_s = k_s' = 1000$ and by treatment of each grating as a layer of thickness equal to the wire diameter with complex reflection and transmission coefficients. Calculations were made for a cell with a nominal gap width d between gratings approximately equal to 3λ and a gap width regulation of about $\lambda/4$. (λ- wavelength of normally incident radiation). These calculations, made by the matrix method with the imaginary part k of the refractive index of the gratings varied over the 0-0.006 range, have yielded the dependence of its optical reflection and transmission coefficients on the dimensionless gap width change $\Delta d/\lambda$ for the various values of k. The cell was tested for the dependence of its electrodynamical properties, namely power reflection and transmission coefficients for E-polarized 2.17-2.27 mm electromagnetic waves on the gap width change $\Delta d/\lambda$, with k also varied over the 0-0.006 range. The results reveal two critical modes: first a resonance mode corresponding to $\Delta d/\lambda$ about 0.04 with the reflection coefficient dipping from 1.0 to a moderate minimum (0.6 when k= 0.006) and the intensity of the magnetic field component in the 20 mm thick absorbing layer rising from zero to a maximum (high sharp peak when k = 0), then a matched mode corresponding to $\Delta d/\lambda$ about 0.26 with the reflection coefficient dipping from 1.0 to a deep minimum (down to zero when k = 0.006) and the intensity of the magnetic field in the absorbing layer rising from zero to a high maximum (highest when k = 0. The cell was also used for experimental study of magnetic resonance at a frequency of the incident electromagnetic wave equal to the Larmor frequency in the resonance mode and in the matched mode, the reflection coefficient of of the paramagnetic absorbing layer also dipping to a deep minimum at that frequency. Figures 4; references 5.

UDC 537.874.4.01

Development of Numerical Method for Solution of Three-Dimensional Vector Problems of Scattering

907K0227I Moscow RADIOTEKHNIKA I ELEKTRONIKA in Russian Vol 35 No 2, Feb 90 pp 438-441

[Article by A.G. Dmitrenko and A.I. Mukomolov]

[Abstract] A modification of the method of auxiliary electromagnetic field sources is proposed for solution of three-dimensional vector problems of scattering, namely selecting an auxiliary surface inside the scatterer body which is similar to its outer surface and representing the scattered field as the sum of the fields of electric dipoles on that auxiliary surface tangential to it. The unknown dipole moments are then determined from a system of linear algebraic equation $Bp = f$ with a 2M x 2N-dimensional matrix B, the boundary conditions being approximated discretely with the number of points M larger than the number of auxiliary dipoles N. A numerical pseudosolution to that system of equations is then obtained iteratively by any applicable method such as solving the system of normal equations $B^*Bp = B^*f$, expansion of that matrix B into a product $U\Sigma V$ product of two unitary matrices U,V and a diagonal one Σ containing its singular values ($p = V^*\Sigma^+U^*f$), or minimization of the functional $\Phi = \|Bp - f\|^2$ (norm squared of the error of that system of linear algebraic equations). As a practical example is considered scattering of a plane electromagnetic wave by a triaxial ellipsoid, the system of normal algebraic equations for this problem having been solved numerically by the Gauss method, the B matrix having been expanded into singular values according to the Forsyte-Malcolm-Mouler program, and the conjugate gradients method having been used for minimization of the error functional. Figures 2; references 4.

UDC 629.7.054.07

Estimation of Efficiency of Various Navigation System Operation Modes

907K0239C Leningrad IZVESTIYA VYSSHIKH UCHEBNYKH ZAVEDENIY: PRIBOROSTROYENIYE in Russian Vol 33 No 3, Mar 90 pp 49-53

[Article by A.A. Ressin, A.D. Troyanovskiy, and B.Ya. Tsilker, Riga Institute of Civil Aviation Engineers imeni Lenin Komsomol]

[Abstract] Three modes of navigation system operation are comparatively evaluated for efficiency in terms of error. Operation modes A_1 and A_2 involve the use of signals from three independent sister systems with the r.m.s. error of each increasing linearly in time, the output signal being the average of the three signals in mode A_1 and the median of the three signals in mode A_2. Operation mode B involves variable use of two different systems, one where the error remains constant and one where the error increases but the error of each system having a zero mean. Here the dispersion of the error increases in time when the first system has failed, the failure rate of that system being constant. The probability of an error exceeding its tolerance limit is calculated analytically for each mode and, as an example, numerically for the error of estimating lateral deviations of an airplane from its route over the Northern Atlantic by means of three inertial navigation system and a long-range radio navigation system. The results indicate that operation mode B performs best in terms of error, assuming an absolute reliability of the inertial navigation system and its continuous correction prior to failure of the radio navigation system. References 8.

UDC 681.3

Bridge-Type Multifunctional Special-Purpose Rational-Fraction Processors

907K0239A Leningrad IZVESTIYA VYSSHIKH UCHEBNYKH ZAVEDENIY: PRIBOROSTROYENIYE in Russian No 3, Mar 90 pp 26-29

[Article by V.B. Smolov, Leningrad Institute of Electrical Engineering imeni V.I. Ulyanov (Lenin)]

[Abstract] The structure and the hardware of special-purpose processors consisting of self-balancing electric bridge circuits are described, each bridge having five controllable resistors of which four are controlled by two input parameters and one is controlled by one output parameter. The four resistors forming the four arms of a bridge have two of them a "controlled conductance" characteristic and two of them a "controlled resistance" characteristic. Their conductance or resistance being linear functions of the input parameter, which can be N/N_{max} (N- length of binary code representing the input quantity), τ/T (τ- duration of square voltage pulse, T- period of pulse sequence), $N/N_{max}+ \tau/T$, $(N/N_{max})(\tau/T)$, $N/N_{max}:\tau/T$, with a constant zero-input term. The fifth resistor has a conductance which is a linear function of the output parameter, which can be N/N_{max} or τ/T, without a constant zero-output term. The transfer function of the bridge is consequently a rational fraction. Such a processor is a multifunctional one in terms of binary code N representing input and output quantities, duration of square voltage pulse τ, and variable pulse repetition rate f readily convertible into duration τ by means of trigger ring, also in terms of class of elementary functions which the rational-fraction transfer function of the bridge approximates with sufficient accuracy. Capacitors are appropriately inserted into the bridge circuit so as to ensure self- balancing under the average over period T unbalance voltage. The use of such a processor demonstrated on elementary functions of a product such as $N/N_{max}\tau/T$ realizable without special digital time-pulse multiplying devices and the processor structure required for realization of such a function is shown schematically. For illustration are considered $N/N_{max}(out) = \tan^{-1}(N/N_{max}\tau/T)$ and $N/N_{max}(out) = (\tan^{-1}\pi/2)(N/N_{max}\tau/T$. Figures 3; references 1. No 3, 90

UDC 581.383:621.391

Estimation of State of Autonomous Off-Platform Inertial Navigation Systems

907K0239B Leningrad IZVESTIYA VYSSHIKH UCHEBNYKH ZAVEDENIY: PRIBOROSTROYENIYE in Russian Vol 33 No 3, Mar 90 pp 44-49

[Article by S.V. Sokolov and I.N. Marinenko, Rostov-na-Donu

[Abstract] A stochastic model of off-platform inertial navigation systems containing three angular velocity transducers and three accelerometers is constructed on the basis of the system of three differential equations describing the instantaneous orientation of its trihedral in terms of the two geographical coordinates (latitude, longitude) and the course, assuming that the trihedral moves tangentially to a sphere around the Earth while at every instant of time remaining oriented with its MZ axis (M- its center) in the local vertical direction and its regular motion does not have vertical component. The vectors of additive noise and accelerometer readings have already been described stochastically so that a stochastic model of the object can be constructed and then a stochastic model of the "object -observer" with the vector equation of inertial navigation reduced to scalar form. On the basis of all these nonlinear stochastic equations describing the instantaneous orientation of the object and corresponding changes in the instrument output signals is then estimated the state vector of such an autonomous inertial navigation system which measures that orientation. The best estimate is obtained by the method of nonlinear filtration, which requires solving first the integrodifferential equation for the

a'posteriori probability density. The solution process can be simplified and the necessary accuracy still ensured by assuming that the changes in the trihedral orientation remain small during the estimation period, that the signal-to-noise ratio is large in all transducer channels, that the dispersion of the vertical acceleration component with zero mean is small, by discarding the quadratic stochastic RW_iW_j- terms as quantities of second-order magnitude ($W_{x,y,z}$- noise in the angular velocity readings $\omega_{x,y,z}$, R- radius of Earth), by assuming that the independent noise in each of the three acceleration readings is a Gaussian white noise of known intensity with zero mean, and by approximating the noise in all three angular velocity readings as well as the vertical velocity component of the object as an n-th order normal linear Markov process. Figures 2; references 4.

Signal Analyzers

907K0243A Moscow PRIBORY I TEKHNIKA EKSPERIMENTA in Russian No 1, Jan 90 p 10

[Article by A. F. Denisov, Yu. P. Donchenko and Ye. F. Kleshchevnikov]

[Abstract] The center for scientific and technical creativity of youth "LUCH" offers in this commercial advertisement several instruments, including a highly sensitive analog-digital convertor performing the functions of an oscilloscope, frequency meter, voltmeter and calculator, as well as a wide band analog- digital convertor for the study of transient processes in signals with amplitudes of 10 mK to 250 V and lengths of 4 ns to 10 s, plus a cathode-ray storage oscilloscope.

CAMAC-Standard Character and Graphic Data Output Module

907K0243B Moscow PRIBORY I TEKHNIKA EKSPERIMENTA in Russian No 1, Jan 90 p 18

[Article by A. D. Mruga, O. V. Minenko and A. A. Nesuck]

[Abstract] This commercial advertisement offers an independent dual-processor microcomputer performing the functions of character and graphic display for connection to the CAMAC box. The module generates synchronization and RGB modulation signals for a video monitor or domestic television set and provides a set of graphic primitives as well as generation of displayed characters.

Hybrid Integrated Circuit Set for Economical Analog Information Collection Systems

907K0243C Moscow PRIBORY I TEKHNIKA EKSPERIMENTA in Russian No 1, Jan 90 p 19

[Article by A. A. Zhurin, A. G. Varenik and S. A. Demidenko]

[Abstract] This commercial advertisement offers a set of hybrid IC's made by hybrid-film technology in standard metal-glass bodies designed for intermediate conversion of voltages from the sensors of various physical quantities, including an integrating voltage-to-time convertor, a programmable pulse signal amplifier and a low-frequency signal amplifier.

UDC 621.373

Hi-power Magnetic Nanosecond Pulse Generators (review)

907K0243D Moscow PRIBORY I TEKHNIKA EKSPERIMENTA in Russian No 1, Jan 90 p 23-36

[Article by A. N. Meshkov, Gorkiy Polytechnical Institute]

[Abstract] This review of the international (primarily Soviet) literature discusses the experience which has been gained in the development of nanosecond pulse generators containing thyristors or thyratons and magnetic ferrite compression elements. Non-linear wave devices for the generation of rectangular pulses are described and the characteristic parameters and design of generators is discussed. Methods for increasing frequency and power are analyzed. This is an area which has seen great expansion in the past 10 years, following the development of designs of very complex non-linear and wave devices, a well as powerful semiconductor devices. The transition to magnetothyristor circuits from thryratrons and discharge circuits can be compared in its qualitative results to the transition to semiconductors in other areas of electronics. References 48: 43 Russian, 5 Western.

UDC 621.396.027.7

Transceiver for Fiber-Optic Communications Line Between Computers.

907K0243E Moscow PRIBORY I TEKHNIKA EKSPERIMENTA in Russian No 1, Jan 90 p 106-109

[Article by A. B. Semenov, V. M. Vatutin and P. G. Vanichkin, Moscow Institute of Electronics, USSR Academy of Sciences]

[Abstract] This article describes a simple transceiver designed to organize communications between SM and Elektronika 60 computers equipped with DLKC devices. The transmitting portion of the transceiver receives a 3-level duobinary signal with positive data and negative synch pulses, converts it to a 2-level signal, generates linear Manchester code and converts the electrical signal to an optical signal. The receiver portion converts the optical signal to an electrical signal, extracts the information and synch pulses and generates the 3-level electrical signal for further transmission. A time diagram of the operation of the decoding portion is presented. References 7: 7 Russian.

UDC 621.375.4

High-Voltage Low-Frequency Class AD Signal Amplifier

907K0243F Moscow PRIBORY I TEKHNIKA EKSPERIMENTA in Russian No 1, Jan 90 p 131-133

[Article by N. A. Fefelov, V. V. Kharchenko and R. V. Chilikina, Planning-Design Bureau of Electrohydraulics, Ukrainian Academy of Sciences, Nikolayev]

[Abstract] An amplifier is described which has higher efficiency, small size and less severe cooling requirements of the output stage than a traditional class AB amplifier. A schematic diagram of the solid-state device is presented, showing the 4- transistor terminal stage, a bridge circuit; 4 identical preterminal stages, galvanically decoupled from each other in both control and power supply; and an overload protection unit for the terminal transistors, a pulse-width modulator with a feedback loop. The amplifier is intended to supply piezoceramic transducers, operating into capacitive and active loads. It produces an output voltage of at least 430 V with a power supply of 500 V, maximum load current 3 A nonlinear distortion over 2 percent, operating frequency range 0-1 kHz. References 4: 3 Russian, 1 Western.

UDC 535.853.4

Method of Measurement of Phase-Frequency Spectra by Quasioptical BWT Millimeter and Submillimeter Wave Band Spectrometer

907K0243G Moscow PRIBORY I TEKHNIKA EKSPERIMENTA in Russian No 1, Jan 90 p 143-144

[Article by A. B. Latyshev, D. A. Lukyanov and I. M. Fedotova, Institute of General Physics, USSR Academy of Science]

[Abstract] This article describes a vector method for measurement of phase, the advantages of which include comparative simplicity of the equipment required, allowing the use of spectrometers not specifically designed for the measurement of phase spectra. This method can achieve high sensitivity, amounting to less than one degree, and high speed of recording of phase spectra, comparable to the speed of recording of amplitude spectra using the same equipment. The method utilizes a backward wave tube as the generator. A block diagram of the measurement system is presented. References 4: Russian.

UDC 621.383

Space-Time Characteristics of Single-Electron FEU-157 Photomultipliers With Single-Crystal GaAs-CsO Photocathode

907K0243H Moscow PRIBORY I TEKHNIKA EKSPERIMENTA in Russian No 1, Jan 90 p 156-159

[Article by Ye. S. Voropay, F. A. Yermalitskiy and T. N. Palts, Scientific Research Institute of Applied Physics Problems Bellorussian State University, Minsk]

[Abstract] Results are presented from a study of the distribution of light sensitivity and resolution over time for various sectors of the photocathodes of an FEU-157 photomultiplier operating in single-quantum mode. It is found that within the operating portion of the photocathode in the photomultipliers studied, the nonuniformity of the light anode sensitivity is 54-98 percent, while the difference in signal transmission time is 0.76- 1.9ns. The variations in time resolution are also significant for different points on the photocathode, 0.4-1.0ns. Diagrams of the distribution of anode sensitivity, duration of response at half- height to subnanosecond gas-discharge tube radiation and difference in time of transmission of signals for various points on the photocathodes of two specimens are presented. The response to radiation of the subnanosecond gas-discharge tube with point illumination of a selected point with minimal and uniform illumination of the central zone of the photocathode is illustrated. Work must be continued on increasing the uniformity of the electric field over the surface of the photocathode in order to achieve greater spacial homogeneity of the light and time parameters of the photomultiplier. References 11: 10 Russian, 1 Western.

Space-Time Characteristics of Single-Electron FEU-157 With Single-Crystal GaAs-CsO Photocathode

907K0243I Moscow PRIBORY I TEKHNIKA EKSPERIMENTA in Russian No 1, Jan 90 pp 156-159

[Article by Ye. S. Voropay, F. A. Yermalitskiy and T. N. Palts]

[Abstract] The distribution of light sensitivity and resolution over time are studied for various sections of the photocathode of an FEU-157 photomultiplier. Nonuniformity of photosensitivity is found to be as great as 98 percent, with signal transmission times varying by up to 1.9 ns. The uniformity of the response can be improved by improving the uniformity of the electrical field over the surface of the photocathode.

UDC 621.375.826

Two-wave Subnanosecond Yttrium-Aluminum Garnet Pulse Generator

907K0243J Moscow PRIBORY I TEKHNIKA EKSPERIMENTA in Russian No 1, Jan 90 p 172-173

[Article by Yu. I. Babikov Kim Synir, V. Ye. Mironov, Joint Institute of Nuclear Research, Dubna]

[Abstract] A description is presented of a subnanosecond master oscillator for a laser system for excitation of plasma waves. The generator is based on a series-produced LTIPCh-8 laser. Designed for investigation of processes of excitation of plasma waves by two-frequency laser radiation, the system produces a pulse of less than 1ns in length in trains of 3 or 4 pulses. The system lases at 1.0615 and 1.0641 μm. A cross-sectional diagram of the discharge unit is presented. References 5: 2 Russian, 3 Western.

UDC 536.422.4:66.047.3

Evaporator for Sputtering Large-Area Thin Films

907K0243L Moscow PRIBORY I TEKHNIKA EKSPERIMENTA in Russian No 1, Jan 90 p 202

[Article by M. I. Fedorov, V. K. Maksimov and N. N. Tyukin, Vologodsk Polytechnical Institute]

[Abstract] An evaporator is described for the production of thin films (0.05-05 μm) on large-area organic semiconductor substrates. The device consists of the actual evaporator, consisting of series-connected elements, plus a frame. The series connection of heating elements assures uniform heating of the substance and the frame fixes the position of the evaporators and assures structural rigidity, allowing films of about 400 square centimeters to be evaporated with thickness deviation of two-three percent over the entire surface.

UDC 621.396.629

Practical Wideband Photoreceptor Circuits

907K0243K Moscow PRIBORY I TEKHNIKA EKSPERIMENTA in Russian No 1, Jan 90 p 174-176

[Article by Ye. G. Volkov, V. A. Zhmud, and Yu. P. Kononenko, Institute of Automation and Electrometry, Siberian Division, USSR Academy of Sciences, Novosibirsk]

[Abstract] Circuits are described for highly sensitive light receivers with pass bands of at least 15 KHz and low internal noise levels. The dynamic band is expanded by several orders of magnitude by subtracting the currents of the photodiodes at the input of the first amplifier stage. The use of a low-noise operational amplifier with a repeater at its input yields a significant gain in signal/noise ratio. An operational amplifier developed by one of the authors and manufactured since 1988 using hybrid technology has a pass band of 80 MHz, a gain of 100 dB and a rise rate of 500 V/μs. Schematic diagrams of the devices are presented. References: 3 Russian.

UDC 53.089.68:531.787

Differential Capacitive Pressure Sensor

907K0243M Moscow PRIBORY I TEKHNIKA EKSPERIMENTA in Russian No 1, Jan 90 p 204-205

[Article by S. N. Afanasyev, V. G. Sevastyanov and A. Yu. Stefanov]

[Abstract] A differential capacitive pressure sensor has been developed allowing an increase in the accuracy of pressure measurement at high temperatures. The design is distinguished by the fact that the comparison chamber is made as a hollow cylindrical body, screen and non-moving electrode placed coaxially, made of a material with identical coefficient of linear expansion, allowing all vacuum seals and electric leads to be placed outside of the high-temperature area. A cross-sectional drawing of the device is presented. It can be used to measure saturated vapor pressure at temperatures up to 1000°C at 0-1000 Torr. References: 4 Russian.

UDC 536.521

Infrared Surface Acoustic Wave Radiometer

907K0243N Moscow PRIBORY I TEKHNIKA EKSPERIMENTA in Russian No 1, Jan 90 p 221-223

[Article by Ye. S. Avdoshin, Tula State Pedogogic Institute]

[Abstract] An infrared radiometer is described including a self-excited oscillator with surface acoustic wave element, the output signal frequency of which depends on the temperature of the object. The radiometer operates on the principle of interaction of thermal radiation with the surface acoustic waves. The output signal varies with frequency of the object in the range of 40-150 ° C. References: 8 Russian.

UDC 621.317.757

Electrical Signal Spectrum Analyzer

907K0243O Moscow PRIBORY I TEKHNIKA EKSPERIMENTA in Russian No 1, Jan 90 p 221-223

[Article by V. I. Zhulev, V. P. Rumyantsev and Yu. M. Suslov]

[Abstract] This device is designed for determination of the spectral density of low-frequency random signal power. It is based on a method of filtration using active RC filters which can be tuned in terms of central frequency and Q. The frequency band is divided by octaves, assuring equality of relative transmission bands

of the filters. The device has a parallel structure, assuring most rapid operation for fast estimation of a signal. The device is based on integrated microcircuits.

UDC 621.378.325

Pulse Shaper for Control of Electroptical Solid-State Laser Gate

907K0243P Moscow PRIBORY I TEKHNIKA EKSPERIMENTA in Russian No 1, Jan 90 p 242

[Article by A. G. Akmanov, V. I. Mikryakov and M. G. Santimirov]

[Abstract] The FIN-1 voltage pulse shaper is designed to control the electrooptical gate of a laser with negative feedback. The operation is based on digital-analog formation of the complex shape. The device allows electronic implementation of various laser operating modes. The technical characteristics of the device are briefly presented.

UDC 621.317.444

Three-component Digital Magnetometer

907K0243Q Moscow PRIBORY I TEKHNIKA EKSPERIMENTA in Russian No 1, Jan 90 p 243

[Article by Yu. D. Klimenko, V. I. Gornostayev and V. V. Potaphov]

[Abstract] This article describes a three-component digital magnetometer designed for measurement of the components of a vector of induction of constant or slowly changing magnetic fields at 0- 0.1 mTl. The sensing element of the instrument is a miniature three-component ferroprobe which is placed in the center of Helmholtz coils and supplied with triangular pulses stabilized at 12.5 kHz. A photograph of the device is presented.

UDC 621.372.853.2

Approximate Solution of Transient Diffraction Problem by Method of Auxiliary Sources

907K0244A Moscow RADIOTEKHNIKA I ELEKTRONIKA in Russian Vol 35 No 3, Mar 90 pp 500-506

[R.S. Zaridze, G.V. Lomidze, and L.V. Dolidze]

[Abstract] A new numerical method of solving transient diffraction problems for electromagnetic pulses in the time domain is proposed, this method involving use of auxiliary sources rather than solution of the Fourier-transform integral equation for an electric or magnetic field. It is demonstrated on diffraction of a normally incident plane electromagnetic pulse by an infinitely long ideally conducting cylinder, assuming that the pulse is polarized in the direction of the cylinder axis and that the cross- section of the cylinder is the same everywhere along the axis. The incident pulse field u_i induces longitudinal surface currents $j_z(t)$ and these emit the scattered field u, which satisfies the wave equation Δu-[d<]sup2u/$c^2\delta t_2$ = 0 and the boundary condition u_i[<i]nfS+ u[<i]nfS = 0 at the cylinder surface S at any instant of time t. Following discretization of the solid reflecting cylinder surface into a grid of thin wires and discretization of time, the assignment of locations for those sources of the scattered field will depend on both form and duration of the incident pulse. The solution to the wave equation, which describes the scattered field, is then expanded into a nonorthogonal series of fundamental solutions in functions u_{ij} $f(r,t,r_1,t_j)$ (r and r_i denoting the distances from origin of cylindrical system of coordinates to observation point and to location of i-th auxiliary secondary source respectively, t_j- instant of time field leaves source on the scatterer surface, t- instant of time field arrives at observation point, [begin set]t_j[end set] = or < t- [r–] r_i[/c], c- speed of light). These functions u_{ij} are linearly independent and complete in the $L_2(S)$ space, for each one a new function Wu_{ij} (W- boundary conditions operator W) being being defined on the surface contour S. Solution of the diffraction problem by this method is demonstrated on a pulse of semiinfinitely long duration containing a packet of sinusoidal waves and an array of parallel infinitely long wires forming a circular cylindrical grid, infinitesimally thin wires in the limiting case and diffraction by a closed cylindrical grid being furthermore analyzed for resonances. The accuracy of this method is evaluated relative to the conventional method involving solution of the Fourier-transform integral equation. Figures 4; references 9

UDC 621.372.8.01

Resonating Cavity Formed by Rectangular Waveguide and Two Coaxial Posts Inside

907K0244B Moscow RADIOTEKHNIKA I ELEKTRONIKA in Russian Vol 35 No 3, Mar 90 pp 514-520

[Article by V.M. Butorin]

[Abstract] Performance and design analysis of a resonating cavity formed inside a rectangular hollow metallic waveguide by two identical coaxial cylindrical metal posts projecting inward from the two opposite horizontal walls is treated as a three-dimensional vector boundary-value problem. The characteristics of such a cavity are calculated accordingly, by the method of partial regions. The fundamental relations are established first, for the electrodynamic model of two coaxial metal posts, the region within which the three-dimensional homogeneous Helmholtz equation must be satisfied having been subdivided into three subregions: I) space surrounding both posts, II) gap between the two posts, III) space beyond the immediate surrounding of both posts. The electromagnetic field in the inner subregions I and II is expanded into a series of cylindrical waves, while in the

outer subregion III it is expanded into a series of natural rectangular-waveguide modes. Satisfying the boundary conditions at points on the boundary between subregions I and III by the collocation method requires solving a system of linear algebraic equations in functions definable on the basis of Maxwell field equations, convergence of the collocation method being demonstrated on the two-dimensional problem of two posts replaced by a single gapless one across the waveguide. The dispersion equation is obtained by equating to zero the determinant of that system equations. Its solution yields the resonance wavelength, which depends on length of the cavity, on both length and diameter of the two posts, also on a downward or upward shift of the gap between the post (not of equal length then). The dependence of the resonance wavelength as well that of the Q-factor and of the wave impedance on these dimensional parameters normalized to the height of the waveguide has been evaluated numerically and compared the respective characteristics of a cavity without posts. All three were found to decrease with increasing length of the posts and with decreasing length of the cavity. The resonance wavelength and the Q-factor were found to increase, but the wave impedance to decrease with increasing diameter of the posts. Shifting of the gap between the posts was found not to have a noticeable effect. Figures 2; references 7.

UDC 621.391.01

Algorithm of Interference Immunity Estimation for Optimized Radioelectronic Tracking Systems According to Composite Information-and- Energy Loss Criterion and Energy Loss Criterion

907K0244C Moscow RADIOTEKHNIKA I ELEKTRONIKA in Russian Vol 35 No 3, Mar 90 pp 527-532

[Article by V.I. Merkulov]

[Abstract] The immunity of high-precision radioelectronic tracking systems to natural and intentional interference is estimated in terms of a coefficient which characterizes the sensitivity of such a system to interference causing additive distortions of its controlled phase trajectory. A composite criterion is selected for this estimation, one which combines tracking error and thus loss of information with inefficiency and thus energy lost in the controls. The model of the given part of the tracking system is $d/x = F_y x_y + B_y u + C_y \xi_y$ (F- state matrix, B- control efficiency matrix, C- interference matrix, x is the n-dimensional vector of tracked and thus controlled coordinates, u is the r-dimensional vector of control signals, ξ is the m-dimensional vector of additive perturbations). The sensitivity coefficient is $\xi_{\xi j} = x_y^T \Gamma_{\xi j} x_y + 2x_y^T \nu_{\xi j} + \mu_{\xi j}$, where Γ is a symmetric matrix, ν is a vector, μ is a scalar, all three depending on the parameters of the given part of the tracking system and analytical expressions for them being needed for estimation of the sensitivity coefficient. They are derived with several simplifying assumptions made regarding the ξ_{yj} component of the interference vector ξ_y, whereupon the algorithm of interference immunity estimation is constructed with interference most generally and most conveniently accounted for. References 8.

UDC 621.391.01

Optimum Estimate of Amplitude-Phase Image of Spatially Diverse Object

907K0244D Moscow RADIOTEKHNIKA I ELEKTRONIKA in Russian Vol 35 No 3, Mar 90 pp 533-540

[Article by A.P. Zhukovskiy and V.I. Chizhov]

[Abstract] Algorithms are constructed for optimum estimation of the amplitude-phase image of a spatially diverse statistically nonuniform and electrophysically nonhomogeneous large object. The optimum estimation is based on the electrodynamical model of correlated partial components of the reflected field, with no constraints on the resolution of signal modulation for space-time processing of the image. The field backscattered by such an object is described in the Kirchhoff approximation, assuming identical polarization of both transmitter and receiver antennas with inclusion of the Doppler frequency shift. The interference is assumed to be a Gaussian white noise with given spectral density and δ-correlation in time as well as in space. The amplitude-phase image is determined by the random complex coefficient of scattering by the object in the presence of noise and interference. This coefficient will be calculated on the basis of the maximum on its a'posteriori probability distribution, the latter being approximately equal to the a'priori probability distribution divided by the likelihood functional. The algorithm involves expansion of the backscattered field into a two-dimensional Kotelnikov series containing discretization integrals and then differentiation of its a'posteriori probability distribution with respect to that field, considering that the distribution of the complex scattering coefficient is a normal one. Equating the derivative to zero leads to a system of equations with the correlation integral of space-time processing on the right-hand side. This discrete estimation algorithm is transformed into a continuous one by replacement of the sum before the triple integral over L_x, L_y, T with a double integral over X and Y. The dispersion of the estimation error is calculated for accuracy evaluation, found to depend largely on the signal-to-noise ratio at a surface resolution element and to be 2-10 times smaller than the dispersion of errors made by a standard synthetic-aperture antennas with holographic image processing. Figures 3; references 4.

UDC 621.391.01

Feasibility of Measuring Distance to Rough Surface by Analyzing Spectrum of Continuous Noise Signal

907K0244E Moscow RADIOTEKHNIKA I ELEKTRONIKA in Russian Vol 35 No 3, Mar 90 pp 548-555

[Article by N.N. Zalogin, A.A. Kalinkevich, K.L. Kirillin, and V.Ya. Kislov]

[Abstract] Measurement of the mean altitude of an aircraft flying above an uneven terrain and simultaneous

determination of the terrain characteristics by the method of dual spectrum analysis is considered, with a radio altimeter which operates with a generator of ergodic noise signals. These signals are sent, through a directional coupler to a circulator and to an adder. The circulator with a vertical transceiver antenna sends these signals down to the ground surface and sends those reflected by that surface to the adder, which combines them with the original signals it has received from the generator through the directional coupler. The adder output signals pass through a sequence of two spectrum analyzers which successively analyze the modulated power spectrum $\Phi(\omega)$ and the secondary spectrum of time delays $s(\tau)$ or modulating "frequencies" Δt_{ik}. Such a radio altimeter differs from the Poirier noise radar (RADIO SCIENCE, Vol 3 No 9, 1968) in that the reflecting ground surface is treated as a statistically uniform one consisting of mutually independent random "shining" points whose reflection coefficient decreases exponentially with increasing distance from the point directly underneath the airborne antenna. Performance analysis of this altimeter is simplified by the assumptions that signals propagate without attenuation, that signals reflected from all "shining" points have constant amplitudes and no phase shift, that the aircraft flies at an altitude much higher than the width of the scanned surface area and than the height of the surface asperities, and that the antenna has a radiation pattern $D^2(r) = D_0e(-r^2/a^2)$. On this basis are calculated the average-over-readings spectral densities $F_1(\omega)$ which characterizes modulation of the power spectrum by different distances from the antenna to points on the ground surface and $F_2(\omega)$ which characterizes modulation of the power spectrum by different path lengths from the antenna to all reflecting points, also the average-over-readings high-frequency spectral density $S_1(T)$ which contains information about the aircraft altitude and the low-frequency spectral density $S_2(T)$ which characterizes the deviation of reflecting points from the mean surface level. Figures 4; references 4.

UDC 621.391.01

Energy Spectra of Pseudonoise Signals of Various Kinds

907K0244F Moscow RADIOTEKHNIKA I ELEKTRONIKA in Russian Vol 35 No 3, Mar 90 pp 556-566

[Abstract] Analytical expressions for the spectral power density (SPD) of phase-shift-keyed (PSK) and frequency-shift-keyed (FSK) compound signals are derived which reveal the mutual relation between the energy spectra of these signals and their both correlation functions characterizing the structure of the respective pseudorandom sequences. These expression reveal furthermore the mutual relation between the statistical characteristics of SPD spikes and those of ACF spikes. Compound signals of the PSK kind are considered for aperiodic and thus single transmission of a pseudorandom sequence, for periodic transmission, for transmission with alternation of two different pseudorandom sequences after periods of time corresponding to duration of an individual pulse so that a mixed periodic cross-correlation function is generated, and for transmission with similar alternation of the basic pseudorandom sequence and the negative one so that meandering inverse autocorrelation function is generated. Among FSK compound signals are considered only those with minimum frequency shift. For a comparative evaluation of their energy spectra as basis for optimum selection, especially with regard to suppression of SPD spikes in each mode of data transmission, PSK and FSK MinFS compound signals were generated by using either $N_E = 127$ long M-sequences or recurrently formed sequences and random sequences. Figures 6; references 8.

UDC 621.375.172

Maximum Attainable Bandwidth of Microwave Transistor Power Amplifiers

907K0244G Moscow RADIOTEKHNIKA I ELEKTRONIKA in Russian Vol 35 No 3, Mar 90 pp 574-580

[Article by A.Z. Kuznetsov]

[Abstract] The maximum attainable bandwidth of microwave transistor power amplifiers under three types of load is calculated, for design purposes, on the basis of Youla's constraints on the series expansion coefficients (IEEE Trans. Vol CT-11 No 1, 1964). The first type of load is an RC-parallel circuit in series with L. The second type of load is an RC_1-series circuit in parallel with C_2 and both in series with L. The third type of load is an RLC_1-series circuit in parallel with C_2. The maximum possible matching bandwidth is calculated first for each case, given the amplitude-frequency characteristic of the matching circuit. The algorithm of matching circuit optimization has been programmed for a microcalculator and use of VSWR tables. Figures 1; tables 1; references 11.

UDC 537.876.23:534

Convolution of Two Surface-Acoustic-Wave Signals in Planar Monolithic Structure

907K0244H Moscow RADIOTEKHNIKA I ELEKTRONIKA in Russian Vol 35 No 3, Mar 90 pp 625-631

[Article by A.B. Lukyanov, V.I. Gavrilin, S.F. Belyy and A.L. Nesterov]

[Abstract] The mechanism of a surface-acoustic-wave convolver, a monolithic thin-film with planar ohmic contact tabs deposited on the semiconductor film of sound propagation for pickoff of the convolution signal,

is analyzed on the basis of a model built on experimental evidence. Accordingly, the convolution voltage V_c is proportional to the relative change in the electrical resistance of the semiconductor film $\Delta R/R$ caused surface acoustic waves and thus equal to the product of bias voltage V_b times that relative resistance change. The convolver, a 150-200 nm thick InSb film as wide as the sound beam aperture deposited through a 50-60 nm thick SiO_x dielectric interlayer on a $LiNbO_3$ sound guide, is excited by an interdigital piezoelectric transducer. The bias voltage is applied to the two-layer structure through aluminum contact tabs and the convolution voltage, picked off the structure by ohmic contact tabs, is sent through a capacitor to an oscillograph. As in the case of a capacitive voltage pickoff, nonlinearity of the charge carrier concentration is considered to be playing the principal role in acoustoelectric interaction. It is furthermore assumed that the two-layer thin-film structure does not load the surface of the piezoelectric structure mechanically and absorbs only an insignificant amount of acoustic energy, also that surface acoustic waves do not influence the charge density at the semiconductor-dielectric interface. The thickness of the semiconductor film is not smaller than the Debye shielding radius, however, so that the piezoelectric SAW field potential varies across the thickness as well as across the width of the structure. The standard system of equations for an n-semiconductor in the quasi-static approximation is solved on the basis of this model, with the aid of both DC and AC equivalent circuit diagrams, for the purpose of design and performance evaluation. Numerical calculations have yielded the dependence of the ratio V_c/V_b (V_{in}- input voltage) on V_{in}^2 (volume electrical conductivity of InSb film in absence of surface acoustic waves $\sigma_0 = 9.85$ S/cm) and on the effective surface charge at the InSb-SiO_x interface when $V_{in} = 10$ V, also its dependence as well as that of $\Delta R/R$ on the volume electrical conductivity of the InSb film when $V_{in} = 10$ V. Figures 5; references 13.

UDC 621.396.67.01

Suppression of Side Lobes of Vertical Antenna While Utilizing Reflections From Boundary

907K0244I Moscow RADIOTEKHNIKA I ELEKTRONIKA in Russian Vol 35 No 3, Mar 90 pp 637-639

[Article by I.S. Falkovich]

[Abstract] A method of suppressing side lobes of a vertical short-wave or ultrashort-wave transceiver antenna arrays is outlined, such antenna being phased so that it can pick up the wave reflected by the ground surface and its directivity at low elevation angles will be enhanced. The method is demonstrated on an array of N only slightly directional elements at altitudes $h_k = kd$ ($k = 1,2,...,N$), its current distribution $J_k = Ia_k\sin(2\eta_k\sin\Delta_0/\lambda)$ (Δ- elevation angle, Δ_0- phasing elevation angle, λ- wavelength) ensuring a radiation pattern which effectively utilizes the wave reflected by the ground surface. Making the current decrease monotonically upward will generally reduce the level of side lobes, especially that of the largest upper and lower ones. The problem is to determine the current- amplitude distribution, characterized by coefficients a_k, which will not also simultaneously broaden the major lobe. It is found by satisfying the condition that the shape of the major lobe change only slightly upon omission of one array element from the phasing system. This condition is most readily attained when the number of array elements is sufficiently large. Figures 1; tables 2; references 2.

UDC 621.372.823.01

Single-Mode Propagation of Various Waves Through Corrugated Circular Waveguide

907K0244J Moscow RADIOTEKHNIKA I ELEKTRONIKA in Russian Vol 35 No 3, Mar 90 pp 643-644

[Article by N.K. Tsibizov and V.Yu. Boronov]

[Abstract] The possibility of a EH_{11}-mode wave propagating through a corrugated circular waveguide having already been demonstrated (ELECTRONICS, LETTERS Vol 13 No 1, 1977), its is now demonstrated that also other single-mode waves can propagate through such a waveguide. The proof is based theoretically on the dispersion characteristics of the first six modes (E_{01}, HE_{11}, EH_{11}, HE_2, EH_{11}, H_{01}) and on the waveguide phase factors, the latter having been calculated according to a known numerical algorithm for corrugated waveguides with arbitrary cross-section. These calculations have also yielded the frequency ranges of those modes, some of them overlapping. The authors thank E.A. Alkhovskiy for helpful discussion of the results. Figures 1; references 3.

UDC 621.371.029.64.001.5

Influence of Uplifted Inversion Layers on Extrahorizontal Propagation of Short Radio Waves

907K0244K Moscow RADIOTEKHNIKA I ELEKTRONIKA in Russian Vol 35 No 3, Mar 90 pp 647-649

[Article by K.V. Koshel]

[Abstract] Extrahorizontal propagation of short radio waves from a source above the Earth and then, particularly, in the presence of coexisting evaporator waveguide and uplifted inversion layers is analyzed by the method the author has used before in analyzing extrahorizontal propagation of short radio waves from a quasi-point vertical electric dipole on the surface of Earth, in that case having been considered the presence of troposhpheric evaporator waveguides at the surface. Solution of this propagation problem involves expansion of the relevant potential A into a series of products of potential

differences A_l- A^{free} and corresponding Legendre polynomials, with the normalized dipole moment of the source appearing as multiplier before the sum of these terms and the potential A^{free} added as an extra term. The problem is reduced to the Riccati equation and solved in a spherical system of coordinates with the origin at the center of the Earth, the solution for free space appearing in the form of Airy functions. On this basis is evaluated the dependence of the wave attenuation on the distance from the source, with altitude of the source, thickness of the inversion layer, complex dielectric permittivity of the medium, electrical conductivity of the surface, and other parameters varied. Calculations were made for 10 cm, for testing their accuracy against calculations by the methods of normal waves and geometrical optics. Figures 2; references 6.

UDC 621.382.082.5:577.391

Automated Optical-Electronic Device for Measuring Coordinates of Laser Beam Power Center

907K0258A Moscow IZMERITELNAYA TEKHNIKA in Russian No 3, Mar 90 pp 20-23

[Article by V. A. Shangin]

[Abstract] The coordinates of the power center of a laser beam, determining the position of the beam axis, can be measured by the use of a method involving measurement of the integral characteristics of the radiation beam. The allows a measurement device to be designed which does not require the use of multiple energy receivers and avoids the error resulting from the discrete measurement field. The procedure involves generation and measurement of a signal proportional to an integral characteristic, with two integral signals obtained using two electronic channels connected to a two-segment photoreceptor used for each coordinate. Figures 2; References: 6 Russian.

UDC 531.76.:085:621.397.6

Influence of Ground-Point Location on Time Scale Matching Error in Satellite Television Channels.

907K0258B Moscow IZMERITELNAYA TEKHNIKA in Russian No 3, Mar 90 pp 25-26

[Article by Yu. D. Ivanova, Yu. A. Fedorov and L. S. Yunoshev]

[Abstract] A previous study discussed synchronization systems in which the results of reception of time signals at the transmitting point and two reference points were used to compute the coordinates of the satellite at the moment when it relayed the signals, which can then be used to determine the time delay at any synchronized point. Continuing these studies, the authors suggest a simple method for estimating the error component of scale matching as a function of the mutual location of the synchronized point, the reference points and the satellite with known time scale synchronization error at the reference points. This allows the creation of a highly effective time scale matching system for television satellite channels with an error on the order of 100 ns for regular matching of standards using existing hardware and communication channels. Figures 2; References 5: 4 Russian, 1 Western.

UDC 621.396.67.012.12

Improvement of Accuracy Characteristics of Measuring Scanners for Determination of Antenna Characteristics.

907K0258C Moscow IZMERITELNAYA TEKHNIKA in Russian No 3, Mar 90 pp 43-45

[Article by R. I. Rumyantsev]

[Abstract] A previous study analyzed the design of a planar scanner made of a radio-absorbing material to decrease the strength of signals reflected from its metal parts. The scanner contains two telescoping sets of cylindrical fittings of the radio-absorbing material for the horizontal and vertical guides of the scanner, allowing the probe to be moved in the scanning plane. Precise estimation of the signals reflected by the scanner is a very difficult task. This article generates such an estimate based on the effective scattering surface of the scanner. The effective scattering surface of the design suggested in the previous article is compared to that of a design consisting of sheets of radio- absorbing material installed before the scanner. Calculated results are compared with experimental data indicating that the new design decreases the effective scattering surface of the scanner by several orders of magnitude. The use of the new design with telescopic covers decreases the strength of signals reflected by the scanner and thus increases the accuracy of measurement of field characteristics in the antenna aperture. Figures 2; References 4: 3 Russian, 1 Western.

UDC 621.317.729.3

Active Dipole Antennas for Measurement of Radio Noise Field Intensity in the Near Field.

907K0258D Moscow IZMERITELNAYA TEKHNIKA in Russian No 3, Mar 90 pp 45-46

[Article by L. A. Mikhalev]

[Abstract] The designs and parameters of active dipole antennas for measurement of radio noise electric field intensity in the near field are described. An active impedance convertor was used, consisting of a differential amplifier stage with crossed feedback transformer. The use of the crossed negative feedback transformer assured high suppression of synphase signal components, low level of combination components in the output signal, high input impedance and the required output

impedance to match the antenna with the feed. As examples of use of the system, active dipole antennas were designed and produced for the 0.01-1000 MHz band. Figure 1; References: 3 Russian.

UDC 502.7:531.708

Metrologic Support of Ocean Hydrophysical Research

907K0258E Moscow IZMERITELNAYA TEKHNIKA in Russian No 3, Mar 90 pp 60-61

[Article by I. F. Shishkin, I. Ye. Ushakov]

[Abstract] The program of the "Ocean" State Committee on Science and Technology for 1986-2000 calls for the development of the scientific, technical, organizational and legal foundation of metrologic support for research in the ocean. The practical metrologic activity must be adapted to the specifics of measurement at sea. The multivariate nature of the object of research must be considered. The organizational basis of metrologic support is the National Metrologic Service. Measurements are mostly performed using non-standardized measurement equipment, manufactured as individual units or in small batches. The resultant reduction in state supervision has not been compensated by any increase in departmental monitoring. It is therefore very important to give marine metrologic regions the status of state regions, thus including them in the State Metrologic Service. The global nature of oceanographic research requires close international cooperation and the development of the corresponding international legal documents.

UDC 621.396.969.14

Elimination of Ambiguity in Carrier Frequency Readings of Coherent Pulse Signal Received With Passive Background Interference

907K0260A Kiev IZVESTIYA VYSSHIKH UCHEBNYKH ZAVEDENIY: RADIOELEKTRONIKA in Russian Vol 33 No 3, Mar 90 pp 8-11

[Article by A.V. Agranovskiy, S.I. Ziatdinov and A.V. Pokrovskiy]

[Abstract] A device is synthesized for measuring without ambiguity the carrier frequency or the Doppler frequency of M sequences of coherent radio pulse packets appearing at the receiver at a different repetition rate each. First is considered the simplest case: a deterministic sequence of radio signals neither amplitude nor phase modulated, all their parameters except the carrier frequency known, and appearing at the receiver together with a white noise. The performance of this frequency meter in the presence of passive interference is then analyzed, with the interference represented as a sequence of radio pulses fluctuating normally with zero mean. Initial phase and envelope of the interference are given, its frequency being equal to the carrier frequency of the sounding signal. The measuring device includes an interference suppressor based on one-shot interperiod subtraction. For a performance evaluation are calculated the probability of correct detection, based on logic processing of signal and interference, as well as the probability of ambiguous frequency reading. The latter can be made not to exceed 10^{-4}. Figures 2; references 2.

UDC 621.372.832

Wideband Microwave Divider-and-Adder Devices

907K0260G Kiev IZVESTIYA VYSSHIKH UCHEBNYKH ZAVEDENIY: RADIOLEKTRONIKA in Russian Vol 33 No 3, Mar 90 pp 59-60

[Article by A.N. Romanov and O.A. Romanov]

[Abstract] Boosting the microwave power in a load by adding signals from arbitrarily many amplifiers through a divider-and-adder bridge formed by directional couplers is considered, binary pairwise connection of directional couplers on coupled strip lines with identical crosstalk attenuation in each being the preferable scheme on account of structral simplicity combined with wide dimensional tolerances and a 4-channel divider-and-adder formed by a one two-segmental and two one-segmental directional couplers being the most efficient power adder with a better economy of space than possible with 8-channel and 16-channel ones. The two-segmental directional coupler consists of two quarter-wave coupled-line segments with different crosstalk attenuations in a cascade connection. It has not only a wider frequency band but also lower lower ohmic and dielectric losses than a symmetric directional coupler consisting of three quarter-wave coupled-line segments. Synthesis of such a device requires first determining both minimum and maximum crosstalk attenuation from the mean attenuation and the attenuation range. The wave impedances of the two segments as well as the overlap of the their operating frequency ranges under cophasal excitation are then calculated on this basis. The two transmission coefficients, to the galvanically coupled arm and to the galvanically decoupled arm, are calculated as the respective elements of the scattering matrix $S2_{12}$, $S2_{13}$ (two-segmental d.c.) and $S1_{12}$, $S1_{13}$1 (one-segmental d.c.), the four transmission coefficients for the divider channel being $k_1 = S2_{12}S1_{12}$, $k_2 = S2_{12}S1_{13}$, $k_3 = S2_{13}S1_{12}$, $k_4 = S2_{13}S1_{13}$. A divider built by connecting a two-segmental directional coupler and two one-segmental ones will put out signals with less nonuniformity than will a single directional coupler when its amplitude-frequency characteristic has two maxima located symmetrically on both sides of the center frequency. Figures 2; tables 1; references 3.

UDC 621.391.2

Efficiency of Signal Search by Group of Independent Receivers

907K0260B Kiev IZVESTIYA VYSSHIKH UCHEBNYKH ZAVEDENIY: RADIOELEKTRONIKA in Russian Vol 33 No 3, Mar 90 pp 11-15

[Article by Yu.P. Ozerskiy]

[Abstract] Signal search prior to tracking an object by a group of independent identical pulsed radio range finders on the basis of time delay measurements is analyzed, the search process involving subdivision of a given time period into n narrow segments and selection of the segment most likely containing the response signal of a duration expected to be shorter than any one of those time segments. The efficiency of search by such a group of N range finders, each subject to an independent interference and each receiving the sought signal with the same time delay, is evaluated and then compared with the efficiency of search by a single range finder. The interrogation signals from these range finders, all tracking the same object, are considered to be time diverse within one pulse repetition period. First the same length of search time is allowed for each range finder and the probability of correct detection by each is assumed to be the same. The length of search time is then not being fixed but treated as a random quantity. Three strategies are considered here, the first one being to wait till all range finders have completed the search. This strategy is correct only when all range finders have selected the same time segment and, therefore, does not work here. The second strategy is to track with the one range finder which has completed the search first, assuming a negligible probability of two or more range finders having completed it simultaneously. All possible situations leading to correct detection are analyzed, taking also into account results of continued signal search by the remaining N- 1 range finders and including the false-alarm probability in all. When the probability of two or more range finders completing the search simultaneously is high, then the third strategy will eliminate the ambiguity which will arise when their readings are different. In this case subsequent tracking is begun after J range finders have completed the search and K of them have given identical readings. This strategy is more easily demonstrated with an odd number N of range finders, but can be extended to any number N. This strategy makes the search not only faster but also more reliable than search by a single range finder. References 1.

UDC 621.396.96

Characteristic Functions Describing Random Phase of Radio Signal

907K0260C Kiev IZVESTIYA VYSSHIKH UCHEBNYKH ZAVEDENIY: RADIOELEKTRONIKA in Russian Vol 33 No 3, Mar 90 pp 29-34

[Article by A.F. Karpov]

[Abstract] The characteristic function which describes the stochastic properties of a random phase of a radio signal is derived, first on the basis of the Rice model and then on the basis of the Tikhonov model. The first model is the probability density function of the phase of a narrow- band normal process, which yields the characteristic function of a random phase not directly but after expansion into a Fourier cosine series with coefficients containing the gamma function and a degenerate hypergeometric function. This characteristic function becomes indeterminate at the singular points $v = 0, +/-1, +/-2, ...$ so that l'Hopital's rule must be applied there. The second model is the probability density function of the phase error in a phase-locked automatic frequency control system, which yields the characteristic function of a random phase after series expansion in modified Bessel functions of orders n from 1 to ∞. Asymptotic approximation of the two probability density functions by way of reconciling the respectively derived characteristic functions of a random phase is proposed, and an analytical relation between the parameters of the two models is established on the basis of these approximations which ensures equivalence of the two models so that preference may be given to use of the simpler Tikhonov model. Figures 3; references 5.

UDC 621.391.1

Simultaneous Filtration of Discrete-Continuous Processes in Real Time

907K0260D Kiev IZVESTIYA VYSSHIKH UCHEBNYKH ZAVEDENIY: RADIOELEKTRONIKA in Russian Vol 33 No 3, Mar 90 pp 34-39

[Article by Yu.G. Bulychev and S.A. Pogonyshev]

[Abstract] Filtration of a mixture consisting of a multicomponent discrete-continuous Markov process λ and an additive white Gaussian noise is described which yields the a'posteriori probability density P of such a process with high accuracy, the values of its discrete parameter forming a simple uniform Markov chain for n states and its continuouus parameters satisfying the Fokker-Planck-Kolmogorov differential equation for $\delta P(t,\lambda)/\tau$. Its solution in the Gaussian approximation is not appropriate here, being sufficiently accurate only for large signal-to-noise ratios. Replacing it with the Stratonovich equation for a non-normalized measure $U(t,\lambda)$ and solving the latter numerically by a method based on fast Fourier transformation is shown to not only yield a more accurate result without constraints on the signal-to-noise ratio but also do it in real time. A modification of the Euler method gives a recurrence relation for this equation. The filtration algorithm involves spatial differentiation of this equation with respect to the L operator in the frequency domain, with the aid of Fourier and inverse Fourier transformations, followed by transition from continuous to discrete Fourier transformation and then transition from the non-normalized measure $U(t,\lambda)$ back to the a'posteriori i probability density. The algorithm is applied, for illustration, to synthesis of an

optimum first-order receiver for signals in system with dual phase-shift keying. Figures 2; references 5.

UDC 621.396.67:621.317.1

Method of Determining Phase Center of Antenna

907K0260E Kiev IZVESTIYA VYSSHIKH UCHEBNYKH ZAVEDENIY: RADIOELEKTRONIKA Vol 33 No 3, Mar 90 pp 43-47

[Article by Yu.I. Gridin, A.N. Lukin and I.F. Strukov]

[Abstract] Holographic determination of the phase center of an antenna is outlined, this method being first applied to an antenna which transmits signals with a spherical wavefront. In this case an interferogram is formed by interaction of a plane wave and a spherical one, the latter in the Fresnel approximation, whose family of equal-intensity lines in the recording plane x0y perpendicular to the direction of wave propagation is described by the relation $(x- \mu)^2 + (y- \nu)^2 + 2rx\sin\alpha = 2r(\cos^{-1}C+ 2\pi n- \varphi)/k$, $n = 0,1,2,...$, (μ,ν- coordinates of the phase center, r- distance from phase center to recording plane, α- angle between wavefront of reference oscillations and recording plane, $k = 2\pi/\lambda$, λ- wavelength of signals from antenna, φ- constant phase difference between signals from antenna and reference oscillations, C- constant angle defining the level of equal-intensity lines. The line on which the phase center of the antenna lies is found by dropping a normal to the recording plane from the center of the hologram at $\alpha = 0$, whereupon its third coordinate r is found either from the radii of two fringes, the n-th and the (n+m)-th, according to that relation of by the method of two holograms. In this way the phase center of an antenna can be found without determining the location and the shape of the equal-phase surface of the antenna radiation field. The holographic method can now be applied to real antennas, which do not have a proper phase center but only an "effective" one and which transmit signals with a usually aspherical wavefront. In this case the relation describing the family of equal-intensity lines on the interferogram will be $(x- \mu)^2+ (y- \nu)^2 = 2\lambda r[n+ \cos^{-1}(C-gf)]/2\pi$ and the procedure for determining μ, ν, r, and $\cos^{-1}(C- \varphi)$ must be modified appropriately. The hologram is approximated with a set of connected fringes according to the method of least squares, necessarily including each fringe and most conveniently in a polar system of coordinates, so that determining the coordinates of an "effective" phase center reduces to solving a linear system of algebraic equations. The method was tested experimentally on a 10γ high antenna with a pyramidal having a $4\gamma x4\gamma$ large aperture and transmitting radio waves in the 3 cm band. Figures 4; references 5.

UDC 621.372.832

Matched and Decoupled High-Power Dividers

907K0260F Kiev IZVESTIYA VYSSHIKH UCHEBNYKH ZAVEDENIY: RADIOELEKTRONIKA in Russian Vol 33 No 3, Mar 90 pp 56-59

[Article by L.G. Korniyenko and N.V. Shcherbakov]

[Abstract] The frequency characteristics of multipole microwave high- power dividers, coaxial quarter-wave transmission lines carrying power from a common source to matched loads and each one laid inside an extended quarter-wave insulator tube, are calculated on the basis of the equivalent circuit and the scattering matrix. The latter yields not only the frequency dependence of the reflection coefficient at the input and the transmission coefficient from input to each output as well as of the reflection coefficient at each output but also that of the traveling-wave-ratio (TWR) at the input and at each output. Four different connection schemes are considered and compared, in two of them the load being represented by an equivalent resistance r normalized to the wave impedance of the feeder and an impedance normalized to the wave impedance of the line formed by the outer conductor and the insulator tube. The divider outputs are connected to the inputs of external devices at the opposite opposite side in the first scheme and on the same side in the second scheme. In the third scheme the matching device is a quarter-wave transformer in the input arm of the bridge and in the fourth scheme the output arms are shorted. The first scheme is that of a divider behaving almost like one with ballast resistors which are not grounded. The fourth divider has the narrowest frequency band. The second divider has a better input matching but a worse decoupling of outputs. The third divider has a worse input matching but the best decoupling of outputs. The results of theoretical calculations were checked against the results of measurements made on a divider built according to the third scheme. The agreement was found to be close: input TWR and output TWR agreeing within two percent and five percent respectively, attenuation from input to output agreeing within 0.5 dB. Figures 4; tables 1; references 2.

UDC 621.396.019.4

Sensitivity of Optimum Quasi-Coherent Diversity Reception Algorithms

907K0260I Kiev IZVESTIYA VYSSHIKH UCHEBNYKH ZAVEDENIY: RADIOELEKTRONIKA in Russian Vol 33 No 3, Mar 90 pp 70-72

[Article by V.V. Bortnikov, A.I. Zvyagin and A.V. Romanov]

[Abstract] Algorithms of quasi-coherent diversity reception of phase-shift keyed signals in a channel with fadeout are analyzed for sensitivity to inaccuracy of a'priori data about the quadrature components of such

signals, assuming that these signals can be treated in the approximation of Markov processes with an exponential normalized autocorrelation function and the a'priori data pertaining to the form of the autocorrelation function as well as to the power dispersion and the width of the fadeout fluctuation spectrum. The probability of error in statistically uniform channels is calculated accordingly for the general case. With a Kalman fadeout fluctuation filter installed in each receiver channel, all designed on the basis of presumably known a'priori albeit inaccurate data about the incoming signal, the optimum bandwidth of these filters which will minimize the dispersion of signal estimates is determined analytically according to V.I. Tikhonov. Realization of Kalman filters by open synthesis and construction of the optimum algorithm minimally sensitive to inaccuracy of a'priori data are demonstrated on estimation of the quadrature components of a signal from an amplifier with a given gain and an instrument RC-filter, the sensitivity of this algorithm decreasing as the fadeout rate decreases and as the diversity reception is made more multiple. Next is analyzed the reception of a signal with a Gaussian autocorrelation function rather than a Markov signal by a quasi-coherent receiver, the receiver shown to have a higher interference immunity when it is an optimum one for Markov quadrature components of an incoming signal. Such a receiver is thus a robust one according to the min-max criterion of maximum interference immunity during "worst signal" reception. Figures 3; references 3.

UDC 537.874.6.01

Diffraction of Cylindrical Wave in Impedance-Angle Domain

907K0261A Moscow RADIOTEKHNIKA I ELEKTRONIKA in Russian Vol 35 No 4, Apr 90 pp 707-718

[Article by V.M. Likhachev and A.I. Stashkevich

[Abstract] Diffraction of electromagnetic waves by an impedance wedge is considered, an asymptotic solution to the problem being sought rather than an exact one in terms of the Sommerfeld integral so that physical and geometrical aspects will become more explicitly evident. The problem is first solved rigorously for a dihedron formed by two impedance planes and excited by an infinitely long magnetic current filament parallel to the line of intersection. This solution is then first transformed by representing the Sommerfeld integration contour in the complex impedance-angle plane as a combination of a closed one around the origin of coordinates and two crossover lines extending infinitely. On this basis are then calculated the radiation field and, particularly, the field of surface waves. Numerical calculations reveal that the magnetic field intensity within the shadow region is largely determined by diffraction of surface electromagnetic waves by the dihedron edge, while the interference pattern in the bright region depends largely on the amplitudes of reflected and diffracted waves. Figures 6; tables 2; references 5.

UDC 621.371.333:551.510.52

Effect of Refraction on Propagation of Metric Radio Waves Near Diffracting Horizon

907K0261B Moscow RADIOTEKHNIKA I ELEKTRONIKA in Russian Vol 35 No 4, Apr 90 pp 730-733

[Article by V.A. Kortunov, Yu.M. Strelnikov, and F.V. Kivva]

[Abstract] An experimental extending over the March-October 1985 period was made concerning the effect of refraction on propagation of radio waves in the 1.5 m band. Radio signals from two television centers located in Kursk (route No 1, channel 6) and in Belgorod (route No 2, channel 12) respectively were picked up at a common reception point in Kharkov, the transmitter antennas being 250 m tall and the wave-duct receiver antennas, arrays of seven elements each, being located approximately 30 m above ground level. The 193 km long route No 1 is closed and equivalent to a 105 km long straight distance commensurate with a diffracting horizon. The 70 km long route No 2 is open and reaches the deflection point of the first interference lobe near the radio horizon. Both routes run almost meridionally so that route No 2, practically a segment of route No 1, could be used for estimating the effect of refraction. Measurements were made with narrow-band receivers having a bandwidth of approximately 300 Hz, with quartz stabilization of the heterodynes and image carrier tuning to ensure an up to -60 dB attenuation. Measurements were made in 2-3 sessions lasting 10-15 min each. The index distribution based on these measurements and readings of electric psychrometers in the atmospheric layer extending from 2 m to 30 m along the open route is fairly consistent with the histogram based on both two-beam and diffraction models. Readings along the closed route have yielded the seasonal variation of the attenuation factor at various probabilities of exceeding certain levels of the latter. The scatter diagram of attenuation factor and effective gradient of index values plotted on the basis of measurements is compared with the dependence of the attenuation factor on the effective index gradient calculated by three different methods, namely according the Bucker-Gordon model, according to the Villars-Weiskopf model, and according to the Kalinin-Troitskiy-Shur coherent theory of scattering. The results indicate that over a short period of time the refractive index is not noticeably influenced by structural nonuniformity of the atmospheric ground layer, contrary to the close functional relation between attenuation factor and effective index gradient according to experimental evidence under conditions of far tropospheric propagation of radio waves but reconcilable with the theory of such a propagation by selection of the proper values of parameters within their experimental range. They also indicate that the variability of signals

increases with their level, the Bucker-Gordon model with m = 0 so that $(\Delta\varepsilon/\varepsilon)^2 = Ch^{-m} = C = 1.4x10^{-12}$ (ε and h denoting dielectric permittivity and height of the atmospheric radio channel) most closely fitting a real atmosphere. The authors thank the Meteorological Service at the Kharkov airport for measurements made with sounding balloons. Figures 4; references 10.

UDC 537.874.4.01

Scattering of Electromagnetic Waves by Bodies Near Boundary of Medium

907K0261C Moscow RADIOTEKHNIKA I ELEKTRONIKA in Russian Vol 35 No 4, Apr 90 pp 734-739

[Article by A.Yu. Andreyev, L.I. Bogin, V.O. Kobak, and V.V. Leontyev]

[Abstract] The problem of scattering of electromagnetic waves by bodies located near the boundary of the ambient medium, the ground surface, is solved by treating reflection by the ground surface in the approximation of geometrical optics and scattering by the body in the approximation of physical optics, inasmuch as the Fock method is not applicable to large generally anisotropic bodies and especially those located within the direct field of view. The resultant scattered field appearing at the receiver is calculated according to the "four rays" model, considering a ground surface with a radius of curvature much larger than that of the body surface and than the altitude of that body, its altitude assumed to be much higher than the wavelength of the incident field. The problem reduces to calculation of the effective scattering area in a nonhomogeneous medium, usually much larger than in free space, and equal to the modulus of the complex scattering coefficient squared. It is solved accordingly for a plane electromagnetic wave impinging on a body near a smooth plane surface characterizied by a Fresnel reflection coefficient so that the resultant scattered field at the receiver can be expressed as the sum of three components: field of a wave propagating through free space and arriving from the scatterer directly + field of a wave arriving from the scatterer "image" (antipode) + field of a wave propagating in free space and arriving from the scatterer after reflection by the ground surface. It is thus equal to the sum of two fields when scattering was monostatic or to double one field when scattering was bistatic, referred to free space in each case. Considered are first the simplest case, namely an ideally conducting isotropic scatterer, then a pair of isotropic point scatterers some distance apart along a line deviating by some angle from the vertical and a generally inclined rectangular metal plate. Numerical calculations made for such a plate reveal the dependence of its effective scattering area on its inclination angle and on the altitude of its center. These calculations were made for an H = 0.8 m wide plate scattering $\lambda = 3$ cm waves, its inclination angle being varied from 0 to 1.5° and incident radiation grazing the ground surface at a $\theta = 1.074°$ angle, with the distance h from center of the plate to receiver either 100 m or ∞. The effective scattering area of a plate near a ground surface with a Fresnel reflection coefficient of -1 approaches zero as the grazing angle of the incident waves decreases and does not depend on the altitude of its center but depends on it passing through four maxima in free space when the grazing angle is $\theta = \sin^{-1}(\lambda/2H)$. Figures 5; references 12.

UDC 621.396.96.01

Synthesis of Optimum Radioelectronic Tracking Systems with High Immunity to Additive Interference

907K0261D Moscow RADIOTEKHNIKA I ELEKTRONIKA in Russian Vol 35 No 4, Apr 90 pp 752-758

[Article by V.I. Merkulov]

[Abstract] Synthesis of high-precision radioelectronic tracking systems is considered, the maximally energy-efficient control law being sought which will ensure not only minimum tracking errors but also minimum sensitivity to interference causing large additive distortions of the tracked phase trajectory. The control law must, accordingly, be optimum with respect to an extension of the Letov-Kalman functional which differs from the latter in that its integrand includes the product of a transposed m-dimensional vector by a symmetric nonnegative penalty matrix, the components of the vector representing sensitivity to multidimensional interference and the matrix elements representing penalty for that sensitivity. This optimum law is sought in the class of quadratic forms and the problem of finding it is solved by a modification of dynamic programming which does not require expansion of the state vector. The four-step algorithm, applicable to determinate systems as well as to stochastic ones, yields a law not essentially different than the control law that minimizes the original Letov-Kalman functional, introduction of the penalty matrix adequately correcting the feedback coefficients with respect to components of the state vector as the penalty of tracking inaccuracy is increased. The optimality of this law is proved by calculation of the sensitivity to any interference component, namely by applying the Bellman sensitivity equation to the extended minimizable functional and the control object. The solution is sought again in the class of quadratic forms. References 7.

UDC 621.396.677.01

Interference Immunity and Directional Characteristics of Antenna Arrays with Digital Formation of Directivity Characteristic

907K0261E Moscow RADIOTEKHNIKA I ELEKTRONIKA in Russian Vol 35 No 4, Apr 90 pp 758-767

[Article by A.Ya. Kalyuzhnyy]

[Abstract] Digital formation of the antenna directivity characteristic for space-time processing of wideband

signals is considered, the procedure involving summation of successively delayed voltage signals from all array elements. Besides usual errors associated with time discretization of the input signals, the time delays of input signals are generally not multiples of the time discretization interval so that readings of the "delayed" signal arrival times will be missing at the input to the digital directivity shaping device. These difficulties are overcome in two methods of digital directivity shaping. The spectrum of the output sequence of voltages from the directivity shaper is calculated first, with the aid of a discrete Fourier transformation, whereupon the spectral power density of these output voltage readings is calculated on the assumption that their spectrum is approximately the same as if it had included readings taken over a long but time period. The receiver is then assumed to be located within the far field of the external interference sources. One method of digital shaping accordingly is rounding the delay times to the time discretization interval, which can be done deterministically or statistically. Another method is interpolation of needed signal values missing in the input sequence of voltages to the directivity shaping device. Both linear interpolation and Kotelnikov interpolation are described, the interpolation filters in all channels having in both cases usually deterministic and identical frequency characteristics so that the radiation pattern of the antenna array is also a deterministic one. Figures 6; references 10.

UDC 621.396.2.01

Estimating Space and Polarization Parameters of Pseudorandom- Frequency-Hopping Signals and of Interference by Radiation Receiver

907K0261F Moscow RADIOTEKHNIKA I ELEKTRONIKA in Russian Vol 35 No 4, Apr 90 pp 767-774

[V.V. Nikitchenko and P.L. Smirnov]

[Abstract] Combining pseudorandom frequency hopping with space-and- polarization processing of useful and interference signals by a radiation receiver with an adaptive antenna is considered, for an analysis and a comparative evaluation of the two available wideband and narrow-band approaches to the reception and parameter estimation problem. The essential difference between the two techniques is that while changes in the parameters of interference signals which occur during wideband reception and estimation are determined solely by the dynamics of the interference pattern within the pseudorandom frequency hopping band, during narrow-band reception and estimation the number of interference signals falling within the receiver passband changes from frequency to frequency within the hopping band depending on their direction of arrival as well as on their polarization and overall level. The advantages and the drawbacks of each technique become particularly evident when the relative contributions of useful signal and an interference to a change in space and polarization parameters are compared. The task of an adaptive receiver antenna-discriminator being to distinguish useful radio signals from interference signals on the basis of space and polarization parameters, a comparative evaluation of several methods of estimating these parameters of pseudorandom frequency hopping signals indicates that the simulation method is sufficiently high-speed and thus may be preferable to other methods of estimation such as linear prediction, Fourier transformation, maximum likelihood, eigenvectors, and "thermal noise". The method of space and polarization simulation can be implemented in either wideband or narrow-band version. It is assumed, for demonstration, that the dynamics of a'priori changes in the unknown space and polarization parameters of a signal and interference pattern can be described by a vector which satisfies a multidimensional stochastic differential equation. The feasibility of measuring space and polarization parameters is determined principally by the geometry of the antenna array and the polarization of its elements, generally a space diversity array of differently polarized elements such as a "crow's nest" antenna. Figures 5; references 13.

UDC 621.391.01

Energy Spectrum Characteristics of Pseudonoise Signal Array

907K0261G Moscow RADIOTEKHNIKA I ELEKTRONIKA in Russian Vol 35 No 4, Apr 90 pp 781-786

[Article by N.I. Smirnov and S.F. Gorgadze]

[Abstract] Compound signals of the phase-shift-keyed (PSK) kind and the frequency-shift-keyed with minimum shift (FSK MinS) kind are analyzed for the statistical characteristics of spikes of the spectral power density (SPD), which are found to depend on the transmission mode. Four modes of transmission are comparatively evaluated with respect to statistical characteristics of SPD spikes and effectiveness of their suppression, namely: aperiodic and periodic transmission, transmission with alternation of the basic pseudorandom sequence and the negative one, and transmission with change of pseudorandom sequence after time periods corresponding to duration of one information carrying pulse. The analysis is based on computer simulation of analytical relations describing the spectral power density in the form of sets of multiplicative and additive components. Both kinds of compound signals were generated by using either all $N_E = 63,...,1023$ long M-sequences or by using over 100 recurrently formed sequences and random sequences. Figures 7; tables 1; references 5.

UDC 621.391.01

Estimation of Effect of Multiplicative Interference on Interference Immunity of Fiber-Optic Transmission Systems

907K0261H Moscow RADIOTEKHNIKA I ELEKTRONIKA in Russian Vol 35 No 4, Apr 90 pp 800-804

[Article by I.V. Zadorozhnyy, Ye.R. Milyutin, and Yu.I. Yaremenko]

[Abstract] The performance of fiber-optic transmission systems subject to multiplicative interference is analyzed, as criterion of interference immunity having been selected the mean reception error probability and for estimation of the latter being needed the probability density function of signal intensity fluctuations. Inasmuch as the probability density can be expressed in terms of a gamma distribution, the mean error probability during noncoherent reception is $p = \exp(-kH^2)/2$ (H^2 denoting the signal-to-noise ratio and coefficient k depending on the type of modulation) with multiplicative interference as well as spontaneous noise and crosstalk disregarded but depends on the signal intensity so that $p(I) = \exp(-AI)/2$ ($A = kH_2/I$) with multiplicative interference taken into account. A more explicit evaluation of p(I) involves representation in terms of the Whittaker function and subsequent asymptotic expansion. The estimate of the minimum reception error probability becomes then $[1- kH^2+ (k^2H^4/2 - ...]/2$, this power series in kH^2 converging to $exp^2)/2$. Figures 1; references 10.

UDC 621.385.69

Gyrotron With Electrostatic Lens

907K0261I Moscow RADIOTEKHNIKA I ELEKTRONIKA in Russian Vol 35 No 4, Apr 90 pp 827-831

[Article by T.F. Dikun, A.A. Kurayev, and B.M. Paramonov]

[Abstract] A gyrotron is described which operates with a straight relativistic electron beam shaped in a cavity behind the amplifier and circularly swept by a rotating E_{1i}-mode, H_{1i}-mode, or T_{00}-mode field in the modulator cavity, a symmetric electrostatic lens being formed within the longitudinal-to-transverse velocity conversion space by placement of a zero-current ring electrode coaxially between the modulator cavity and the precollector beam-stalling energy-extracting cavity under a negative potential relative to both. The performance analysis of such a gyrotron is based on a system of three equations describing the motion of electrons in a high-frequency field of both modulator and extractor cavities, the initial conditions being determined on the mode of modulator operation. This system of equations therefore must be solved continuously from the modulator entrance section on, the initial conditions at that section being zero velocity components except the longitudinal one for a thin straight electron beam without scattering of electrons. An analysis of numerical solution reveals that the effect of an electrostatic lens on the velocity conversion process in an adiabatically building up magnetostatic field is to increase its efficiency, owing to the peculiar path of the trajectory along which an electron circulates while advancing through the lens. Figures 3; references 9.

UDC 621.396.9

Relative Radio Navigation

907K0261J Moscow RADIOTEKHNIKA I ELEKTRONIKA in Russian Vol 35 No 4, Apr 90 pp 845-848

[Article by Ye.A. Mosyakov, A.A. Sosnovskiy, Yu.G. Shatrakov, and M.S. Eydelson]

[Abstract] Relative radio navigation for the benefit of sea or air vessels carrying radar equipment is analyzed for accuracy, this method of navigation often not requiring estimation of absolute coordinates but only the relative disposition of of objects located within the same field. As a common technique is considered multistation difference-ranging radio navigation, generally and with three radar stations as a specific case, assuming invariant weather conditions. The mathematical expectation of the error vector are calculated, of a vector representing the error of relative coordinates based on measurement of some radio navigation parameter by each radar station at the same time in the case of a stationary object and at different instants of time in the case of a moving one. By the method of least squares are then calculated other statistical characteristics of this random vector, namely its dispersion and its correlation matrix, assuming mutual independence of instrument errors in each user's equipment and equality as well as independence of all other components of the vector of parameter readings. Theoretically according to this analysis, the readings taken at the same instant of time by two user's radar set sets at the same location within the radio navigation field can differ only by the magnitude of the instrument error. An analysis of experimental estimates confirms this conclusion, a moving surface vessel having been steered to the reference point with its coordinates estimated accurately within 10-30 m on the basis of averaging over a 30 min period and similar experiments performed in the United States with the "NavStar" satellite radio navigation system indicating that an accuracy within about 1 m is attainable with use of centimetric radio waves for landing guidance. Tables 1; references 9.

UDC 621.373.7:621.373.121.131

Discretely Tunable Parametric Oscillator Based on Surface-Acoustic-Wave Resonator

907K0261K Moscow RADIOTEKHNIKA I ELEKTRONIKA in Russian Vol 35 No 4, Apr 90 pp 849-856

[Article by L.V. Rodionov and M.S. Sandler]

[Abstract] A discretely tunable parametric oscillator is described which consists of a multifrequency surface-acoustic-wave (SAW) resonator as the signal stage followed by a tunable idler and a pump generator coupled through a nonlinear reactance. Its main advantages of this oscillator over one with several SAW single-frequency resonators or delay lines and thus discretely tunable by switching from one to another are the much simpler construction and generation of signal much stabler than the pump. As idler and coupling nonlinear reactance can be used an LC-parallel circuit and a varicap respectively. The behavior of this multifrequency SAW resonator and idler plus varicap combination are analyzed theoretically according to conventional circuit theory, considering that such a device with a capacitor capacitance varying at the pump frequency constitutes a negative admittance at the signal frequency. The performance characteristics of such a parametric oscillator are then evaluated on the basis of experimental data, a tunable SAW oscillator on a ST-cut quartz substrate operating at a frequency of 203 MHz having been used as the pump which delivered an output power of 25 mW. The resonator consisted of two short-circuit interdigital reflectors with 200 pairs of bar electrodes each, spaced 1500 wavelengths apart on an ST-cut quartz substrate, and an interdigital transducer with 100 pairs of bar electrodes in the middle. The idler circuit consisted of a fixed inductance a variable capacitance. The idler and the resonator were matched by a fixed parallel inductance loading the interdigital transducer. The reactance of the matching coil at the idler frequency was low while the reactance of the resonator was high so that neither of them influenced the idler circuit. The pump and the nonlinear coupling reactance were matched by an LC-series circuit. A filter consisting of two resistors and three capacitors separated the high-frequency voltage from the bias voltage. The oscillator performance was monitored and its output signals picked up by two interdigital transducers with 25 pairs of bar electrodes each, one at a ⅝ wavelength distance behind each reflector toward the resonator edges. The test results indicate that one of the two requirements for suppression of phase fluctuations in the parametric oscillator, namely a pump signal with a "pure" spectrum, is fulfilled by using a single-frequency SAW oscillator as pump. The other requirement, namely an idler circuit with a bandwidth smaller than the frequency separation between resonator modes, is not easy to fulfill so that some phase fluctuations will occur. Figures 5; references 12.

UDC 537.874.2.01

Synthesis of Two-Reflector Antennas Transforming Plane Waves as Required

907K0261L Moscow RADIOTEKHNIKA I ELEKTRONIKA in Russian Vol 35 No 4, Apr 90 pp 877-879

[Article by E.E. Gasanov]

[Abstract] Transformation of plane waves by two successive reflections is described by a system of two differential equations of geometrical optics and energy conservation respectively in two coinciding Cartesian systems of coordinates, for simplicity assuming that the second reflection puts a wave on a path parallel to its original one. On the basis of this model model is formulated the problem of synthesizing a two-reflector antenna which will transform the wavefront boundary and will have the required gain characteristic. In order to solve this problem, it is necessary to determine the conditions which the wavefront boundary functions must satisfy. Two conditions are found to need to be satisfied by the wavefront boundary coordinates and the intensity gain. The coordinates of the wavefront boundary being functions of time, the characteristic directions are shown to be invariant relative to transformation of the time parameter so that the wavefront boundary functions are characteristic functions when and only when these two conditions are satisfied. Two characteristic directions are found to exist when the gain is negative and none when the gain is positive. As an example is considered transformation of a circular wavefront. The wavefront boundary functions for the general case are best selected with the aid of a computer, unless the right-hand side of the equation of energy conservation admits separation of the two variables (coordinates in the planes of the wavefront). The surface profile of the first reflector is synthesized accordingly and that of the second reflector determined from the requirement the length of the optical path be the same for all rays. Figures 1; references 3.

UDC 621.396.96.01

Synthesis of Nontracking Multichannel Direction Finder Receiving Unknown Signals From Array of Sources

907K0261M Moscow RADIOTEKHNIKA I ELEKTRONIKA in Russian Vol 35 No 4, Apr 90 pp 888-893

[Article by F.M. Andreyev and V.L. Seletkov]

[Abstract] A nontracking M-channel direction finder receiving unknown signals from an array of K sources is synthesized mathematically on the assumption that the angular coordinates, while entirely arbitrary to begin with, remain invariant during the measuring period. Estimates are made on the basis of an M-dimensional

vector representing an l-dimensional sample of a narrow-band process, considering that the angular coordinates of signals may not necessarily be resolvable on the basis of of the Rayleigh criterion. The procedure is essentially an extension of that for synthesis of an M-channel single-source direction finder receiving unknown signals with Gaussian background noise in the channels. Calculations and analysis of the results reveal that the resolving power of such a direction finder will not be appreciably enhanced by simply increasing the number of channels, no matter how large the signal-to-noise ratio is. Rather the closeness to linear mutual independence of the channels, numerically described by elements of the approximation matrix, is shown to determine the maximum attainable resolving power and measurement accuracy. References 5.

UDC 621.385.6.01

Use of Equation of Electron Beam Stability in Optimization of Miniature Microwave Electron Vacuum-Tube Devices

907K0261N Moscow RADIOTEKHNIKA I ELEKTRONIKA in Russian Vol 35 No 4, Apr 90 pp 902-904

[Article by Yu.L. Bobrovskiy, S.R. Zarembskiy, and N.N. Popova]

[Abstract] Inasmuch as optimization of miniature microwave electron vacuum-tube devices involves synthesis of interaction spaces, the equation of electron beam stability in a cylindrical such space is used as basis for optimization of these devices. This equation is generalized so as to be useful for a wide range of applications, whether for electron bunching optimization with respect to density in klystrons or for synchronization of the electromagnetic wave with the electron beam. The equation of stability is reduced to Child's law for the maximum nondestabilizing current and the concept of an "asymptotic" voltage is introduced here, namely the supply voltage for a given beam power below which a given magnitude of the static stability factor can be attained only with a certain combination of supply voltage and length-to-radius ratio but at and above which any combination of supply voltage and length-to-radius ratio will yield only a smaller static stability factor. This asymptotic voltage thus represents the upper bound for the static stability of the electron beam presenting as major constraint on tube design and performance. An expression for this voltage is obtained by letting the ratio of transverse electron transit angle to longitudinal electron transit angle approach zero, this ratio being equal to the length-to-radius ratio, which makes this voltage proportional to the two-fifth power of the ratio of beam power to static stability factor. Figures 1; references 6.

UDC 621.396.67.01

Method of Synthesizing Optimum Antenna Radiation Patterns for Power Transmission by Microwave Beam

907K0318A Moscow RADIOTEKHNIKA I ELEKTRONIKA in Russian Vol 35 No 5, May 90 pp 921-928

[Article by V.A. Vanke, A.A. Zaporozhets, and A.V. Rachnikov]

[Abstract] Use of microwave beams for power transmission from space solar power plants or other remote energy sources is considered, the radiation patterns of transmitter antennas needing to be specially shaped and the efficiency of receiver antennas needing to be maximized for this application. The optimum radiation pattern of such a transmitter antenna, namely the amplitude distribution of electric field intensity in its aperture which will maximize the efficiency of power transmission is synthesized analytically on the basis of the Fresnel-Kirchhoff diffraction theory, calculations by this mathematically simple method yielding sufficiently accurate data on the form of the major lobe and of the nearest side lobes. Along with the efficiency of power transmission are also calculated the surface utilization factors for both transmitter and receiver antenna. The method is demonstrated on discrete staircase antenna arrays, specifically on a 10-step one. Figures 3; references 36.

UDC 621.396.67

Power Transmission by Microwave Beam Over Channel With Radial Field Polarization of Antennas

907K0318B Moscow RADIOTEKHNIKA I ELEKTRONIKA in Russian Vol 35 No 5, May 90 pp 928-933

[Article by V.A. Vanke, A.A. Zaporozhets, and A.V. Rachnikov]

[Abstract] In connection with power transmission from space solar power plants by microwave beams, the amplitude distribution of the electric field in the plane of a transmitter aperture is synthesized for maximum efficiency of such a power transmission and corresponding distribution of the electric field in the plane of the receiver aperture. The problem is simplified by considering transmitter antenna arrays with the number of elements so large and their dimensions so much smaller than the antenna radius that such arrays can be treated as approximately continuous rather than discrete ones. The phase distribution of the electric field is assumed to be a quadratic one and the receiver antenna to be located within the Fresnel region. The problem of synthesis is solved on this basis, the optimum transmitter antenna array being sought as one with an amplitude distribution in its aperture describable by a Zernike polynomial

series. The efficiency of power transmission, the surface utilization factors for both transmitter (A,a) and receiver (R,r) antennas, also the maximum levels of the nearest side lobes have been calculated accordingly as functions of a wave parameter $\tau = (\pi R_a R_r/\lambda D$ (wavelength, D- distance between antennas). For a performance analysis of such a power transmission system operating typically at the 12.25 cm wavelength, numerical calculations were made for transmitter antenna and receiver antennas with radial field polarization separated by a distance of 36,000 km. The maximum power density was assumed to be 23 kW/m^2 on the transmitter antenna and 23 mW/cm^2 on the receiver antenna. A comparative performance evaluation of different variants of such power transmission channels must also include a cost analysis, for which the Kerwin-Jezewski-Arndt formula for unit cost in $/kw.h (PROCEEDINGS, INTERSOCIETAL ENERGY CONVERSION ENGINEERING CONFERENCE in N.Y. 1981, Vol 1) is proposed. Figures 3; tables 1; references 15.

UDC 621.391.01

Robust Invariant Detection and Discrimination of Signals

907K0318C Moscow RADIOTEKHNIKA I ELEKTRONIKA in Russian Vol 35 No 5, May 90 pp 1021-1028

[Article by V.A. Bogdanovich]

[Abstract] Robust detection and discrimination of signals on the basis of a sample consisting of n independent readings is considered, the form of the signals $\theta S^{(k)}$ with k = 1,...,m and with the energy parameter θ in $(0,\infty)$ set assumed to be known. The problem is treated as one of testing two hypotheses, whether the sample represents an interference distribution characterized by some scale factor and some bias or represents a distribution of signal+interference mixture also characterized by some scale factor and some bias. The problem of detector synthesis is solved by the min-max technique, the decision rule for the detector to be invariant relative to both scale factor and bias. The mean missed-signals probability is, moreover, to be invariant relative to a'priori probabilities of signals, inasmuch as their probabilities are rarely a'priori given. Correlation detectors asymptotically optimum with respect to the decision rule and particularly M-detector are considered, the false-alarm probability here being invariant and thus dependent on neither the scale factor nor the bias. References 8.

UDC 621.373.5:621.382.2.029,64

Power, Phase, and Noise Characteristics of Injection-Locked Si and GaAs IMPATT-Diode Oscillators

907K0318D Moscow RADIOTEKHNIKA I ELEKTRONIKA in Russian Vol 35 No 5, May 90 pp 1044-1053

[Article by Ye.M. Gershenzon, A.A. Levites, L.A. Plokhova, and A.I. Smetanin]

[Abstract] The performance of externally injection-locked IMPATT-diode oscillators is analyzed on the basis of a model of such a diode and its equivalent series circuit which consists of an impedance representing the space-charge region and a resistance lumping all losses in the base region, the oscillator tank circuit being represented by an equivalent LC-series combination. Their performance is characterized essentially by the power delivered to a resistive load, the phase difference between locking signal and locked signal, and the spectral densities of noise which consists principally of amplitude and frequency fluctuations. For theoretical calculations, all these characteristics are expressed through both amplitude and phase of the load current. Its amplitude and phase as well as their fluctuations are assumed to be slowly varying functions of time, with the variance remaining much smaller than the average amplitude and phase respectively Regarding the space-charge region, its resistance is assumed to be frequency-independent and its reactance is assumed to be a capacitive one and thus inversely proportional to the oscillator frequency. Only avalanche noise is taken into consideration, its in-phase and quadrature components being noncorrelated, and the contribution of low-frequency noise to high-frequency noise through "up-down" conversion is ignored. The theoretical data are compared with experimental ones, three GaAs and one trial Si IMPATT-diode oscillators having been tested. The experimental data are based on measurements covering capacitance of the p-n junction, breakdown voltage, differential resistance, running current, starting current under conditions of a weak coupling to the load and under conditions of a selected coupling to the load, and external Q corresponding to the starting current in the latter case. The quantitative agreement between calculations and measurements is fairly close as long as measurements are made with the oscillator operating in the single-frequency mode, the discrepancy between them widening appreciably otherwise. Figures 5; tables 1; references 10.

UDC 621.371.36

Effect of Earth's Nonhomogeneous Ionosphere on Accuracy of Satellite Trajectory Measurements

907K0318E Moscow RADIOTEKHNIKA I ELEKTRONIKA in Russian Vol 35 No 5, May 90 pp 1081-1084

[Article by V.A. Andrianov, V.A. Arkhangelskiy, V.V. Bobrov, A.I. Yefimov, and V.I. Rogalskiy]

[Abstract] Passage of satellite radio signals through Earth's nonhomogeneous ionosphere is analyzed for the resulting fluctuation errors in their phase and frequency measurement along their trajectory, taking into account not only the relevant characteristics of several different satellites (1963-38C, Maritime Navigation Satellite, P76-5) but also the parameters of various measuring methods which use different carrier frequencies (162 MHz, 1620 MHz or other frequency within the 1-2 GHz

range) and the transfer function of a typical measuring instrument. In addition to phase and frequency fluctuations, are accordingly also considered fluctuations of the distance to the satellite and fluctuations of its radial velocity. The calculations are based on analytical expressions for their r.m.s. values, the spectra of phase fluctuations being quite closely approximated with power functions in the range of high Fourier frequencies and their spectral density being almost uniform in the range of low Fourier frequencies. Tables 2; references 9.

UDC 621.396.6:681.3.06

Algorithm for Analysis of Quasi-Periodic Processes in Nonlinear Radio Engineering Systems

907K0330A Kiev IZVESTIYA VYSSHIKH UCHEBNYKH ZAVEDENIY: RADIOELEKTRONIKA in Russian Vol 33 No 6, Jun 90 pp 12-17

[Article by V.N. Lantsov and A.S. Merkutov]

[Abstract] An algorithm is constructed for analysis of quasi-periodic processes in nonlinear radio engineering systems and particularly microwave devices, as a part of the radio circuit design procedure. It is based on equations of harmonic balance, the method of least squares being used for determining the spectral composition of the current in a nonlinear circuit component under a quasi-periodic voltage and Newton's method being combined with analytic continuation for finding the roots of equations parametrically. The discrete formalism of nonlinear relations is applied to sine and cosine transforms, voltages being sought in the form of generalized Fourier series and their spectral composition being found through analysis of a linear multipole network in the frequency domain by the method of node potentials. The 14-step algorithm was applied to a single-stage transistor amplifier and its performance analysis in two modes of operation on the basis of the Ebers-Moll model. First was considered a linear two-frequency small-signal mode with an input voltage consisting of two components, 87 MHz and 100 MHz, of 0.01 V amplitude each and with a bias voltage of -0.2 V. This mode was analyzed with the aid of Volterra series. Next was considered a single- frequency large-signal cutoff mode with a 100 MHz input voltage of 0.5 V amplitude. The algorithm has been programmed for a Standard System 1045 computer. Figures 1; tables 2; references 4.

UDC 621.396.6

Formalization of Macromodeling Process for Analog Integrated Circuits

907K0330B Kiev IZVESTIYA VYSSHIKH UCHEBNYKH ZAVEDENIY: RADIOELEKTRONIKA in Russian Vol 33 No 6, Jun 90 pp 50-55

[Article by V.F. Gerasimenko and A.S. Kabak]

[Abstract] One possible way of formalizing a macromodel of analog integrated circuits is proposed, beginning with classification of leads into four groups: 1) input leads receiving electric signals to be processed by the circuit, 2) output leads to user of processed signals, 3) corrective leads to external circuits which influence processing of input signals, 4) parametric input leads transmitting external electrical or nonelectrical influencing actions. The model must include leads of groups 1) and 2), some of those of group 3) are optional, and inclusion of leads of group 4) is not advisable inasmuch as it would complicate and more ill-condition the model. The next step is synthesis of the macromodel in two stages, synthesis for the linear mode of operation followed by incorporation of nonlinear effects without structural modification. Construction of the macromodel in the form of an equivalent multipole electric network is proposed, in preference to a system of equations, the process then reducing to synthesis of such a network on the basis of an available Y or Z matrix whose elements y_{ij} or $_{ij}$, with the required degree of accuracy, describe given y or z elements of the circuit. The next step is setting up equations of the $H_{ij} = \Delta_{ij}/D$ kind which relate primary and secondary parameters of the linear circuit, H_{ij} denoting the transfer function between i and j nodes, D denoting the determinant of the matrix of primary parameters x describing the sought elements, and Δ_{ij} denoting the algebraic complements of that matrix, whereupon equations of the same kind are set up for the secondary parameters. Taking into consideration ill-conditioning of the problem, the system of equations is then solved by first reducing it to the operator equation Ax = y (A- operator over the primary parameters defined within the region D(A) with values within the set R(A) of solutions based on the set I of possible input data values y). The selection of input data must be based strictly on minimum sensitivity of the solution to variation of given secondary ỹ parameters from the set of solutions. References 7.

UDC 681.325.65:621.3.049.77

Method of Designing Circuits of Clocked Triggers

907K0330C Kiev IZVESTIYA VYSSHIKH UCHEBNYKH ZAVEDENIY: RADIOELEKTRONIKA in Russian Vol 33 No 6, Jun 90 pp 61-66

[Article by Yu.I. Rogozov]

[Abstract] The principle of ratios is considered relative to circuit design for large-scale integration, where the values of parameters of identical components can vary over an up to 15 percent range from chip to chip while the ratio of their values on one chip must be maintained within a 0.01 percent tolerance. Logic arithmetic is treated from this standpoint so that, since the difference between the sums of two arguments (a_i, b_i) which determine the j-th predicator p_j of the generated logic function

must be equal to 0 or 1, the arithmetic operation of subtracting becomes equivalent to the operation of comparing and thus ratioing the sums of input arguments. A method of applying this principle together with the principles of differentiation and integration is proposed, and demonstrated on the circuit design of clocked triggers. An ideal D-trigger is regarded as a combination of a main trigger and an auxiliary one connected in series, the latter one built with conventional NAND or other logic elements but the main one requiring new logic arithmetic element $\&(\tau)_i$-NOT with a controllable time delay $\tau = f(D,C,Q)_{t-1}$ (function of input variables and of the state of the auxiliary trigger). The circuit of the main trigger circuit is designed on the basis of time ratios, which can be implemented by stipulation of switching delay according to a physical process such as current flow. The design procedure begins with selection of the analytical expression describing the trigger structure in conventional circuit terminology, selection of the types of elements optimally covering the logic functions in that expression. The equations of trigger operation are selected by optimal balancing of two criteria. The number of ratios between currents I_1 and I_2 is maximized by exclusion or minimization of the logic module while technological capabilities limit that maximum number. The procedure is demonstrated on the design of a bipolar D-trigger which performs an addition and a subtraction according to an equation containing two ratios: $I_1/I_2 = I_{n1}/I = T_1/T_2 < 1$ ($D = 0$, $I_y = 0$) and $I_1/I_2 = (I_{n1} + I_y)/I_{n2} = (T_1 + I)/T_2 > 1$ ($D = 1$, $I_y = 1$), where $I_1 = I_y + I_{n1}$ and $I_2 = I_{n2}$ are respectively the levels 1 and 2 of the direct current. The method allows for changing the number of current ratios. The design by this procedure is analyzed for a D-trigger built on transistor-transistor logic. It consists of two invertor transistors VT1-2 and two conjunctor transistors VT3-4, two resistors R_1 and R_2 acting as direct-current sources T_1 and T_2 respectively, and a another transistor VT5 with another resistor R5 forming the controllable source of current I_y. A comparison of this design with the design of a trigger involving only one current ratio indicates that the chip area can be decreased by decreasing the number of interconnections. It also indicates that parasitic time delays of invertor switching can be utilized for raising the trigger efficiency. Figures 5; tables 1; references 4.

UDC 621.382.82.001

Computer-Aided Modeling of Structures With Uneven Boundaries

907K0330D Kiev IZVESTIYA VYSSHIKH UCHEBNYKH ZAVEDENIY: RADIOELEKTRONIKA in Russian Vol 33 No 6, Jun 90 pp 71-73

[Article by Mulyarchik, A.V. Popov, and V.G. Solovyev]

[Abstract] Automation of two-dimensional numerical modeling of microelectronic elements with nonplanar boundaries is analyzed, two key problems being constructing the space discretization grid and setting up linear systems of equations solvable by iterations of the Hummel kind. The problem with constructing the space discretization grid is that two contradictory requirements need to be satisfied, namely that the number of nodes must not be to large so as not to excessively raise the order of the system of linear algebraic equations but sufficiently large to correctly describe the solution and the nonplanarity of boundaries. Considering that nodes of the grid must lie on continuous boundaries, it is proposed to construct a continuous rectangular grid with triangular elements by drawing lines parallel to the Y-axis through points where lines parallel to the X-axis intersect nonplanar boundaries and drawing lines parallel to the X-axis through points where lines parallel to the Y-axis intersect nonplanar boundaries. In order to avoid indefinite drawing of lines, in the case of asymmetry, or even an excessive density of lines in the case of symmetry, lines are not drawn at distances smaller than some given length from already existing ones. The problem with setting up the system of linear algebraic equations is that for each node of the grid one must know about existence of boundaries running along diagonals of the corresponding discretization cell. For approximation of the dopant distribution, therefore, a data array should be used each element of which contains information about existence of a diagonal boundary in the upper left quadrant of the corresponding discretization cell and also about its orientation. The program of two-dimensional modeling of integrated-circuit components by this method is designed to solve discrete analogs of the equations of continuity for electrons and holes and the Poisson equations, all of which having been linearized to the form $Ax = B$. The coefficients in this system of linear algebraic equations are calculated by adding the contributions of the quadrants of a discretization cell. The program is universal in so far as various different boundary conditions can be accommodated in one algorithm of computer-aided solution of that system of equations. Figures 3; references 5.

UDC 621.317.7

Digital Multichannel Maximum-and-Minimum Meter

907K0167C Novocherkassk IZVESTIYA VYSSHIKH UCHEBNYKH ZAVEDENIY: ELEKTROMEKHANIKA in Russian No 3, Mar 90 pp 92-95

[Article by Valeriy Petrovich Grinchenkov, candidate of technical sciences, docent, Novocherkassk Polytechnic Institute, Petr Yefimovich Sergiyenko, candidate of technical sciences, department manager, and Valeriy Petrovich Chernov, engineer, All-Union Scientific Research Institute of Electric Drives]

[Abstract] A multichannel instrument which includes a high-speed analog-to-digital converter and sequential scan of measuring channels has been developed for simultaneous real-time determination of the global maximum and minimum in each channel. It combines a significant economy of hardware with high accuracy of data recording and storage. It consists of a clock pulse generator, a synchronizer, a digital commutator switch, an address counter, an analog commutator switch, a high-precision detector, a sign comparator, an analog-to-digital converter, an initial recording stage, a memory space control, a recording control, a memory, and a digital comparator. The pulse generator and analogously the synchronizer can be blocked when a "sample/readout" signal appears at the generator input. The operation of the instrument, maximum-and-minimum recording in each channel followed by feeding the read values to a data processing device, can be controlled by three signals from a microcomputer: "sample/readout", "clock pulse sequence", "reset". The microcomputer can also be used for subsequent data processing. The sign comparison cycle is followed by storage in the memory of the code which the A-D converter has generated, if: 1) a memory space has been allocated for minimum values of the measured signal and the converter output code is shorter than the code of the measured quantity stored in the memory; 2) a memory space has been allocated for maximum values of the measured signal and the converter code is longer than the code of the measured quantity stored in the memory. Initial recording is included in the instrument, to prevent codes longer than the dynamic range of signals from entering the memory by storing in the latter all data except comparator data. The instrument was tested and found to be accurate within 3 percent during measurement with a 1000 Hz signal repetition rate in each channel. Figures 1; references 4.

The XXXVI International Exhibition-Competition

907K0182b Moscow ELEKTRICHESKAYA I TEPLOVOZNAYA TYAGA in Russian No 2, Feb 90 p 44

[Article by S. L. Dovgvillo]

[Abstract] This study reports the events at the XXXVI International Model Railroad Exhibition-Competition Sponsored by the Brno (Czechoslovakian Soviet Socialst Republic) Model Railroad Club. Model railroad enthusiasts from Hungary, the German Democratic Republic, Poland, the USSR, and Czechoslovakia participated in the competition. More than 150 papers were presented to the international judges. These include operating rolling stock models from steam-driven engines through modern electric and diesel locomotives. The twelve-member judge panel reviewed each model and prototype in 14 categories and subcategories. Forty-four exhibits were awarded prizes.

The VL10U Electric Train: Electrical Circuit Troubleshooting

907K0182a Moscow ELEKTRICHESKAYA I TEPLOVOZNAYA TYAGA in Russian No 2, Feb 90 pp 19-22

[Article by V. S. Artsybashev, A. V. Orlov]

[Abstract] This is a continuation in a series of articles devoted to the service and maintenance of the VL10U electric train. This article discusses fault localization and troubleshooting of electrical circuitry including the low-voltage current pick-off circuits, failures in the low-voltage circuits of auxiliary equipment, failures in the motor compressor control circuitry, faults in the BB-1 low-voltage network, and first position network failures. In addition to various fault localization and troubleshooting procedures, the article provides step-by-step instructions for troubleshooting and repair operations of these and other equipment.

UDC 621.313.322:621.319

Efficacy of Charging Devices for High-Voltage Capacitive Energy Storage Banks

907K0267B Novocherkassk IZVESTIYA VYSSHIKH UCHEBNYKH ZAVEDENIY: ELEKTROMEKHANIKA in Russian No 3, Mar 90 pp 88-91

[Article by Boris Vladimirovich Gandybin, candidate of technical science, deputy director of educational and research activity at Interdisciplinary Institute of Personnel Upgrading and Retraining, Robert Yakovlevich Klyayn, candidate of technical sciences, docent, Vitaliy Ivanovich Popov, candidate of technical sciences, docent, and Konstantin Aleksandrovich Khorkov, doctor of technical sciences, professor, Tomsk Polytechnic Institute]

[Abstract] Four types of 3-phase charging devices for high-voltage capacitive energy storage banks are evaluated, namely a 3-phase step-up transformer: 1) followed by a capacitor-diode voltage multiplier, 2) preceded by an inductive-capacitive voltage pretransformer and followed by a diode rectifier bridge, 3) preceded by a 3-phase saturable reactor and followed by a diode rectifier bridge, 4) preceded by a 3-phase thyristor bank and followed by a diode rectifier bridge. As the criterion of comparison has been selected the composite design and performance indicator $K = W\eta/Mt$ (W- energy transferred to storage capacitor bank, η- integral efficiency of charging device, M- mass of charging device, t- charging time). They are also compared with charging devices which do not include the intermediate 3-phase step-up transformer but operate directly from a high-voltage synchronous generator, such schemes offering significant advantages in terms of smaller mass and higher efficiency. A comparison of a salient-pole generator construction and a cylindrical one relative to mass of active materials, overall mass, and specific storage of kinetic energy reveals significant advantages of the salient-pole construction. Figures 5; tables 3; references 4.

Decreasing Interference From External Sources in K-60p Transmission System Channels

907k0289a Moscow AVTOMATIKA, TELEMEKHANIKA I SVYAZ in Russian No 5, May 90 pp 20-23

[Article by V. I. Kurgalkin]

[Abstract] In addition to thermal noise and crosstalk interference, the high-intensity electromagnetic fields created by high-voltage AC transmission lines and railroad contact systems, various types of radio stations, and lightning discharges are sources of interference for audio-frequency channels. Ways of reducing the effect of these sources on cable communication lines are considered: elimination of the interfering effect of radio stations on cables lines, interference suppression by countercoupling circuits, and interference suppression by balun circuits. Methods of checking the protection efficacy and locating interference sources in aluminum-sheathed cables, primarily in the cable sleeves, are described. Procedures for coordinating radio station frequency plans with the location of unmanned cable communication line repeater stations and cable routes are suggested. Figures 7, tables 1.

UDC 656.254.16:621.372.8

Combined Train Radio Communication Bypass Waveguide Line

907K0289B Moscow AVTOMATIKA, TELEMEKHANIKA I SVYAZ in Russian No 5, May 90 pp 31-32

[Article by V. P. Gurtovenko, Shevchenko Division of the Odessa Railroad]

[Abstract] High-voltage automatic interlocking lines are often used as waveguides; when the interlocking system power supply line is cabled, bypass waveguide lines must be used. The 1.8-km-long cable insert used as the bypass waveguide line in order to insure reliable radio communication along a section of the railroad at the Viska station is described; it is made of clad metal communication line wires which are energized in antiphase by induction with the help of the ASU-ZhR-3M antenna matching device. The driving wires are suspended 0.6 m from the aerial interlocking system wires. Methods of tuning the bypass waveguide lines are described. The combined waveguide line has been in operation for three years and has demonstrated is ability to insure stable and reliable radio communication between trains and fixed radio stations. Figures 1.

UDC 621.315:621.3.029.7

Optical Fibers for Fiber Optic Lines

907k0313a Moscow AVTOMATIKA, TELEMEKHANIKA I SVYAZ in Russian No 6, Jun 90 pp 9-12

[Article by V. V. Vinogradov, V. N. Nuprik, Leningrad Railroad Engineers Institute]

[Abstract] The experience of developing fiber optic cable communication systems shows their great advantage over conventional lines. The discussion of the structure of optical fibers and fiber optic cables manufactured by the domestic industry as well as their design and electric parameters which began in ATiS No. 1, 1990 is continued. The physical processes occurring in fiber optic waveguides, especially those made of quartz glass and polymers, the parameters and designs of trunk, area-wide, city-wide, and installation-wide optical cables, and the performance requirements of optical communication cables are examined. Approaches used in developing the specifications of various types of fiber optic cables for railroad communication networks are considered. It is shown that the development and production of optical cables by the domestic industry will greatly increase the operational reliability of trunk fiber optic communication lines. Figures 7; tables 1.

UDC 656.4:656.257-83

Improved Control Circuit of All-Electric Interlocking Switches in Industrial Railroad Transport

907k0313b Moscow AVTOMATIKA, TELEMEKHANIKA I SVYAZ in Russian No 6, Jun 90 pp 25-27

[Article by M. Z. Gurgenidze, G. P. Zgudadze, G. A. Lomtatidze, T. Sh. Iashvili, Georgian Polytechnic Institute]

[Abstract] The analysis of switch control in all-electric interlocking switches in industrial railroad transport which began in ATiS No. 3, 1987 is continued. The design of enlarged trigger units and trigger circuits used for controlling all the switches in a yard neck and their typical shortcomings are examined. A new trigger circuit design which is free of these shortcomings is suggested by the authors. The improved electric switch drive control circuit with one trigger equipment set makes it possible to operate a single switch and eliminates the danger that other switch drives may operate until one working algorithm is executed. The circuit also makes it possible to transfer any switch to any position regardless of the trigger relay's initial state and return the switch to the initial position simply by pushing one's own switch button; the other switches remain unaffected. Prototype tests confirmed the high degree of the new circuit protection from dangerous failures resulting from incorrect operator actions. Figures 1, tables 1.

UDC 656.25:621.315:621.316.9

Combined Cable Communication Line Protection Method

907k0313c Moscow AVTOMATIKA, TELEMEKHANIKA I SVYAZ in Russian No 6, Jun 90 pp 28-29

[Article by V. M. Sorokin, Wire Communication Department at the USSR Railroad Ministry Directorate of Signaling Control, Communication, and Computer Equipment]

[Abstract] The discussion of automation device and communication cable protection from dangerous effects of AC electric railroads which began in ATiS No. 4, 1990 is continued. A combined method of protecting communication lines with the MKPAShp-7x4x1.05+5x2x0.7 cable from the effect of AC electric traction using OSGR-4x4/8 reduction transformers, FZ-1 protection circuits, remote power supply filters, isolation transformers, and low-pass filter input protection units is examined. The combined method was developed by experts from the Minsk Branch of the Transelektroproyekt Institute and the All-Union Science Research Institute of Railroads for protecting high-frequency trunk lines multiplexed by the K-60p equipment, as well as selective communication lines and signaling and all-electric interlocking systems. Dangerous and interfering voltages and protection measures were analyzed for one section of the South-Eastern Railroad to be switched to AC traction. Figures 6.

Analysis and Outlook for Reducing Accident Rate

907k0312a Moscow ELEKTRICHESKAYA I TEPLOVOZNAYA TYAGA in Russian No 6, Jun 90 pp 2-4

[Article by B. N. Zimting, ETT correspondent]

[Abstract] Chairman of the Locomotive Teams and Locomotives Management Department at the USSR Ministry of Railroads A. M Krivnoy discussed the causes of some industry failures with an ETT correspondent. In 1989, the volume of shipments was 99.1 percent of target, labor productivity rose 1.1 percent vs. a target of 5.7 percent, operating cost overruns reached 79 million rubles, first quarter 1990 targets were not met, and the safety record did not improve over 1988: there were 12 crashes resulting in two deaths and a loss of 2.4 million rubles. Mr. Zimting described the circumstances of some accidents and their possible causes, primarily poor maintenance and lax discipline; he specifically singled out long working hours, excessive overtime, and the lack of basic amenities. He expects that implementation of computers, automatic safety control systems, and new management methods will improve railroad safety.

UDC 621.336.332.004.5:621.337.2

ChS4 Electric Locomotive: Fixing Electrical Circuit Faults

907k0312b Moscow ELEKTRICHESKAYA I TEPLOVOZNAYA TYAGA in Russian No 6, Jun 90 pp 14-16

[Article by Yu. N. Sokolov, V. I. Khomchik, Kiev Passenger Depot, Southwestern Railroad]

[Abstract] The most common locomotive malfunctions and ways of dealing with them are discussed. Suggestions are made for diagnosing and fixing problems in the following units: current collectors, cam switches, and contact system; traction engines and reversal circuits; acceleration circuits; piston engine air-pressure and mechanical components; piston engine control valves; deceleration circuits; automatic safety circuit breakers; interlocking system grounding; relay circuit grounding; and auxiliary motors. The suggestions are expected to be helpful to young engineers and their assistants.

Circuit Designs of the ER2T Electric Train

907k0312c Moscow ELEKTRICHESKAYA I TEPLOVOZNAYA TYAGA in Russian No 6, Jun 90 pp 16-19

[Article by B. K. Prosvirin, Engineer-Instructor at the October Railroad Moscow Depot]

[Abstract] A fourth article in a series which began in ETT Nos. 3, 4, and 5, 1990. A general description of the design, function, and operation of the following ER2T electric locomotive components is given: control circuit power supply sources; auxiliary compressor circuits; current collector control circuits; and converter start-up circuit. To be continued in subsequent ETT issues. Figures: 7.

Circuit Designs of the 2TE10Ut Diesel Locomotive

907k0312d Moscow ELEKTRICHESKAYA I TEPLOVOZNAYA TYAGA in Russian No 6, Jun 90 pp 20-23

[Article by V. P. Gayvoronskiy, S. N. Petrushchenko, Voroshilovgradteplovoz Production Association and Locomotive Facilities Department of the USSR Ministry of Railroads]

[Abstract] Circuit 2179.70.01.000 E3 for the new 21TE10U[u] diesel locomotive whose batch production began at the Voroshilovgradteplovoz Production Association is a modified version of the TE10M locomotive's circuit 2139.70.01.005 E3. The new double-unit locomotive, a modification of the TE10M model, has a design speed of 120 km/h and is intended for both freight and mail trains because of its electrical compressed air brakes. It is also equipped with a new GP-311BMU2 traction generator which is a modified version of the GP-311B, enabling it to deliver up to 26 tf of traction per unit. The power circuit, diesel start-up procedures, traction generator power and cooling chamber control procedures, electrical instruments, fire alarms, and the automatic locomotive safety indication system are described in detail. To be continued. Figures: 3.

UDC 681.3.02

Principles for Increasing Logical Modeling Adequacy of Digital Integrated MIC and CMIC Circuits

907k0158a Kiev ELEKTRONNOE MODELIROVANIE in Russian Vol 12 No 1, Jan 90 pp 60-64

[Article by V. N. Kozlov, V. V. Khatylev, Riga]

[Abstract] The level of integration of modern VLSI circuits has risen dramatically due to advances in microelectronics. Such VLSI circuits can be designed only on computers by using specialized CAD systems which incorporate electrical (circuitry) and logical modeling subsystems. Peculiar features of modeling metal-insulator-conductor and complementary metal-insulator-conductor circuits at their gate-transistor representation level and the principles of increasing the logical modeling adequacy of such circuits are examined. Since an analysis of a large number of various circuits shows that VLSI circuits on the basis of both MIC and CMIC technologies have similar characteristics and peculiarities, only the MIC circuits are examined. The results are extended to CMIC circuits without significant modifications. The multi-layer model hierarchy makes it possible to describe and simulate digital circuits on a scale of up to 100,000 equivalent gates or 70,000 transistors in the framework of the software used in the analysis. A 50,000-gate model occupies 6.8 Mbytes of memory while the modeling time per one input set is 0.48 s without writing the results into a library and 3.3 s with writing. References 6: 5 Russian, 1 Western; figures 6; tables 2.

UDC 681.3

Programmable Logic Structure Test Diagnostics

907k0158b Kiev ELEKTRONNOE MODELIROVANIE in Russian Vol 12 No 1, Jan 90 pp 64-68

[Article by A. Ye. Lyulkin, Belorussian State University, Minsk]

[Abstract] The use of LSI circuits with a logic structure (programmable logic arrays, PROMs, programmable logic arrays with memory) in the development of various computer and control system devices makes it possible to increase the dimension of problems formally solved at the design stage, employ standard circuit designs, and shorten the design time. The properties of faults in such programmable logic structures as well as in multiplexers and other devices and various test diagnostics methods are examined. The results show that by analogy with programmable logic arrays, in solving the problems of test diagnostic of digital devices with programmable logic structures, an analysis of just the installation and relocation faults would suffice, making it possible easily to modify the automated diagnostic test facilities for use with other digital devices and other types of programmable logic structures. References 12: 11 Russian, 1 Western; figures 1.

UDC 681.324:658.52.011.56

Increasing Authentication Service Computer Network Survivability

907k0158c Kiev ELEKTRONNOE MODELIROVANIE in Russian Vol 12 No 1, Jan 90 pp 99-100

[Article by L. M. Ukhlinov, Moscow]

[Abstract] Computer network authentication services control access of users to data distributed in a network and are executed as an added software feature at an open system interaction benchmark model session layer; they also interact with the representation and transport layers. Access is controlled during the logical interconnection process. All checks are based on the access control information which is stored by the authentication service and is transmitted between network nodes if necessary. A criterion is suggested for evaluating the authentication service survivability which considers the requirements for the probability of recovering and keeping the confidentiality of access control data. A method of selecting an optimal version (relative to the proposed criterion) data distribution arrangement for restoring internal authentication service data if they are distorted or erased is examined. The proposed methods can be used to determine the optimal ratio of authentication service data distribution parameters in order to increase its survivability allowing for the network nodes' probability features. References 7: 2 Russian, 5 Western; tables 1.

Third Regional Seminar on 'Distributed Data Processing'

907k0158d Kiev ELEKTRONNOE MODELIROVANIE in Russian Vol 12 No 1, Jan 90 pp 108-109

[Article by M. S. Tarkov]

[Abstract] On 2-6 July 1989, the third regional seminar on distributed data processing was held in Ulan-Ude; it was organized by the Siberian Branch of the USSR Academy of Sciences, the Siberian Territorial Group of the Soviet National IMACS Committee, the Novosibirsk oblast directorate of the Scientific and Technical Society of Radio Engineering, Electronics, and Communications imeni A. S. Popov, the Semiconductor Physics Institute at the Siberian Branch of the USSR Academy of Sciences, and the Eastern Siberian Technological Institute. Today's state and efficient ways of developing, implementing, and using distributed data processing and parallel application-oriented signal processing computer systems were discussed at the seminar. Experts from 12 cities representing 38 organizations participated in the seminar and presented 64 reports to two sections dealing with architectural concepts of parallel computer systems, application-oriented image processing systems, parallel

computation methods, methods of developing parallel algorithms and parallel programming languages, distributed decentralized operating systems, computer system elements and units, computer system reliability, survivability, and diagnostics, and parallel computer system operating experience. The seminar recommended that the best reports be published in periodicals. The fourth All-Union distributed data processing seminar is tentatively scheduled for 1991.

UDC 621.865:681.3

Plotting Speedwise Optimum Trajectory for Travel of Manipulator Robot

907K0168A IZVESTIYA VYSSHIKH UCHEBNYKH ZAVEDENIY: ELEKTROMEKHANIKA in Russian No 11, Nov 89 pp 31-36

[Article by Mikhail Borisovich Krivonogov, candidate of technical sciences, docent, Tula Polytechnic Institute]

[Abstract] The problem of plotting the optimum control trajectory for a robot to ensure the fastest manipulator travel along a given geometrical trajectory is solved on the basis of the PUMA-560 manipulator model with hinge joints, which includes not only kinetic energy and moments of gravitational forces but also moments of Coriolis and centrifugal forces. The geometrical trajectory is defined by a sequence of reference points in a generalized system of coordinates and, for simplification, in a parametric form with displacement along the trajectory selected as the parameter and with an Lagrange interpolation polynomial converting discrete functions of displacement into continuous ones. Differentiation of the matrix equation of manipulator dynamics and of the equation of manipulator motion yields the system of second-order differential equations which is to to be solved. The algorithm of the solution consists of six steps: 1) integration with respect to time from point zero (zero velocity and maximum acceleration) to intersection with the limit curve, 2) integration in the reverse direction from end point (zero velocity and minimum acceleration) to intersection with the limit curve or to the switchover point on curve one obtained on the preceding step; 3) plotting the uppermost deceleration curve (minimum acceleration) from curve one to the zero-velocity point; 4) plotting the uppermost acceleration curve from curve two to curve three or to the zero-velocity point; 5) locating the extremum-point of the limit curve between the end points of curves three and four, then plotting the uppermost acceleration curve below that extremum point from curve three to intersection with the limit curve; 6) plotting the uppermost deceleration curve from curve five to intersection with curve four, this being the optimum trajectory, or to the zero-velocity point an repeating steps five-six for curves six and four. The problem is solved on a computer by successive use of programs LAGRANGE - DOPUSK-(tolerances) - TRAYEKT(trajectory in discrete space) - MAPPING with auxiliary programs GETNEXT, SOLVEQ, GETMOMOMENT along the road. Figures 3; references 3.

UDC 62-506

Design of Self-Regulating Electric Drives for Robots

907K0168B Novocherkassk IZVESTIYA VYSSHIKH UCHEBNYKH ZAVEDENIY: ELEKTROMEKHANIKA in Russian No 11, Nov 89 pp 36-40

[Article by Vladimir Fedorovich Filaretov, candidate of technical sciences, docent, Far-Eastern Polytechnic Institute]

[Abstract] A design procedure for electric drives with self-adaptive regulators ensuring stability during fast changes in the equivalent moment of inertia loading the motor shaft is outlined, such drives being required for satisfactory performance of industrial robots. The procedure is based on combining the equation which describes transient electric processes in the armature circuit of a d.c. motor with separate field excitation or a permanent-magnet field and the equation of moments acting on the motor shaft within the linear range of the power amplifier operation. The necessary supplementary corrective device with two time constants and a transfer function $W(s) = (T_1s+ 1)/(T_2s+1)$ is synthesized by any conventional method, assuming that the system parameters remain constant, whereupon the law of voltage regulation which will stabilize the dynamic drive parameters and thus also the motor performance is calculated on the basis of the characteristic third-order differential equation with four constant coefficients, assuming a long time constant L/R of the armature circuit. Typical underdamped transients of motor rotation with not more than two oscillation cycles and typical values drive parameters are shown for illustration. Figures 2; references 9.

UDC 621.316.925:681.325.5

Methods and Means of Softwave Development for Microprocessor-Aided Protective Relaying Systems

907K0169A Novocherkassk IZVESTIYA VYSSHIKH UCHEBNYKH ZAVEDENIY; ELEKTROMEKHANIKA in Russian No 1, Jan 90 pp 13-19

[Vladislav Ivanovich Antonov, candidate of technical sciences, senior instructor, Chuvash State University, Cheboksary, Nikolay Viktorovich Podshivalin, senior engineer, Information and Computation Center branch, Chuvash State University, and Goda Semenovich Nudelman, candidate of technical sciences, deputy department manager, All-Union Scientific Research Institute of Relay Construction, Cheboksary]

[Abstract] Industry-wide experience in development of software for microprocessor systems is systematically overviewed for application to protective relaying. The development stages successively covered are formulation of tasks and requirements, microprocessor design for modular programming or step-down programming, coding of algorithms in symbolic language for logic operations (AND, OR, NOT, MAJ, TRG, TIMR, EQ, BIF, INIT, INIV) and annunciator operations (DEFIN, DYNST, SIGN, COUNT) or programming in higher-level languages, debugging, testing, documentation, and tracking. Most important is shown to be proper planning of the software development stages. The development process can be simplified and accelerated by using special-purpose program languages and automatic generators of application programs oriented toward specific relaying tasks, preferably adaptive application programs designed to maximize the response speed of protective relays. Figures 1; tables 1; references 12.

UDC 621.313

Calculation of Magnetic Field Distribution in Arched and Semicircular Slots of Finite Depth

907K0169B Novocherkassk IZVESTIYA VYSSHIKH UCHEBNYKH ZAVEDENIY; ELEKTROMEKHANIKA in Russian No 1, Jan 90 pp 30-34

[Article by Ivan Pavlovich Streltsov, candidate of technical sciences, docent, Far-Eastern Institute of Public Utilities Technology]

[Abstract] A method of designing groined-arch and round rotor slots for inductor alternators with a smooth stator bore is outlined, considering that the slot depth must necessarily be limited and that Z-slots are impractical here. The slot design must yield the magnetic field distribution and thus also the electric potential distribution in the slots and in the air gap above them necessary for specific alternator performance requirements. The magnetic field distribution is calculated by solving the Laplace equation in a bicylindrical system of coordinates for two regions, one slot and the associate quasi-rectangular air gap segment above it, with the appropriate boundary conditions each. A solution is obtained by the method of space discretization and reduction to a system of algebraic equations, which yield the sought universal parameter which characterizes the slot depth and is included in the argument of a hyperbolic tangent function. Figures 2; references 2.

UDC 621.313.17

Efficiency of Short-Term Electromechanical Energy Converter in Circuits With Capacitive and Inductive Integrators

907K0307B Kiev TEKHNICHESKAYA ELEKTRODINAMIKA in Russian No 3, May-Jun 90 pp 70-77

[Article by A. D. Podoltsev, Electrodynamics Institute at the Ukrainian Academy of Sciences, Kiev]

[Abstract] A simplified model of an electromechanical energy converter with a constant resistance and a variable time-dependent equivalent inductance is examined. Capacitive (YeN) and inductive (IN) integrators are used as the pulsed power supply source. A comparative analysis of these sources is made from the viewpoint of their conversion efficiency. The use of this model makes it possible to derive empirical expressions and graphic plots for estimating the energy conversion efficiency. It is shown that for YeN, the maximum efficiency is reached when the inductance variation law is linear or parabolic; in the case of IN, efficiency rises when inductance grows faster. Under practicable conditions, the use of YeN is preferable to IN since they make it possible to attain higher efficiency in converting previously stored energy into mechanical work given a linear dependence of inductance on time. References 10; Figures 5.

UDC 621.313.2-752

Magnetic Vibration in DC Motors

907k0307a Kiev TEKHNICHESKAYA ELEKTRODINAMIKA in Russian No 3, May-Jun 90 pp 55-58

[Article by S. P. Kalinichenko, Yu. S. Kalinichenko, Science Research Institute at the Elektrotyazhmash Plant, Kharkov]

[Abstract] Magnetic vibration due to the main magnetic flux fluctuations caused by the armature core serration is the worst in four-pole DC motors with a wave winding and an odd number of slots; it often hinders the development of modern heavy-duty motors. Vibrations lead to alternating forces and may cause frame resonance oscillations. A computer analysis of the main pole permeance made for various armature positions at a 0.02 tooth step revealed the pattern of permeance fluctuations as a function of the number of slots. Several methods of decreasing magnetic vibration are discussed. Wave windings with "dead" sections are the most expedient for eliminating the cause of magnetic vibration and reducing the resulting noise; their large-scale use is recommended for modern quadripole DC motors in place of conventional wave windings since other methods of preventing magnetic vibration appear to be less efficient. References 3: 2 Russian, 1 Western; Figures 3.

UDC 621.316:681.3

Issues of Developing Efficient Procedures of Simulating Processes in Complex Electric Power Installations

907k0307c Kiev TEKHNICHESKAYA ELEKTRODINAMIKA in Russian No 3, May-Jun 90 pp 70-77 Issues of Developing Efficient Procedures of Simulating Processes in Complex Electric Power Installations

[Article by V. G. Levitskiy, A. V. Kirilenko and A. F. Butkevich, Electrodynamics Institute at the Ukrainian Academy of Sciences, Kiev]

[Abstract] Raising computation efficiency, primarily the speed of algorithms for finding the solution within an acceptable time, is especially important in a wide range of process simulation problems for complex electric power systems and other entities. Numerical simulation efficiency largely depends on the method of solving the set of algebraic equations which describe steady-state (quasistationary) and transient processes, given certain assumptions and differential equation algebraization. An equation ordering algorithm which differs from known methods in that the ordering problem is solved before forming Jacobi matrices is considered. The proposed algorithms make it possible to take into account the matrix sparsity, increase computer speed, and utilize computer memory more efficiently. They also confirm their efficacy for diagnosing electrical circuits of automation systems. The software developed on the basis of these procedures is rather versatile and can be applied to systems and entities for various purposes regardless of their functions. Appendices 1; References 4; Figures 4.

UDC 621.382

Comparison of Schottky Gate Si and GaAs FET Characteristics

907k0326a Moscow MIKROELEKTRONIKA in Russian Vol 19 No 4, Jul-Aug 90 pp 323-327

[Article by I. Yu. Lapushkin, V. I. Ryzhiy and G. Yu. Khrenov, Physical Technology Institute at the USSR Academy of Sciences]

[Abstract] The use of GaAs and Si-based semiconductors in high-speed integrated circuits is expanding due to their high charge carrier mobility and the possibility of their applications in the high T_c technology, making them completive not only in traditional but also VLSI circuits. Based on numerical simulation, characteristics of Si and GaAs FETs with a 0.1-1 μm long gate were compared. The lattice temperature was assumed to be equal to 300K while a constant threshold voltage was maintained. The results show that under these conditions, GaAs Schottky gate FETs on a semiconductor base were three- to fivefold superior to Si FETs on an insulator base with respect to transconductance, saturation current, and speed while being significantly inferior with respect to their threshold voltage and cost. To identify the limit of the FETs' capabilities at 77K, a Si transistor with a 0.1 μm gate was simulated, showing that it was virtually identical to a GaAs FET operating at 300K. References 8: 4 Russian, 4 Western; figures 2; tables 1.

UDC 621.382.8

Effect of Mask Material on Reactive Ion-Plasma Etching Characteristics of Single Crystal Silicon

907k0326b Moscow MIKROELEKTRONIKA in Russian Vol 19 No 4, Jul-Aug 90 pp 360-366

[Article by G. V. Vasilyev, A. V. Ivanov, V. Yu. Kireyev and Ye. A. Mishenkova]

[Abstract] The main VLSI circuit development trend is toward decreasing the chip area by integrating its elements vertically. The best-developed method of producing such structures in single crystal silicon is ion-plasma etching (RIPT) in chlorine- and bromine-containing gases or their mixtures with fluorine-containing compounds. Films of positive photoresist and silicon dioxide or their combinations are used as masks. The effect of the mask material on RIPT properties was examined. The FP-051MK positive photoresist and thermal silicon oxide were used as masks while mixtures of khladon-113 and sulfur hexafluoride or molecular chlorine and sulfur hexafluoride were used as reagents. Etching was performed in a planar diode reactor with an individual wafer treatment at 13.56 MHz. It was established that the mask material had a significant effect on the etching profile and anisotropy and was localized, i.e., characterized by a certain active zone depending on the masking coating area and the etching rate. In all RIPT processes, the etching anisotropy was higher in the khladon-113 and sulfur hexafluoride mixture than in the chlorine and sulfur hexafluoride mixture due to an additional passivation of the groove walls with khladon-113 decomposition products. The considerable effect of pressure on the active zone size confirms the transport of the mask etching products to the gaseous phase. References 6: 4 Russian, 2 Western; figures 6.

UDC 621.315.592:621.382

Optical Sounding of Elastic Stress in Silicon Structures During Planar Gettering

907k0326c Moscow MIKROELEKTRONIKA in Russian Vol 19 No 4, Jul-Aug 90 pp 380-386

[Article by V. V. Artamonov, M. Ya. Valakh, B. N. Romanyuk, I. V. Rudskoy, V. V. Strelchuk and G. I. Khokhotva, Semiconductors Institute at the Ukrainian Academy of Sciences]

[Abstract] Structures of getter areas formed on the working side of the wafer in an immediate proximity to active subcircuits using local high-energy Ar^+ implantation and subsequent film build-up are examined whereby the gettering is concurrent with the epitaxial film growth. Since gettering is accompanied by the development of considerable elastic stresses in the film surface layer, the stress distribution in the circuit was analyzed by laser light Raman scattering. Wafers sliced from the same KDB-10 Si ingot grown by Czochralski's method were examined. An investigation of elastic stresses in the working sections of epitaxial silicon structures adjacent to planar getter areas made it possible to establish the getter area interaction range as a function of the implantation dose and the pad size and draw the conclusion that in developing getter areas of certain configurations, the effect of the resulting mechanical stress asymmetry must be taken into account. References 10: 2 Russian, 8 Western; figures 6.

UDC 621.382.8.001.2

Optimization of Speed and Energy Characteristics of Digital IC

907K0326D Moscow MIKROELEKTRONIKA in Russian Vol 19 No 4, Jul-Aug 90 pp 387-391

[Article by V. I. Staroselskiy, Moscow Electronic Engineering Institute]

[Abstract] In digital integrated circuit design, the problem of optimal power resource distribution must be solved in order to attain the maximum speed. To this end, logic circuits consisting of a series of logic gates are analyzed. An iteration technique is proposed for optimizing the power distribution in a randomly branching logic circuit. The method is applicable to digital bipolar

or MISFET LSI circuits and requires minimal computational facilities. Particular cases where the iteration loop may be eliminated are also considered. It is shown that power resource distribution optimization not only raises the IC speed but also reduces the spread of IC characteristics due to the component parameters' spread. References 5: 4 Russian, 1 Western; figures 2; tables 1.

UDC 621.382.323.001.24

Numerical Simulation of Nonlinear Equivalent Circuit Characteristics of Microwave Submicron Schottky Gate GaAs FETs

907k0326e Moscow MIKROELEKTRONIKA in Russian Vol 19 No 4, Jul-Aug 90 pp 392-399

[Article by G. Z. Garber]

[Abstract] The dependence of output power on the input microwave power of Schottky gate FETs is an important parameter for designing centimetric and millimetric band amplifiers. This dependence may be derived efficiently using a nonlinear equivalent circuit of the FET's active region. A two-dimensional inertial diffusion-drift model which is a modification of a quasihydrodynamic model is used. The analysis shows that the contribution of the transient Gunn domain to the equivalent circuit's electric properties may be ignored. A method is proposed for smoothing the equivalent circuit characteristics in the transient Gunn domain region; it is similar to the least squares method. An avalanche multiplication current generator model is developed on the basis of the analytical avalanche transit time diode theory. References 11: 9 Russian, 2 Western; figures 3.

UDC 621.382.8

Read Amplifiers for GaAs RAM LSI Circuits

907k0326f Moscow MIKROELEKTRONIKA in Russian Vol 19 No 4, Jul-Aug 90 pp 400-406

[Article by V. I. Staroselskiy, V. A. Bratov, V. I. Suetinov, Moscow Electronic Engineering Institute]

[Abstract] GaAs RAM LSI circuits deliver the best speed and energy characteristics. These circuits' active components are Schottky gate FETs. Efficient methods of designing read amplifiers on GaAs RAM LSI circuits which make it possible significantly to shorten the signal delay in the storage cell are analyzed. The methods are based on increasing the read current amplitude or decreasing the read signal voltage. It is shown that the latter method is more promising in that it makes it possible to shorten the signal delay in the storage-amplifier circuit to a level comparable to that in a conventional logic gate. The computer analysis thus confirms the efficacy of the proposed read amplifiers with a low read signal amplitude. References 10: 5 Russian, 5 Western; figures 5.

UDC 621.314.2/6:537.312.62

Determination of Power Losses in Superconducting Devices.

907K0250A Kiev TEKHNICHESKAYA ELEKTRODINAMIKA in Russian No 2, Mar 90 pp 27-32

[Article by Yu. P. Chernavskiy, A. V. Kuzmin, Electric Power Institute imeni G. M. Krzhizhanovskiy, S. V. Nepogodyev, Institute of Power Conservation Problems, Ukrainian Academy of Sciences, Kiev.]

[Abstract] A method is studied for determining thermal losses in superconducting devices by immersing a converter in a bath of liquid helium with known volume. Heat is lost in the latent heat of evaporation. By measuring the quantity of vapor formed it is possible to determine the thermal losses in the superconducting device. It must be considered that the thermal losses represent only a portion of the heat absorbed by the liquid helium. Another portion arrives through the walls of the cryostat, from power and measurement leads and from radiation. These losses represent a background level which must be subtracted. Figures 5; References 3: 1 Russian, 2 Western.

UDC 621.382.333

Local Mathematical Model of Gallium Arsenide Schottky-Gate Field Effect Transistor

907K0250B Kiev TEKHNICHESKAYA ELEKTRODINAMIKA in Russian No 2, Mar 90 pp 52-56

[Article by B. M. Bondarenko, S. V. Zakharova, Institute of Electrodynamics, Ukrainian Academy of Sciences, Kiev]

[Abstract] A study is made of a mathematical model of a field-effect transistor with a Schottky barrier. The model rather precisely reflects the processes occurring in the field-effect device with Gate length over 1 μm. Using the model, it is possible to compute changes in the instantaneous values of energy, drift velocity, charge-carrier concentration, electric field intensity and potential in the transistor channel with known topologic dimensions of the device. When it is necessary, static volt-ampere characteristics of the device and the parameters of the substitution circuit can be determined. The model is very simple and can be used to design circuits based on field-effect transistors with Schottky-barrier gates. Figures 4; References 3 Russian.

UDC 621.316.723.3

Variable Reactive Power Sources Based on Condenser Batteries

907K0250C Kiev TEKHNICHESKAYA ELEKTRODINAMIKA in Russian No 2, Mar 90 pp 63-66

[Article by V. S. Sidorov, Lvolv Polythechnical Institute]

[Abstract] Studies have been recently conducted to optimize the transmission of very high AC and DC voltages by the use of thryistor compensators. This article suggests a plan allowing a battery of condensers to be used as a variable source of reactive power, showing ranges of smooth regulation of the reactive power output at 35 to 220 kV. An example is presented of selecting equipment and the results of calculations of steady operation for a reactive power source at 35 kV using a static condenser battery with an installed capacity of 36 Mvar. The battery consists of 24 series-connected type KSKG-1.05-125 condensers in four parallel branches. Figures 3; References 12 Russian.

UDC 629.79.064.5:621.355

Analysis of Requirements For Mathematical Models of Batteries For Design of Nuclear Electric Power Systems.

907K0250D Kiev TEKHNICHESKAYA ELEKTRODINAMIKA in Russian No 2, Mar 90 pp 78-82

[Article by A. B. Tokarev, N. B. Zhirnova, Moscow Institute of Power Engineering]

[Abstract] The design of independent nuclear power supplies requires mathematical models of the individual elements, including the primary power source, the buffer accumulator and the load. This article studies the design of nuclear power supplies and suggests mathematical models for batteries used as buffer accumulators. A universal static mathematical model for a battery is suggested. Figures 2; References 2 Russian.

UDC 600

W Power Supply for CO_2 and CO Lasers

907K0250E Kiev TEKHNICHESKAYA ELEKTRODINAMIKA in Russian No 2, Mar 90 p 112

[Article by A. P. Koba, V. V. Pshenichnyy]

[Abstract] Power supplies are described for lasers with 7-14 kV excitation voltage and 10-mA discharge current, suitable for the ILGN-703, 704, and 708 lasers. Two models are supplied, for gas- discharge tubes with grounded anode or cathode. A compensation circuit based on an invertor with variable frequency and an inductive-capacity converter is used to stabilize the current. The discharge current is very stable and there is

a standby operating mode allowing remote or internal switching in not over 0.02 s. The maximum switching frequency is at least 10 Hz. Technical characteristics of the power supplies are listed.

UDC 621.31.008.004.5

Organization of Accounting for Electric Power

907K0252A Moscow PROMYSHLENNAYA ENERGETIKA in Russian No 4, Apr 90 pp 5-6

[Article by V. I. Kiriyenko, "Tsentrogosenergonadzor" Regional Directorate, Moscow]

[Abstract] Analysis of reports on 60 examinations of the accounting system for generation, distribution, and consumption of electric power have revealed a number of problems in the organization of accounting for electric power in systems. There is a constant shortage of electric power meters. Funds for spare parts for meters cover only 10-30 percent of the demand, and plants manufacture low-quality spare parts, frequently quite unusable. There is a shortage of test stands and standard instruments for verification of power meters. There is a shortage of personnel and of repair equipment. Many meters in use have passed the time for maintenance and testing, and many consumers are billed on the basis of installed capacity rather than metered use of power. The requirements of the operating rules are not met in terms of metering of high-capacity power transmission lines. Automated monitoring systems have started to be put in use in various power systems around the country. A special group has been organized to coordinate operations in power systems related to improvement of accounting and monitoring of electric power. One of the tasks of this group is to monitor the organization of accounting for electric power and provide methodological and technical assistance in the improvement of accounting and monitoring of electric power use.

UDC 658.012.011.56:002.5:621.311.4

Automated System for Monitoring and Control of Enterprise Electric Power Consumption

907K0252B Moscow PROMYSHLENNAYA ENERGETIKA in Russian No 4, Apr 90 pp 6-8

[Article by Yu. A. Kochkarev, Doctor of Technical Sciences, G. T. Oleynik, Candidate of Technical Sciences, N. S. Solovyev, Cherkassa Branch, Kiev Polytechnical Institute]

[Abstract] Some of the problems in the area of monitoring and management of electric power consumption at an enterprise are discussed, including the lack of cooperation between power management enterprises and power consuming enterprises, the unavailability of standard flexible plans considering the variety of equipment in use, and the lack of organizations involved in timely revisions of standard plans for specific enterprises. The introduction of automated systems for monitoring and management of electric power consumption at enterprises is therefore still proceeding at a slow pace, with 330 systems installed in the first quarter of 1989 in the Ukraine of 717 systems which have been acquired. Several steps are suggested to speed up the process, including orientation of the automated systems not toward improvement of accounting with energy supply organizations, but rather toward separate accounting for electric power by subdivisions within the consuming enterprise; assignment of a number of supplementary functions related to the automation were simplification of management of enterprise power consumption to the automated system; development of a standard automated system design to be revised quickly to meet the conditions of a specific enterprise; development of modular information-measurement system designs to allow selection of modules for specific conditions; organization of the delivery of spare circuit board and microcircuit modules, as well as organization of measurement equipment at energy monitoring enterprises; and the transition to open-market trade of automated system elements.

UDC 621.31:665.6(571.1)

Development of Electric Power Engineering for Western Siberian Oil and Gas Complex

907K0252C Moscow PROMYSHLENNAYA ENERGETIKA in Russian No 4, Apr 90 pp 8-11

[Article by N. Z. Pokonov, A. P. Finkel, "NEFTEGAZSPETSMONTAZHPROYET" Planning-Design and Technology Institute, USSR Oil and Gas Industry Construction Ministry, Moscow, G. I. Illarionova, National Design Institute and "ENERGOSETPROYEKTE" Scientific Research Institute, Moscow.]

[Abstract] During the past two decades, a large electric power system has been set up in Western Siberia. At present, a plan has been developed for the prospective development of power engineering in this region through the year 2000. This plan defines the basic strategy for development of the Tyumen power system; bypassing the stage of creating territorially isolated power units with small electric power plants, move forward immediately to the creation of a large power system based on high- capacity thermal electric power plants and major 500 kV power transmission lines. The increase in electric power consumption has exceeded even the calculations of the government planning organizations. A program of equipment modernization has been developed and is now being implemented to increase the reliability and stability of the power supply system for enterprises in the oil and gas industry and the oil and gas industry construction ministry. However, it has long been known that the large synchronous motors now being installed do not fully meet the demands for dynamic stability in cases of temporary reduction in voltage. The Tyumen power system is unique in that compressors and pumping stations are driven by large synchronous motors,

allowing effective regulation of the reactive power of consumers. New and economic designs of power transmission line supports, power substations and equipment have been developed for use in this area. Some 8000 km of 220 kV power transmission lines and over 3000 km of 500 kV transmission lines are to be constructed in this area, as well as 220-500 kV reducing substations with a capacity of about 30 million kVA. Steps must be taken to improve the sophistication of equipment and intense labor in the performance of construction, installation and adjustment operations, the manufacture of equipment and structures, products and mechanisms for use in this area.

New Electric Power Equipment

907K0252D Moscow PROMYSHLENNAYA ENERGETIKA in Russian No 4, Apr 90 p 54

[Abstract] Brief technical descriptions and tables of characteristics are presented for new electric power equipment, including high-voltage RRZ-35/1000UZ, RRZ-35/2000 UZ breakers, type VBChE-10 vacuum 3-pole breakers, RE12 current relays and RE14 voltage relays without standard reset ratio. Names and addresses of manufacturing plants are presented.

UDC 621.311

Influence of Capacity and Location of Electric Power Plants on Power System Organizations.

907K0268A Moscow ELEKTRICHESKIYE STANTSII in Russian No 4 Vol 25, Apr 90 pp 16-20

[Article by D. L. Faybisovich, A. N. Zeyliger, Energosetproyekt, Scientific Research Institute of Direct Current]

[Abstract] The development of the electric power systems of the USA and the USSR over the past fifteen years is compared. The USSR has built and plans to build considerably more very high voltage power transmission lines (500 kV and higher). This difference results from the difference in location and construction of power plants in the two countries, the concentration of production of electric power and the balance between the development of electric power plants for regional and combined power systems with respect to the growth of power system loads. The USSR has concentrated more on the construction of large hydroelectric power plants located far from major areas of power consumption. The USSR also builds larger nuclear power plants, with capacities averaging almost twice as great as in the USA. Future Soviet plans call for reduced concentration of power generating capacity, with determination of the optimal concentration of the generating facilities in consideration of economic, ecologic and social factors. References: 4 Russian.

UDC 621.311.027.89.016.35

Study of Static Stability in Combined Power System Containing 1150 kV Power Transmission Lines.

907K0268B Moscow ELEKTRICHESKIYE STANTSII in Russian No 4 Vol 25, Apr 90 pp 21-27

[Article by D. L. Balyberdin, T. A. Gushchina and A. Kh. Yesipovich Scientific Research Institute of Direct Current.]

[Abstract] This article studies problems of assuring static stability against cumulative hunting and effectiveness of damping electromechanical oscillations in the USSR unified electric power system as the system-forming 1150 kV power transmission system is brought on line. Control facilities studied included strong-acting systems for automatic regulation of excitation for power-plant generators and regulating systems for reactive power compensation devices. The purpose was to determine whether adjustment parameters of the excitation regulating equipment can be constant for all situations, or to suggest an adaptation logic for the transition from mode to mode. The mathematical and experimental studies demonstrate that the adjustment can be constant, limiting the operating modes of the 1150 kV power transmission lines and assuring good quality damping of electromechanical oscillations. Calculation and experimental results agree well. The experiments confirm the effectiveness of the introduction of stabilization channels to the regulating structure in weakly damped systems. References: 4 Russian.

UDC 621.311.2:620.97

Crimean Experimental Solar Electric Power Plant.

907K0268C Moscow ELEKTRICHESKIYE STANTSII in Russian No 4 Vol 25, Apr 90 pp 60-62

[Article by V. A. Dubovenko, V. S. Galushchak, A. I. Kuryatov, V. M. Markin, Crimean Electric Power Association.]

[Abstract] The Crimean experimental solar electric power plant SES-5 transmits power into the unified national Soviet power system for the first time on 25 Sep 1985. The tasks of the plant included determination of the capability for using solar energy by its conversion to electric power using the classical thermodynamic system of a thermal electric power plant, as well as the development, manufacture, fine tuning and accumulation of experience in using new types of equipment and systems for this type of solar electric power plant. The plant consists of three basic systems: the optical system, thermal electric power generating system and power output system. It is a basin-type power plant with the heat receiver mounted at some height in the center of a circular field of heliostats forming a parabolic optical system. The SES-5 plant uses 1600 GE-500 heliostats manufactured in Czechoslovakia, each measuring 5 X

5M, with their motion controlled by three SM computers. Maximum electric power output has been 5.7 MW, annual power production 250 kW · hr, continuous operating time over 10,000 hours. A Thermal accumulation system has been developed capable of generating 1.5 MW ·. References: 3 Russian.

UDC 621.3:62.5.001.24

Methods of Constructing the Boundaries of the Working Capacity Area of Electrotechnical Objects

907K0269A Moscow ELEKTRICHESTVO in Russian No 4, Apr 90 (manuscript received 7 Jul 1988) pp 14-19

[Article by A. V. Saushev]

[Abstract] The working capacity of an electrotechnical object is defined by a region, G, which is the intersection of the acceptable region of the set of input parameters of an object and the set of limitations on the input parameters.

The boundaries of G are used in optimization problems and the parametric synthesis of electrotechnical systems and devices, as well as quality and stability control. The effectiveness of the solution is determined by the means of constructing the boundaries of G.

This article examines a goal-oriented method of determining the boundaries of G, the parallel straight lines method, which does not have the drawbacks of the secant method. R-functions are used to simplify the algorithm to find the boundary points of G.

The parallel straight lines method can be used for any electrotechnical object for which the working conditions are defined and for which there is a link between input and output parameters. Accuracy depends only on the degree of discreteness of the varied input parameter. Figures 3; tables 1; references 10.

UDC 621.314.6:537.312.62.001.57

Experimental Model of a Three-Phase 50 Hz Cryotronic Transformer

907K0269B Moscow ELEKTRICHESTVO in Russian No 4, Apr 90 (manuscript received 25 Nov 1987) pp 55-58

[Article by Sh. I. Litidze, Doctor of Technical Sciences, V. Ye. Ignatov, I. V. Karlash, Candidates of Technical Science, and V. N. Noskov, Engineer]

[Abstract] Superconducting transformers based on cryotrons are being developed as devices to supply, regulate, and stabilize the current of multi-ampere coils of superconducting magnetic systems.

The power of cryotrons must be increased by increasing the number of phases and the frequency of the working voltage, and by using fine disperse superconducting materials with high Debye temperatures and high dielectric permeability for the valves.

The specific resistance ρ of the superconducting material indirectly determines the power of the transformer. For cryotrons $\rho = 10^{-6}$-$10^{8}\Xi$m is desirable.

The authors theoretically analyzed the electromagnetic transition processes in the three-phase cryotron. The parameters of its basic elements were determined experimentally.

Power losses were decreased and cooling was improved after heating due to resistive losses caused the cryotron to fail.

The deviation of experimental data from theoretical did not exceed 10 percent and a method was developed to evaluate the performance of the three-phase cryotrons in commutating resistance and EMF.

Figures 4; references 4: 1 Russian 3 Western.

Conference on the Transmission of Ultra-high Voltage

907K0269C Moscow ELEKTRICHESTVO in Russian No 4, Apr 90 (manuscript received) pp 84-86

[Article by I. I. Kartashev, O. A. Nikitin]

[Abstract] A conference on ultra-high voltage (UHV) power transmission was held on 25-30 September 1989 in Moscow and Kokchetav. Specialists from a number of nations attended.

In three days of round table discussions over 50 participants discussed 25 reports on the technology of UHV transmission. An important feature of the conference was a visit to the Kokchetav 1150 kV substation.

In choosing a UHV transmission scheme, many factors aside from economic ones must be considered, for example, stability, reliability, viability, ecological limitations, regional significance, and industrial capabilities.

No decision was reached on the maximum working voltage of UHV systems, but it was decided that selection of one standard level would be expedient, as well as standards for the acceptable ecological effect of UHV transmission lines.

Reports were given on new designs in AC systems, including a Soviet self-compensating high voltage line and six-phase systems.

The ideal flexible AC transmission system was discussed again at the conference. The section on AC UHV transmission lines discussed ten reports and letters.

The visit to the 1150 kV substation demonstrated the feasibility of UHV systems.

UDC 621.311.019.34.001.24

Estimation and Guarantee of Reliability of Large Power Pools

907K0283A Moscow ELEKTRICHESTVO in Russian No 5, May 90 (manuscript received 12 Oct 88) pp 1-9

[Article by L. L. Bogatyrev]

[Abstract] The steadiness of the operation of present-day large electric power systems can be maintained and the reliability of their operation can be improved only by the extensive introduction of automatic situation control systems employing computers that can adapt to emergency situations and can identify the power systems's state. The control of these systems requires the enlistment of qualitative—so-called semantic—information. The controlled system evolves over time and its structure changes, and this causes the control process itself to evolve. The control system needs to be designed on the basis of specific knowledge concerning the controlled system that reflects the basic properties of electric power systems. This article presents various methods of forming a knowledge base for a system for controlling the operating trouble states of power systems, depending on the knowledge representation language and inference algorithms used when the control system makes decisions. Also presented are methods of identifying, in the process of solving long-term planning problems, efficient control options and power system development strategies based on a set of reliability indices when the initial data are uncertain. Various decision rules are discussed, e.g., one for determining the value of the post-accident permissible power flow for a section having an 8-percent static stability margin, taking into account irregular power fluctuations when a 500-kV power tranmission line is cut off. The methods of pattern recognition theory, fuzzy sets and fuzzy evidence are found to be effective for the estimation of reliability indices in real time. In the case cited, the device of fuzzy sets and fuzzy evidence is found to be adequate for the process studied when the initial data are uncertain and makes possible the control system's adaptation as the controlled system evolves. The distinction is drawn between stochastic uncertainty—caused by random factors—and linguistic uncertainty—caused by the fuzziness of the goal of the system's functioning and of the limitations placed on the system, i.e., the fuzziness of such concepts as "high," "good" and "proper." Quantitative reliability indices for electric power systems are proposed that can be used in designing power systems and solving problems of their long-range development and control. Statistical decision functions obtained by the methods of pattern recognition theory and fuzzy sets can be used effectively in estimating in real time a power system's functioning reliability. The control system's knowledge base must be formed by using a production, relational and predicate language. Figures 3; references 14 (Russian).

UDC 537.811.001.24

Electromagnetic Field of Shielded Two-Wire Line

907K0283B Moscow ELEKTRICHESTVO in Russian No 5, May 90 (manuscript received 20 Oct 86) pp 50-53

[Article by V. P. Zakharov, A. V. Kisletsov, A. V. Krivopustov and A. Yu. Mosolov]

[Abstract] The problem of the electromagnetic compatibility of a heavy-current electrophysical plant operating in the pulsed mode with the set of equipment used with it reduces to the determination of the intrinsic field generated by the plant, i.e., is equivalent to studying the shielding properties of the plant's shell in relation to internal electromagnetic pulse sources. This article presents a technique for calculating the characteristics of the magnetic field generated by a current pulse of arbitrary shape passing through a shielded two-wire line, serving as an example of a standard component of high-tension power systems. Edge effects are disregarded, resulting in a two-dimensional problem. A pair of wires is examined, at a distance of 2a from one another and placed in a cylindrical shield of radius R and thickness d . An expression is found for the strength of the external field, disregarding the relationship between the shielding material's permeability and the amplitude of the strength of the intrinsic acting field of the two-wire line. The intrinsic field is represented as the superposition of the strengths of the fields of concentrically arranged multipoles for current pulse durations of on the order of 10^{-9} s. The shielding factors are defined for the individual multipoles and an expression is derived for the shield's pulse response for a fixed multipole number, m . An expression is obtained for the external magnetic field strength components of a shielded two-wire line through which a current pulse of arbitrary shape is passing. A program—the MSLW program—was written that implements the system of equations presented, for the purpose of revealing the main features of the radiated field of shielded two-wire lines. Amplitude-time characteristics are presented for the magnetic field strength of such a line at the outer surface of the shield. The shield exerts a substantial influence on the amplitude and shape of the magnetic field pulse. Currents induced in the shield create fields that oppose alteration of the pulsed field of the two-wire line. The approximate analytical expressions presented for the external magnetic field strength components can be used for engineering approximation calculations. Figures 4; references 3 (Russian).

UDC 537.523.4:536.421.1.001.24

Calculation of Heating of Walls of Metal Objects Under Effect of Lightning on Them

907K0283C Moscow ELEKTRICHESTVO in Russian No 5, May 90 (manuscript received 28 Oct 88) pp 56-59

[Article by N. R. Abramov and I. P. Kuzhekin]

[Abstract] The thermal problem was solved in previous studies for the case of the effect on the walls of metal

objects of the lasting component of lightning current. Here it was assumed that there is no heat transfer between the wall and ambient air and that the current of the lasting component of the lightning does not change over time. Current amplitudes of the order of hundreds of amperes and durations of scores and hundreds of milliseconds were used in experimental verification of the calculation procedure. The present article is devoted to an analysis of the influence on the temperature change in the walls of metal objects of a high-velocity air flow and of the drop in current over time, and of the applicability of the proposed procedure for the calculation of thermal fields when the current has a duration of single numbers of milliseconds. The thermal effect of lightning on metal objects is associated mainly with the intake of energy from the region near the electrodes when lightning current passes through after the main discharge. The heat flux is assumed to be surface flux. A system of equations is presented that describes the process of the heating of a plane unbounded wall of thickness h under the effect of a heat source of radius r_0. It is assumed that the material's thermal properties do not depend on the temperature and that the heat flux density does not depend on time current of the lightning's lasting component. An analysis is made of the influence of heat transfer on the temperature distribution, using a thin plate as an example, in which the thermal process takes place more intensely. An analysis is made of the influence of heat transfer on heating of the walls of metal objects when there is an air flow of velocity v present. It is shown that with velocities of v = 100 to 200 m/s heat transfer does not result in a substantial change in the wall's temperature. Even at the hottest point (r = 0) the temperature is lowered by only 15 percent with v = 200 m/s and t = 1 s. Calculated data show that the change in the melting radius, r_{pl}, of an object's wall over the range of durations of the constant component of the lightning's current, taking into account heat transfer between the wall and a high-velocity air flow, is insignificant with t = 1 s, and the disagreement is nine percent for v = 0 and v = 200 m/s. The analytical expressions obtained for the thermal fields can be used for calculating the melting of the walls of metal objects under currents of the lasting lightning component when these currents last from single numbers to hundreds of milliseconds and when the current changes over time. Figures 3; references 6 (Russian).

UDC 621.315.21

High- and Superhigh-Voltage Cables With Insulation Made of Synthetic Materials

907K0290A Moscow ENERGETICHESKOYE STROITELSTVO in Russian No 5, May 90 pp 55-58

[Article by A. I. Gershengorn, engineer]

[Abstract] Previously only impregnated paper insulation was used in cables for underground and submarine high-voltage power transmission lines. The low manufacturing cost of cables with insulation made of synthetic materials such as polyvinylchloride and polyethylene quickly made them competitors of paper-insulated cables. In addition, they have the advantages of lower weight, the ability to be laid both manually and by machine, and to be laid directly in the ground without additional protection from mechanical damage; and long single-core cables can be laid without splicing. Also, their connections are more reliable and they have a smaller permissible bending radius, making it easier to lay them under cramped conditions. They have smaller power losses and can withstand short-duration overloading and considerable short-circuit current. The advantages and disadvantages and areas of application of cables having various types of synthetic insulation are contrasted and compared, and the history of their development and introduction in electric power systems in Europe, the USA and Japan is summarized. Special attention is paid to crosslinked polyethylene (XLPE)—produced by the extrusion of low-density thermoplastic polyethylene—as an insulating material for high- and superhigh-voltage cables. XLPE insulation can withstand a rise in temperature to 90° C under long-time use, and to 100-to-105 and 250° C, respectively, during overloading and short circuiting. Though an excellent insulator, even a small amount of impurities will worsen its insulating properties, it is labor-intensive to produce, and it is more flammable than ordinary polyethylene. Cables having XLPE insulation began to be used for laying high-voltage distribution cable lines in the 60s in the USA, Japan and West Europe. In 1987 in the USA, 90.1 percent of the total length of these lines had been laid with these cables. The structure of 20-kV and 187-kV XLPE-insulated cables is shown, and the concrete block used in Switzerland for running high-density polyethylene conduits through, through which, in turn, high-voltage cables are run. Reliable new extruded connecting sleeves are making it possible to construct extended cable lines for even higher voltages. Figures 4; references 14 (Western).

Metal Tower for Areas With High Wind Loads

907K0290B Moscow ENERGETICHESKOYE STROITELSTVO in Russian No 5, May 90 pp 75-76

[Article by Ye. A. Kruglikov, A. S. Golovchenko and B. A. Lenitskiy, engineers]

[Abstract] The design of a special intermediate tower for use in areas with high wind loads is discussed. Anchored corner poles were previously used as two-circuit intermediate poles for 330-kV aerial power transmission lines in these areas because of the lack of a unified design for these supports. Heavy footings had to be built and too much steel was used. The tower described was developed by the Ukrainian branch of Energosetproyekt [All-Union State Design and Surveying and Scientific Research Institute of Power Systems and Electric Power Networks] with the participation of the Yuzhelektrosetstroy Trust and the Donetsk High-Voltage Pole Plant. The tower is designed for the suspension of 2XAS300/39 or

2XAS400/51 wires and one or two type S-70 lightning-protection cables in areas having a maximum wind load of 800 Pa and belonging to glazed-frost zone IV and line-wire dancing zone III. The tower has four crossarms, and the distance to the ground from the point where the wires are attached to the bottom crossarm is 20 meters. The bolt-construction tower has a rectangular cross section in plan and measures 8 x 6 with an overall height of 26 m, or 6.3 x 4.6 m with an overall height of 20 m. Its principal structural members are made of galvanized rolled angle stock. Standard precast reinforced concrete footings are used to fasten the tower to the ground. The new type A2M towers were used for the first time in a 330-kV 23-km aerial line. They can also be used in 220-kV aerial lines being constructed in areas with high wind loads, such as in the Far East. Figures 1.

New Design of Footing for Steel Aerial Line Poles

907K0290C Moscow ENERGETICHESKOYE STROITELSTVO in Russian No 5, May 90 pp 76-77

[Article by N. S. Milykh, engineer]

[Abstract] The supporting capacity and deformability of the base of footings installed in earth with the earth's structure undisturbed are higher than for footings placed in a pocket in a ditch that has been backfilled. The main difficulty in installing a precast reinforced concrete footing in a drilled hole is making the connection between the footing and the undisturbed earth. The design of a pile footing that solves this problem is described in this article. The stem of the footing is square in cross section. Four main and four additional hinged blades connected to the footing and to one another by means of links are located at the bottom of the stem at a spread heel that is round in cross section. In assembled form the blades encompass the footing along the perimeter of the drilled hole. There are notches in the lateral edges of the main blades. The free ends of each pair of additional blades are furnished with stops that can enter the notches of the respective adjoining main blades. The stops restrict the movement of the additional blades in the notches of the main blades. There are metal insertion parts installed near the heel at the bottom of the stem that have ears rigidly connected to them. There is a chamfer on the inside of the ears with which the lower parts of the main blades engage. The ends of pull rods designed for adjusting the blades' position and withdrawing the piles from the hole, when necessary, are attached to the main blades. There are prongs at the bottom of the edges of the main blades. The collapsible blades are raised before the pile footing is placed into the drilled hole, and the footing is lowered into the hole without disturbing the earth's structure. Then the blades are pressed into the earth by means of a device that has the shape of a tubular beam. The hole is then filled with a sand-and-gravel mixture that is tamped layer by layer. The result is a reliable connection to undisturbed earth. The main blades are fastened so that in the working position they engage with the footing and absorb the alternating loads acting on it. Figures 1.

UDC 621.31:65.015.3

Certain Results of the USSR Energy Ministry Operation in 1989

907k0323a Moscow ELEKTRICHESKIYE STANTSII in Russian No 7, Jul 90 pp 2-6

[Article by V. Ye. Denisov, Soyuztekhenergo]

[Abstract] The Soyuztekhenergo annually analyzes the reliability and economic indicators of power generating enterprises in the industry and energy losses to power transmission, making it possible to evaluate the performance of individual power plants and enterprises as the well as the ministry as a whole. The results of such an analysis for 1989 are presented, showing that a total of 1,722 billion kWh of electric energy was generated in the country in general an 1,422.8 billion by the USSR Energy Ministry's enterprises. Fossil fuel plants generated 1,201.0 billion kWh. The following rates of increase over 1988 are reported: 1.5 percent by all power plants, 2.4 percent by fossil fuel plants, and 2.9 percent by hydroelectric plants. Heat deliveries by all power plants in the industry dropped by 25,000,000 Gcal to 1,091,800,000 Gcal and deliveries by fossil fuel plants decreased by 25,600,000 Gcal to 973,300,000 Gcal. The rate of fuel and energy resource conservation at fossil fuel plants has decreased significantly in recent years. Other economic and performance indicators, such as the availability factor, installed capacity utilization, specific fuel consumption, and MTBF are also summarized. The conclusion is drawn that perennial troubles with equipment failures continued in 1989 and that the year was not an exception with respect to the lag between the available and installed capacity of hydroelectric plants. Tables 1.

New Ceramic Element Converts Gaseous Fuel Energy Into Electrical Energy

907K0292 Moscow NAUKA V SSSR in Russian No 3, May-Jun 90 pp 55-56

[Article by I. A. Zudov]

[Abstract] Scientists at the Institute of Electrochemistry of the Urals Division of the USSR Academy of Sciences have developed a ceramic element which converts the electrical energy of a gaseous fuel directly into electrical energy with an efficiency of up to 55-60 percent. At present the experimental model can power only a 100-W light bulb.

Specially prepared natural gas and air pass through channels in the element. Oxygen in the air oxidizes the hydrogen and carbon monoxide, and the liberated energy is converted to electricity. The by-products are nitrogen, water vapor, and carbon dioxide.

The elements are made of a solid solution of oxides of metals such as yttrium, scandium, and zirconium. Vacancies of oxygen ions are formed in the solution. Oxygen can migrate along the nodes of the crystal lattice, which gives the ceramic its unusual properties. Sensors in the element are used to monitor combustion so that it can be regulated and made more efficient.

Prospects for the use of this new technology in automobile engines and power engineering are discussed.

UDC 538.3

Influence of Ferromagnetic Part on Magnetic Field of Source

907K0311A Novocherkassk IZVESTIYA VYSSHIKH UCHEBNYKH ZAVEDENIY: ELEKTROMEKHANIKA in Russian No 5, May 90 pp 11-16

[Article by Lemark Aleksandroovich Cherednichenko, candidate of technical sciences, docent, senior scientific associate, Central Scientific Research Institute 'Morfizpribor' (Maritime Physical Instruments)]

[Abstract] A solid or hollow ferromagnetic cylinder between two conductors of a transmission line carrying a sinusoidally alternating current is considered and its influence on the originally uniform plane- parallel magnetic field of that current is evaluated theoretically. As parameters characterizing that influence are selected the constant coefficient D^n in the expression for the magnetic vector potential as the sum of all n space harmonics $A_e = \Sigma (C_n r^n + D_n r^{-n}) \sin(n\varphi)$ from n = 1 to n = ∞ (n = 1 for a uniform magnetic field), the magnitude of this coefficient being determined from the boundary conditions, and also the equivalent magnetic permeability μ_{en} of the cylinder material. Analysis and calculations reveal that the influence of such an inclusion, even of one with a high magnetic permeability, is even at low line frequencies determined principally by eddy currents when the inclusion is large and by magnetization of the material when it is small. The critical fundamental frequency separating these two ranges drops fast as solid cylinders with larger radii are inserted in the magnetic field and the critical frequencies for the higher harmonics are, in the first approximation, proportional to orders of the harmonics squared. Hollow cylinder are considered next, of special interest being one whose inside radius approaches the outside radius and thus an infinitesimally thin one so that Bessel functions of the second kind $Y_n(z)$ must be replaced with a Hankel functions $H_n^{(1)}(z)$. The critical frequency is most strongly dependent on the inside radius when the cylinders are thin and made of a weakly ferromagnetic material, the critical frequency then rising as the inside radius is increased and the thickness of the cylinder becomes smaller than the field penetration depth so that the skin effect vanishes. It is almost independent of the inside radius when the cylinders are thick with a small inside radius, the limiting case being a solid cylinder. Figures 1; tables 3; references 3.

UDC 621.313.33

Method of Designing Armature for Cylindrical Linear Induction Motor

907K0311B Novocherkassk IZVESTIYA VYSSHIKH UCHEBNYKH ZAVEDENIY: ELEKTROMEKHANIKA in Russian No 5, May 90 pp 28-34

[Article by Yuriy Fedorovich Kabachkov, candidate of technical sciences, docent, and Nelya Mikahylovna Kravchenko, senior instructor, Magnitogorsk Institute of Mining and Metallurgy]

[Abstract] A method of designing the armature-rotor for cylindrical linear induction motors is outlined, using as basis the dependence of the p.u. magnetic impedance on the acting surface magnetic field intensity according to V.M. Kutsevalov's graph approximately fitting the relation $[Z<]\text{inf}(1) = 0.88 \times 10^4 H_e^{0.417}$ rather than its proportionality to the square root of the electrical conductivity divided by the magnetic permeability at a given operating point on the magnetization curve with the complex proportionality factor A = 1.13+ j1.85 according to the L.R. Neyman formula. On this basis are calculated the equivalent-circuit parameters of a rotor with toroidal windings for such a motor driving a ram. Such a motor was built to specifications for a ram and its performance than evaluated according to classical procedure, on the basis of no-load and short-circuit tests. The rotor diameter is 0.237 m, the 10-pole stator with a 0.04 m pole pitch is 0.407 m long. Energized from a 220/380 V power line, it delivers a force of 10,150 N (9,526 N calculated) while drawing a current of 141 A (136.3 A calculated) at start (short circuit) when mounted vertically for a 0.3-0.4 m downward travel aided by the force of gravity. When mounted horizontally for a 1.5 m travel, its acceleration can be boosted by means of a winch with a speed reducer. Another variant

of a rotor was designed and built for a horizontal ram motor, one having a laminated iron core glued together with epoxy compound and having no copper winding. Its measured performance characteristics agreed within 4-5 percent with the theoretically predicted ones. Figures 2; tables 1; references 10.

UDC 621.822:621.318.3

Synthesis of Stabilization System for Electromagnetic Suspension Supporting Test Models in Wind Tunnel

907K0311C Novocherkassk IZVESTIYA VYSSHIKH UCHEBNYKH ZAVEDENIY: ELEKTROMEKHANIKA in Russian No 5, May 90 pp 48-57

[Article by Aleksandr Vladimirovich Kuzin, candidate of technical sciences, senior scientific associate, Moscow Institute of Aviation]

[Abstract] Following an analysis based on the fundamental equation of motion of a body in a stationary system of coordinates, a three-dimensional stabilization system is synthesized schematically for an electromagnetic suspension supporting a test model containing a magnetic core in a wind tunnel. The equation of motion is expanded so as superpose constant and variable external aerodynamic perturbing forces and moments on the acting electromagnetic forces and moments. The equation of motion is supplemented with linear equations of electric circuit dynamics, ignoring eddy currents and magnetic hysteresis. Equations of static equilibrium are excluded, on account of their irrelevance here. As the criterion for optimum synthesis is regarded the maximum stability region in the space of state variables. As the first example is considered roll, pitch, and yaw stabilization of a slender horizontal body in the vertical plane in the interpolar space of electromagnets at both its nose and tail ends. As the second example is considered roll stabilization only, by means of a single control element. Figures 6; references 9.

Analytical Synthesis of Digital Regulators for Nonlinear Electromechanical Systems

907K0311D Novocherkassk IZVESTIYA VYSSHIKH UCHEBNYKH ZAVEDENIY: ELEKTROMEKHANIKA in Russian No 5, May 90 pp 57-60

[Article by Sergey Eduardovich Lyashevskiy, candidate of technical sciences, senior scientific associate, Moscow Institute of Aviation]

[Abstract] Analytical synthesis of robust digital regulators for nonlinear electromechanical systems by a simple procedure is outlined, perturbed motion of such a system being described by the equation $dx/dt = f(x,u)$ (x- vector of state coordinates in space R^e, u- vector of control coordinates in space R^m, f(x,u)- nonlinear vector function). The mathematical model of the regulator is converted from a system of differential equations with indeterminate parameters to one matrix-form difference equation $x_{n+1} = [A_n + \Delta A_n(z)]x_n + [B_n + \Delta B_n(p)]\, u_n$ (A,B - matrices of coefficients, $\Delta A, \Delta B$ - matrices representing parametric indeterminacies, z,p - vectors of indeterminate parameters). As the criterion for optimum synthesis is then selected minimization of the functional $J = \Sigma [W_1(x_n) + W_2(u_n) + W_3(x_n)]$ (W- functions of x representing estimated losses due to transients). Synthesis based on this criterion involves solution of the Bellman functional minimization equation with the Lyapunov function appearing in quadratic form. Variations of the parameters $\Delta A_n(z)$ and $\Delta B_n(p)$ are first disregarded, to obtain the closed-loop control $u_n = -K_{0n}x_n$, whereupon they are reduced to and calculated as $\Delta A_n(z) = \Delta A_{0n}z$ and $\Delta B_n(p) = \Delta B_{0n}p$ with $[z] = \text{or} < I$ and $[p] = \text{or} < H$. The equation of controlled motion of the electromechanical system is then becoming modified accordingly, the necessary and sufficient conditions for stability of the closed-loop system it describes being that the first difference of the Lyapunov function be negative-definite and the matrix K_n in space R^{eXe} be positive-definite. The condition $W_1(x_n) + W_2(u_n) + W_3(x_n) > 0$ must then also be satisfied. If stability has not been thus ensured, then the destabilizing influence of the semidefinite function $W_3(x_n)$ must be compensated, which is done by modifying the weight matrix. The procedure is demonstrated on synthesis of a robust regulator for an electric drive with a synchronous motor. References 6.

UDC 666.189.2:535

Correction to Abel Integral Evaluation for Interpretation of Polarization Interferometry Data on Fibers

907K0223A Leningrad OPTIKA I SPEKTROSKOPIYA in Russian Vol 68 No 2, Feb 90 pp 442-446

[Article by I.K. Nekrasov]

[Abstract] Polarization interferometry of highly birefringent optical fibers is considered, interpretation of interferograms requiring evaluation of the Abel integral. A correction to this integral is also needed, however, because at the fiber-coating interface the longitudinal refractive index and thus also the difference between this index and the transverse one are actually lower. The correction is demonstrated on interferograms of double refraction by polymer fibers, polyparaphenylene terephthalamide and polyamidobenzimidazole ones, taken under a BIOLAR microscope (made in Poland). This microscope had a Wollaston prism built in for regulation of image doubling so that differential as well as integral interferograms could be viewed. It has been found that the fringe displacement is smaller than estimated due to bending of light rays at the fiber surface, due to birefringence at the fiber surface, and due to an index gradient inside the fiber. The correction is applying Tikhonov's regularization method to this ill-posed problem, the effect of an index gradient being best included according to the Iga theory (1977) and the effect of surface birefringence not being critical. The author thanks B.I. Molochnikov and L.N. Tsvetkov at the State Institute of Optics imeni S.I. Vavilov for supplying the immersion fluid for coating the fibers. Figures 2; references 13.

UDC 621.372.8:535

Waveguide Modes in Divergent Waveguide Excited by Linear Source

907K0223B Leningrad OPTIKA I SPEKTROSKOPIYA in Russian Vol 68 No 2, Feb 90 pp 447-451

[Article by A.S. Starkov]

[Abstract] Excitation of a divergent waveguide between two media by a linear point source near the critical cross-section is considered, the critical cross-section being the one where the thickness of the waveguide layer is sufficiently small for cutoff. The problem of waveguide modes in such a configuration is solved by the Born-Wolf method, with both E and H fields expressed through a scalar function u which in any refractive medium satisfies the equation $(\Delta + k^2n^2)u = -\delta(x - x_1)\delta(z - z_i)$ (Δ- Laplace operator, x_1,z_1- coordinates of the excitation source in rectangular Cartesian system of coordinates x,z) and the condition of continuity of its tangential components at the boundaries between media. The thickness h of the waveguide layer is assumed to be a slowly increasing smooth function of the x-coordinate so that the problem with a small parameter p = max[h](x) << 1 can be solved by asymptotic expansion with the principal term in the approximate solution for a layer of uniform thickness as reference. Expressions are obtained on this basis describing the field amplitudes of waveguide modes and the critical layer thickness for each mode at which its amplitude becomes zero. Local asymptotic expansion within the vicinity of a critical cross-section yields the size of the region within which significant transformation of an incident wave takes place, buildup of the corresponding mode being described by a special function. Figures 2; references 6.

UDC 534.522:535.345.6

Wide-Aperture Acoustooptic Filter for Intermediate Infrared Range of Spectrum

907K0223C Leningrad OPTIKA I SPEKTROSKOPIYA in Russian Vol 68 No 2, Feb 90 pp 452-457

[Article by V.B. Voloshinov and O.V. Mironov]

[Abstract] A wide-aperture acoustooptic filter for the intermediate infrared range of the spectrum is described, such a filter necessarily being a wideband one. The filter, with a specially cut highly anisotropic paratellurite TeO_2 single crystal as acoustooptic cell and with an X-cut $LiNbO_3$ single crystal as piezoelectric transducer, has a 52° aperture angle and a high spectral resolving power. Normal incidence on the front face of the filter corresponds to a 38.1° Bragg angle. The transducer induces in the cell an ultrasonic acoustic shear mode whose vector makes an 18.9° angle with the [110] axis of the latter and a 57° angle with the radiation vector. The front face and the rear face of the filter are not parallel but at a 9.5° angle to each other. The design and performance analysis of this filter is based on theoretical relations and experimental data, the latter pertaining to the dependence of its diffraction efficiency on the angle of radiation incidence and on the frequency of the ultrasound. The angle of radiation incidence was measured in the (1-11) plane from the front face (θ) and in the (001) plane from the front face (θ^*), the frequency f of ultrasound in the respective plane being referred to correspondingly. The diffraction efficiency was measured as a function of the angle of incidence over the θ = 45-135° range and the θ^* = 70-110° range respectively, with the frequency of theultrasound varied over the 39.85-41.20 MHz range. The data fit on a family of single-peak narrow-band and double-peak wideband curves depending on the frequency of the ultrasound. On the basis of these curves have been calculated θ-f curves on which the angles of incidence for maximum diffraction efficiency can be read. Most relevant to design of a wideband filter are the double-peak efficiency curves and frequencies of the ultrasound yielding such curves, the required filter aperture being equal to the difference between the angles of incidence which correspond to the two not necessarily equal maxima of diffraction efficiency. The maximum number of a filtered image resolvable according to the Rayleigh criterion is equal to one half the product of

angular and linear filter apertures divided by the radiation wavelength, the linear aperture being equal to the dimension of the sound column in the reference (1-11 or 011) plane. The authors thank I.P. Ponomarev and V.Ya. Molchanov for producing the acoustooptic cell. Figures 4; references 7.

UDC 522.6

Cosmic Dust Influx Model, Part III

907k0324a Ashkhabad IZVESTIYA AKADEMII NAUK TURKMENSKOY SSR: SERIYA FIZIKO-TEKHNICHESKIKH, KHIMICHESKIKH I GEOLOGICHESKIKH NAUK in Russian No 2, Mar-Apr 90 pp 19-24

[Article by V. N. Lebedinets, M. Begkhanov, Turkmen State University imeni A. M. Gorkiy]

[Abstract] Today, radar and photographic observations of meteors yield the most reliable data on the density of meteor bodies of varying mass. The authors selected the most reliable measurement data; radar and photography meteor and bolide research data and recordings of micrometeor collisions with spacecraft were used as the basis. The influx of the dust particles which cannot be detected by most instruments and weighing up to 10^{-17} g were examined. Based on available data, a model integral average flux density distribution by the mass of meteor bodies was plotted. Its complex behavior can be explained by the interplanetary dust cloud model. The following main conclusions were drawn from this model and other sources: above 30 km, all the particles largely have a meteor origin; above 140 km, only primary cosmic dust particles of the same size are found in the atmosphere; they have the same concentration as those in the interplanetary space but a higher flux density; in the 30-100 km range, micrometeors with a mass below 10^{-8} g are present as well as particles of the same mass which are the product of breakup of larger meteor bodies. The rate of the meteor influx toward the earth is equal to 1.0×10^{-16} gram/square centimeter per second or between 5×10^3 and 6×10^4 tons per year. References 36: 12 Russian, 24 Western; figures 2.

Photoelectric Device for Automating TV and Optoelectronic Observations of Weak Meteors

907k0324b Ashkhabad IZVESTIYA AKADEMII NAUK TURKMENSKOY SSR: SERIYA FIZIKO-TEKHNICHESKIKH, KHIMICHESKIKH I GEOLOGICHESKIKH NAUK in Russian No 2, Mar-Apr 90 pp 25-28

[Article by S. Mukhamednazarov, G. Nechayev, A. Atayev, and V. Shulgin, Engineering Physics Institute at the Turkmen Academy of Sciences]

[Abstract] The random and unexpected nature of the meteor appearance and their brief stay in the sky make it difficult to record them optically. The design and development of a photoelectric device for automating the weak meteor image recording from an image converter tube or a video monitoring TV screen is described. The recording equipment permeating capacity is between $+9^m$ and $+10^m$, hence the photoelectric device under study must have the same sensitivity; since its task is to produce the command signal for the movie or photo recording camera, its response time to the luminance increment must be shorter than the meteor life and the TV or image converter equipment signal afterimage. Two practical design versions are suggested and their operating principles are described. Pilot tests of the device developed by the authors show its suitability for automating meteor recording using video monitoring and image converter devices. References 5: 3 Russian, 2 Western; figures 2.

UDC 621.373.826

Optical Bistability of Self-Focusing Elliptical Beam

907k0325a Minsk DOKLADY AKADEMII NAUK BSSR in Russian Vol 34 No 7, Jul 90 pp 603-605

[Article by A. M. Goncharenko, P. S. Shapovalov]

[Abstract] Self-focusing is observed during the propagation of intense circular light beams in media with a cubic nonlinearity. Bistable devices are designed on the basis of this phenomenon. For elliptical beams, the light spot shape also depends on the light intensity. As the beam power increases, the light spot ellipse shape oscillates. A bistable cell consisting of a nonuniform medium, a stop, and a semitransparent mirror is examined. An opaque screen with an elliptical rather than round aperture is used as the stop. The dependence of the beam's output power on the input power is measured. It is shown in the framework of a Gaussian beam approximation that a bistable device can be designed on the basis of the light spot shape oscillation of an elliptical beam as a function of its power during propagation in a nonlinear medium. References 4: 3 Russian, 1 Western; figures 2.

UDC 621.385.6.01

Gyroresonant Devices With Four-Mirror Traveling Wave Cavities

907k0325b Minsk DOKLADY AKADEMII NAUK BSSR in Russian Vol 34 No 7, Jul 90 pp 610-612

[Article by A. A. Kurayev, Minsk Radio Engineering Institute; submitted by Belorussian Academician V. A. Labunov]

[Abstract] The main problem in the advancement of EHF gyroresonant oscillators and amplifiers is the dynamic separation of the electron current whose radial dimensions greatly exceed the cavity's working mode wavelength. Probably the only possible way of preventing the electron current separation in EHF gyroresonant devices is suggested. The principle is based on

using the traveling wave formed by a four- (or more) mirror reflector system as the working oscillator. The transverse field inhomogeneity in the working area is insured by the T-wave field independence from transverse coordinates (relative to the propagation direction) while the wave's traveling structure determines the phase grouping independence of any electron current layer from the point of its injection into the cavity's working area. The main equations describing the interaction in the devices under study and the results of their efficiency optimization at the first three gyroharmonics are cited. References: 4; figures 1.

Effect of Infrared Lighting on Photocarrier Conduction in Intrinsic Amorphous Semiconductor

907k0329a Leningrad FIZIKA I TEKHNIKA POLUPROVODNIKOV in Russian Vol 24 No 5, May 90 pp 844-848

[Article by A. G. Abdukadyrov, Ye. L. Ivchenko, Engineering Physics Institute imeni A. F. Ioffe at the USSR Academy of Sciences, Leningrad]

[Abstract] The use of two light sources, one visible and one infrared, opens up important opportunities for studying the mechanics of photoconduction and photoluminescence in amorphous semiconductors, particularly hydrogenated amorphous silicon. Photoconduction of intrinsic amorphous semiconductor is examined using the dual-beam technique at a low temperature where up-energy photocarrier tunneling jumps can be ignored. The distribution function of localized photocarriers generated under steady-state optical excitation of amorphous semiconductor to higher bands is used. Photocarrier distribution function variations under the effect of steady-state infrared radiation is calculated. It is established that absorption of this additional radiation causes photoexcitation of localized photocarriers to delocalized states which is followed by their rapid repeated capture by one of the localized states and an energy relaxation of these states terminating in a radiative recombination with another kind of carrier or another transfer to the delocalized state band. The authors are grateful to S. D. Baranovskiy, A. V. Zherzdev, A. I. Kosarev, and A. B. Pevtsov for discussing the results. References 5: 2 Russian, 3 Western; figures 2.

Effect of Hot Electrons on GaAs Luminescence

907k0329b Leningrad FIZIKA I TEKHNIKA POLUPROVODNIKOV in Russian Vol 24 No 5, May 90 pp 883-891

[Article by B. M. Ashkinadze, V. V. Belkov, A. G. Krasinskaya, Engineering Physics Institute imeni A. F. Ioffe at the USSR Academy of Sciences, Leningrad]

[Abstract] Low-temperature luminescence of sufficiently pure GaAs crystals is determined b the emission of free and bound excitons. The effect of electrons heated in a microwave field on the luminescence of pure GaAs crystals is examined. It is established that in a number of cases exciton luminescence is quenched monotonically and gradually with an increase in the electric field intensity. It is shown that this us caused by a decrease in the free exciton production cross section with an increase in the electron energy; moreover, as the electron life or light intensity increase, quenching curves may change shape and become "threshold" curves. Such a behavior may be due to the nonuniform static electric field distribution in the sample. The results enable us to draw the conclusion that excitons bound to small donors and acceptors are produced and ionized by the free exciton attachment to (or detachment from) the center, whereby excitons bound to deep acceptors are produced by successively capturing particles. The authors are grateful to V. V. Rossin for providing intrinsic GaAs samples. References 16: 6 Russian, 10 Western; figures 5.

'Energy Quasiballistics' in GaAs Microstructures at Low Temperatures

907K0329C Leningrad FIZIKA I TEKHNIKA POLUPROVODNIKOV in Russian Vol 24 No 5, May 90 pp 928-931

[Article by Yu. V. Dubrovskiy, I. A. Larkin, S. V. Morozov, A. V. Borisov, G. G. Bunin, S. A. Inozemtsev, V. G. Lapin, B. A. Malakhov, Institute of Microelectronics and Especially Pure Materials Engineering Problems at the USSR Academy of Sciences, Chernogolovka]

[Abstract] For the first time, characteristics of electron transport were examined experimentally in the case where the free path length is much shorter than the structure length under study which, in turn, is shorter than the energy relaxation length. These features are attributed to the electron temperature nonuniformity along the channel and its saturation under the channeling voltage applied to the sample on the order of the optical phonon energy. The electron motion which is virtually free of energy relation is referred to as the "energy quasiballistics". Measurements were taken in GaAs samples with a Schottky gate FET topology made from epitaxial films. The channel's incremental resistance was measured as a function of the channeling voltage between the drain and the source. The dependence of the incremental resistance behavior on the Schottky gate length was established. Subsequent numerical estimates are consistent with experimental data and confirm the validity of the physical model adopted. The authors are grateful to I. B. Levinson and V. A. Tulin for discussing the results. References 4: 2 Russian, 2 Western; figures 2.

Hypersound Amplification Under Interimpurity Light Absorption in Semiconductors

907k0329d Leningrad FIZIKA I TEKHNIKA POLUPROVODNIKOV in Russian Vol 24 No 5, May 90 pp 933-936

[Article by M. V. Vyazovskiy, Volgograd State Teachers Institute imeni A. S. Serafimovich]

[Abstract] Acoustic and optical phonon production in semiconductors during the interaction of a strong elec-

tromagnetic wave with lattice modes through the electron subsystem, especially in the case where the phonon subsystem becomes unstable and, consequently, individual lattice modes are generated or amplified, is analyzed. The possibility of the hypersonic wave generation or amplification during the interimpurity absorption of light in semiconductors with a nonforward forbidden gap is examined. The hypersound electron attenuation constant, lattice attenuation constant, and the buildup increment are calculated in a partially or fully compensated silicon-type semiconductor with a nonforward forbidden gap where light is absorbed by the donor-acceptor pairs and the light absorption is accompanied by the emission and absorption of phonons. References 9.

UDC 535.376

Epitaxial Garnet Structures as Scintillation Detectors of Ionizing Radiation

907k0334a Minsk ZHURNAL PRIKLADNOY SPEKTROSKOPII in Russian Vol 52 No 6, Jun 90 pp 967-972

[Article by Yu. V. Zorenko, S. S. Novosad, M. V. Pashkovskiy, A. B. Lyskovich, V. G. Savitskiy, M. M. Batenchuk, P. S. Malyutenkov, N. I. Patsagan, I. V. Nazar and V. I. Gorbenko, Lvov Science Research Institute of Materials]

[Abstract] Of all $Y_3Al_5O_{12}$ garnets suitable for use as scintillation detectors, single crystal films doped with rare earth ions which are characterized by interconfigration transitions between the 5d and 4f-shell states are the most interesting. Since these transitions are permitted, their luminescence attenuation time does not exceed 0.1 μs. Of these, $Y_3Al_5O_{12}$:Ce are the most promising. Certain uses of such compounds as film-type scintillation detectors of low-penetration ionizing radiation are examined. It is found that such epitaxial structures can be used to detect α- and β-particles. It is also established that "Fosvich"-type scintillators formed by one or two epitaxial single crystal layers on a garnet base and a bulk single crystal phosphor layer can be used to detect partial components of mixed ionizing fluxes, such as X-rays or γ-quanta. Scintillation characteristics of these detectors are described. References 9: 8 Russian, 1 Western; figures 3.

UDC 543.422

On the Issue of Smoothing of Spectral Curves

907k0334b Minsk ZHURNAL PRIKLADNOY SPEKTROSKOPII in Russian Vol 52 No 6, Jun 90 pp 988-994

[Article by D. K. Buslov, L. A. Meleshchenko, N. A. Nikonenko, Physics Institute imeni B. I. Stepanov at the Belorussian Academy of Sciences, Minsk]

[Abstract] The method of smoothing the experimental curves is used to increase the stability of the computer-based spectrum processing results. In order to eliminate as many random errors as possible without loosing the features of the spectrum under study, the smoothing problem is considered as a certain optimization problem. Two criteria of optimal smoothing are examined and expressions which describe the transfer functions of the corresponding digital filters used for the smoothing are derived. These equations are employed for determining the parameters of the low-pass digital filters which are matched with the signal and noise. Measurement limits of the white noise dispersion during the oscillatory spectra smoothing are evaluated, making it possible to synthesize optimal smoothing filters and automate the analysis of their parameters which is necessary for lowering the effect of subjective factors on the selection of smoothing methods and parameters, attain better spectral curve smoothing results, and estimate quantitative and qualitative noise variation during the smoothing. The authors are grateful to R. G. Zhbankov for his constant attention and help. References 5: 2 Russian 3 Western; figures 3.

UDC 621.382

Functional Microelectronic Devices Based On Superconducting Quantum Interferometers

907K0295A Moscow MIKROELEKTRONIKA in Russian Vol 19 No 3, May 90 (manuscript received 20 Feb 1989) pp 221-231

[Article by A. A. Zubkov, V. I. Makhov, A. N. Samus]

[Abstract] The use of a superconducting quantum interferometer (SQUID) in logic circuits provides speeds on the order of tens of picoseconds and low energy scattering.

The SQUID is a superconducting circuit containing one or more Josephson contacts regulated by clock signals from a magnetic flux. The contents of one interferometer acting as memory is read by another. A logical 1 indicates the capture of a quantum of magnetic flux.

The memory was numerically modeled, and it was found that when parameters are optimized, a record-read cycle can be reduced to less than 300 picoseconds. In reality, the speed of the device is determined by the geometric size of the element and the speed of peripherals forming the control currents.

An experimental model was built and tested. The size and switching dynamics may be optimized, and SQUID may be used as shift registers or XOR elements. These devices can be used in communications, image processing, and delay measurement. Figures 6; references 15: 8 Russian 7 Western.

UDC 621.382

Switching Processes of Information Cells in Magneto-Optic Controlled Transparencies. 1. Critical Parameters of the Monodomain State

907K0295B Moscow MIKROELEKTRONIKA in Russian Vol 19 No 3, May 90 (manuscript received 21 Jan 1989) pp 232-238

[Article by L. G. Onopriyenko, A. Ya. Chervonenkis]

[Abstract] Magneto-optically Controlled Transparencies (MOCT) with electrical addressing have come into widespread use for flat displays, fast printers, and real time systems of optical signal processing. MOCT are spatial-temporal light modulators based on an magneto-optic medium.

A cellular matrix can be formed in the film medium by local diffusion annealing in the presence of a reducing agent (usually silicon). A periodic system of magnetized (M_1) cells is formed in a film with an initial magnetization (M_2) and a labyrinth domain structure. When [M<]inf2[i]s small the cells have a stable monodomain structure suitable for recording binary information. The stability of this state depends on M_1/M_2 and other factors. The magnetic and geometric parameters of a film with a cellular structure are found for which a monodomain state is realized. It is only possible to use a cellular-structure film as a MOCT at certain correlations of magnetic and geometric parameters. The film is not suitable for MOCT when a critical quality factor is exceeded or when $M_1 > M_2$. A monodomain state can only be maintained for small cell size, which is impractical. Figures 5; references 4: 2 Russian 2 Western.

UDC 621.382.8.001.2

Probabilistic Distribution Law of the Lengths of Interconnections

907K0295C Moscow MIKROELEKTRONIKA in Russian Vol 19 No 3, May 90 (manuscript received 18 May 1989) pp 304-308

[Article by B. N. Fayzulayev, V. V. Kamenskiy and A. S. Pervov]

[Abstract] While integration has increased, and the size of elements and switching delays have been reduced, the length of connections between chips had changed only slightly. The length of these connections determines the size of casings and the arrangement of chips on boards.

The use of average lengths of these connections is inadequate. This article obtains a probabilistic law for the distribution of lengths of interconnections, and compares these results with experimental distributions.

The law is found for optimized, partially optimized, and nonoptimized arrangements of elements, and for several special cases. A Rayleigh distribution if found to be a sufficiently good approximation of the lengths of interconnections. Figures 3; references 5.

UDC 621.382.8.001.2

The Average Delay of Signal Propagation in VLSI Interconnections

907K0295D Moscow MIKROELEKTRONIKA in Russian Vol 19 No 3, May 90 (manuscript received 18 May 1989) pp 309-311

[Article by B. N. Fayzulayev]

[Abstract] Unlike the linear dependence of signal delay on the length of the communication line in wave propagation, the dependence of the average signal delay in the interconnections of VLSI circuits with distributed RC parameters on the length of communication lines is quadratic.

Thus, the mathematical expectation of a signal propagation delay in VLSI interconnections is dependent on the distribution law for the length of communication lines.

Special cases are examined which illustrate the effect of the probabilistic law of the length distribution of lines on the average signal propagation delay in the interconnections.

Determination of the average signal propagation delay from the average length of interconnections is valid only for wave propagation, not diffusion propagation. For RC type interconnections, losses in the line cannot be ignored, and the delay increases proportionally to the square of the interconnection length. The average delay in propagation depends on the probabilistic law of line length distribution, and substantially exceeds estimates based on average lengths. Figures 1; references 2: 2 Russian, 2 Western.

Foreign Broadcast Information Service (FBIS) and Joint Publications Research Service (JPRS) publications contain political, military, economic, environmental, and sociological news, commentary, and other information, as well as scientific and technical data and reports. All information has been obtained from foreign radio and television broadcasts, news agency transmissions, newspapers, books, and periodicals. Items generally are processed from the first or best available sources. It should not be inferred that they have been disseminated only in the medium, in the language, or to the area indicated. Items from foreign language sources are translated; those from English-language sources are transcribed. Except for excluding certain diacritics, FBIS renders personal and place-names in accordance with the romanization systems approved for U.S. Government publications by the U.S. Board of Geographic Names.

Headlines, editorial reports, and material enclosed in brackets [] are supplied by FBIS/JPRS. Processing indicators such as [Text] or [Excerpts] in the first line of each item indicate how the information was processed from the original. Unfamiliar names rendered phonetically are enclosed in parentheses. Words or names preceded by a question mark and enclosed in parentheses were not clear from the original source but have been supplied as appropriate to the context. Other unattributed parenthetical notes within the body of an item originate with the source. Times within items are as given by the source. Passages in boldface or italics are as published.

SUBSCRIPTION/PROCUREMENT INFORMATION

The FBIS DAILY REPORT contains current news and information and is published Monday through Friday in eight volumes: China, East Europe, Soviet Union, East Asia, Near East & South Asia, Sub-Saharan Africa, Latin America, and West Europe. Supplements to the DAILY REPORTs may also be available periodically and will be distributed to regular DAILY REPORT subscribers. JPRS publications, which include approximately 50 regional, worldwide, and topical reports, generally contain less time-sensitive information and are published periodically.

Current DAILY REPORTs and JPRS publications are listed in *Government Reports Announcements* issued semimonthly by the National Technical Information Service (NTIS), 5285 Port Royal Road, Springfield, Virginia 22161 and the *Monthly Catalog of U.S. Government Publications* issued by the Superintendent of Documents, U.S. Government Printing Office, Washington, D.C. 20402.

The public may subscribe to either hardcover or microfiche versions of the DAILY REPORTs and JPRS publications through NTIS at the above address or by calling (703) 487-4630. Subscription rates will be provided by NTIS upon request. Subscriptions are available outside the United States from NTIS or appointed foreign dealers. New subscribers should expect a 30-day delay in receipt of the first issue.

U.S. Government offices may obtain subscriptions to the DAILY REPORTs or JPRS publications (hardcover or microfiche) at no charge through their sponsoring organizations. For additional information or assistance, call FBIS, (202) 338-6735,or write to P.O. Box 2604, Washington, D.C. 20013. Department of Defense consumers are required to submit requests through appropriate command validation channels to DIA, RTS-2C, Washington, D.C. 20301. (Telephone: (202) 373-3771, Autovon: 243-3771.)

Back issues or single copies of the DAILY REPORTs and JPRS publications are not available. Both the DAILY REPORTs and the JPRS publications are on file for public reference at the Library of Congress and at many Federal Depository Libraries. Reference copies may also be seen at many public and university libraries throughout the United States.